



Results

Chapter I

Regulation of Nogo and Nogo receptor during the development of the entorhino-hippocampal pathway and after adult hippocampal lesions

Ana Mingorance, Xavier Fontana, Marta Solé, Ferrán Burgaya, Jesús M. Ureña, Felicia Y. Teng, Bor L.Tang, David Hunt, Patric N. Anderson, John R. Bethea, Martin E. Schwab, Eduardo Soriano and José A. del Río.

Molecular and Cellular Neuroscience (2004) 26: 34-49

Regulation of Nogo and Nogo receptor during the development of the entorhino-hippocampal pathway and after adult hippocampal lesions [☆]

Ana Mingorance,^a Xavier Fontana,^a Marta Solé,^a Ferran Burgaya,^a Jesús M. Ureña,^a Felicia Y.H. Teng,^b Bor Luen Tang,^b David Hunt,^c Patrick N. Anderson,^d John R. Bethea,^e Martin E. Schwab,^f Eduardo Soriano,^a and José A. del Río^{a,*}

^aDevelopment and Regeneration of the CNS, Barcelona Science Park-IRBB, University of Barcelona, E-08028 Barcelona, Spain

^bNCA Laboratory, Institute of Molecular and Cell Biology, Singapore, Singapore

^cDepartment of Immunology and Molecular Pathology, The Wellcome Institute, University College London, London W1T 4JF, UK

^dDepartment of Anatomy and Developmental Biology, University College London, London WC1E 6BT, UK

^eMiami Project for Cure Paralysis, University of Miami School of Medicine, Miami, FL 33136, USA

^fDepartment of Neuromorphology, Brain Research Institute, University and ETH, Zurich, Switzerland

Received 31 July 2003; revised 11 December 2003; accepted 6 January 2004

Available online 21 March 2004

Axonal regeneration in the adult CNS is limited by the presence of several inhibitory proteins associated with myelin. Nogo-A, a myelin-associated inhibitor, is responsible for axonal outgrowth inhibition in vivo and in vitro. Here we study the onset and maturation of Nogo-A and Nogo receptor in the entorhino-hippocampal formation of developing and adult mice. We also provide evidence that Nogo-A does not inhibit embryonic hippocampal neurons, in contrast to other cell types such as cerebellar granule cells. Our results also show that Nogo and Nogo receptor mRNA are expressed in the adult by both principal and local-circuit hippocampal neurons, and that after lesion, Nogo-A is also transiently expressed by a subset of reactive astrocytes. Furthermore, we analyzed their regulation after kainic acid (KA) treatment and in response to the transection of the entorhino-hippocampal connection. We found that Nogo-A and Nogo receptor are differentially regulated after kainic acid or perforant pathway lesions. Lastly, we show that the regenerative potential of lesioned entorhino-hippocampal organotypic slice co-cultures is increased after blockage of Nogo-A with two IN-1 blocking antibodies. In conclusion, our results show that Nogo and its receptor might play key roles during development of hippocampal connections and that they are implicated in neuronal plasticity in the adult.

© 2004 Elsevier Inc. All rights reserved.

Introduction

Myelin-associated inhibitors Nogo-A, myelin-associated glycoprotein (MAG), and oligodendrocyte-myelin glycoprotein (OMgp) are thought to prevent axon regeneration in the lesioned nervous system in vitro and in vivo (Chen et al., 2000; Kottis et al., 2002; McKerracher et al., 1994; Mukhopadhyay et al., 1994; Schwab and Bartholdi, 1996; Tang, 2003). These inhibitory proteins exert their effects through a common neuronal receptor (the Nogo receptor or NgR) (Fournier et al., 2001). Nogo-A is the longest isoform encoded by the *nogo* gene (RTN4), which also gives rise to Nogo-B and Nogo-C (Chen et al., 2000). All three isoforms present a common C-terminal region with two putative transmembrane domains, whereas Nogo-A and -B share an amino terminus of 172 amino acids (Chen et al., 2000; see also Oertle and Schwab, 2003 for review). RTN4/*nogo* belongs to the Reticulon (*Rtn*) gene family (together with RTN1–3), whose transcripts are mainly retained in the endoplasmic reticulum (reviewed by Oertle and Schwab, 2003). However, a low percentage of Nogo-A is present at the cell membrane of oligodendrocytes (Chen et al., 2000; GrandPre et al., 2000), and together with OMgp, Nogo-A is also expressed by neurons (Huber et al., 2002; Hunt et al., 2002; Josephson et al., 2001; Tozaki et al., 2002).

Several studies have pointed out that Nogo-A has two inhibitory domains: the Nogo-66 loop, which is also present in Nogo-B and -C, and the amino Nogo (or NiG) (Chen et al., 2000; Fournier et al., 2001; Oertle et al., 2003b; Prinjha et al., 2000). Oligodendrocytic Nogo-66 interacts with NgR at the neuron surface and inhibits axonal outgrowth through the activation of p75 (Fournier et al., 2001; Wong et al., 2002). On the other hand, NiG corresponds to a central region specific to Nogo-A, and it is also assumed to be exposed at the cell membrane (Oertle et al., 2003b).

[☆] Supplementary data associated with this article can be found at doi:10.1016/S1044-7431(03)00003-X.

* Corresponding author. Development and Regeneration of the CNS, Barcelona Science Park-IRBB, University of Barcelona, Josep Samitier 1–5, E-08028 Barcelona, Spain. Fax: +34-93-4037116.

E-mail address: jario@pcb.ub.es (J.A. del Río).

Available online on ScienceDirect (www.sciencedirect.com.)

Different strategies have been used to prevent the Nogo-A-induced inhibition of axonal regeneration in CNS lesions. For example, the blockage of the Nogo-66 interaction with NgR using the agonistic peptide NEP1–40 increases functional recovery and axonal regeneration after spinal cord injury (GrandPre et al., 2002). Similarly, the binding of the monoclonal antibody IN-1 to NiG promotes regeneration of lesioned fiber tracts (Bregman et al., 1995; Brosamle et al., 2000; Schnell and Schwab, 1990; Thallmair et al., 1998). However, the effects of IN-1 interaction with NiG are not clearly established. Besides promoting neuronal regeneration, IN-1 treatment also induces the sprouting of unlesioned neurons and activates the transcription of different growth promoting genes such as GAP43 (Buffo et al., 2000; Zagrebelsky et al., 1998). In addition, Nogo-A interacts with a novel mitochondrial protein of unknown function (NIMP, Hu et al., 2002) and with the cytoskeletal protein tubulin (Taketomi et al., 2002). Furthermore, recent studies report a role for Nogo and NgR in apoptosis (Li et al., 2001; Oertle et al., 2003a; Watari and Yutsudo, 2003) and cell adhesion (Fournier et al., 2002, He et al., 2003).

The regenerative potential of the CNS disappears gradually during development and coincides with the formation of myelin sheaths, around the second postnatal week for the entorhino-hippocampal connection in vivo (e.g., Li et al., 1995; Prang et al., 2001; Savaskan et al., 1999). The main myelinated afferents to the hippocampus (entorhinal and commissural axons) terminate in a non-overlapping fashion along the dendrites of the granule cells in the dentate gyrus and the pyramidal neurons in the hippocampus proper (Amaral and Witter, 1995). Perforant path lesions cause profound alterations in the deafferented hippocampus such as the activation of glial cells, the overexpression of extracellular matrix proteins, the infiltration of serum-derived elements, and changes in myelin (Bovolenta et al., 1993; Fagan and Gage, 1990; Jensen et al., 1997; Meier et al., 2003; Turner et al., 1998). In addition, entorhino-hippocampal lesions lead to anterograde degeneration of presynaptic elements in the outer two-thirds of the dentate molecular layer and in the stratum lacunosum-moleculare (Hjorth-Simonsen and Jeune, 1972). Nogo-A and NgR are expressed in the entorhino-hippocampal formation during embryonic and postnatal stages (Huber et al., 2002; Hunt et al., 2002; Josephson et al., 2001, 2002; Meier et al., 2003). However, the correlation of the developmental expression of Nogo and NgR with the ingrowth and maturation of hippocampal afferents is as yet unknown.

In the present study, we correlate the expression pattern of Nogo and NgR in the hippocampal formation with the development and maturation of hippocampal afferents. We also investigate the possible role of Nogo during embryonic hippocampal development. Our results show that Nogo fails to inhibit neurite outgrowth of E15 hippocampal neurons. Furthermore, we determine the cell types expressing Nogo and NgR in the hippocampus and examine whether neuronal Nogo and NgR are regulated in the adult by insults such as axotomy of the entorhino-hippocampal afferents or intraperitoneal kainic acid (KA) administration. We provide evidence that NgR expression is regulated by neuronal activity and is strongly altered after lesion. Lastly, we tested the regenerative potential of treatment with IN-1 antibodies after entorhino-hippocampal lesions in vitro, and showed that the blockage of NiG induces the regrowth of axotomized axons into the lesioned hippocampus.

Results

Developmental expression of Nogo and NgR mRNAs in the entorhino-hippocampal formation

We examined the spatial and temporal patterns of Nogo and NgR mRNAs in the entorhino-hippocampal formation by *in situ* hybridization (ISH) analyses (Fig. 1). The Nogo probe used recognized a 3' region shared by Nogo-A, -B, and -C and will be called 3'-Nogo. A probe recognizing a 3' region of NgR was also used. Digoxigenin-labeled sense probes produced no signal (not shown). 3'-Nogo mRNA was observed in the pyramidal layer of the hippocampus proper at E16 (Fig. 1A). There was an overall increase in the hybridization signal between E16 and P0, with pyramidal neurons displaying the highest labeling (not shown). Low labeling occurred in the prospective dentate gyrus as well as in the stratum lacunosum-moleculare. In contrast, the interphase radiatum-lacunosum-moleculare and the stratum radiatum contained a moderate number of 3'-Nogo-labeled cells (not shown). The distribution pattern of the 3'-Nogo mRNA expression from P5 upwards remained essentially the same as P0 (Fig. 1H). In addition to pyramidal and granule neurons, cells in the hilus of the dentate gyrus were also labeled, and a few cells in plexiform hippocampal layers (e.g., stratum lacunosum-moleculare) displayed moderate signals at P15 adult stages (Figs. 1H and J). 3'-Nogo mRNA was also observed in the entorhinal cortex with signal levels increasing from E16 to the adult stage (Figs. 1L, N, and P).

In contrast to Nogo, NgR mRNA expression signal was very low at E16 and increased at P0. 3'-NgR labeling was essentially in the pyramidal layer of the CA3 region (Figs. 1B–C). From P5 onwards, the pyramidal layer of the hippocampus proper displayed the highest signal levels, with the CA3 region being more intense than the CA1 (Figs. 1D, E, and I). In the dentate gyrus, the upper portion of the granule cell layer displayed high hybridization labeling at P5 (Fig. 1F). At P15, hybridization signals were present in the granule cells in the outer two-thirds of the granule cell layer (Fig. 1G). In the adult, granule cells were homogeneously labeled (Fig. 1I). In contrast to the hippocampus, the first low NgR mRNA signals in the entorhinal cortex were seen at P0; they then increased until the adult stages (Figs. 1K, M, and O).

Expression of Nogo-A and NgR during development and in the adult entorhino-hippocampal formation of the mouse

To determine the expression levels of Nogo-A and NgR during development, protein extracts from developing hippocampi were analyzed by Western blotting. Immunoblot analysis using the rabbit α -Nogo-A antibody detected a band of approximately 210–220 kDa (Fig. 2A). Nogo-A levels were found to increase from E16 to P0–P5 stages, after which they decreased until the adult stages (Fig. 2A). Immunoblot analysis using α -NgR antibody detected two bands of about 80–85 kDa in hippocampal protein extracts from P0 onwards (Fig. 2B). Levels of NgR protein were found to increase from P0 until P7 (Fig. 2B).

At E16 and P0, strong Nogo-A immunoreactivity occurred in pyramidal neurons of the hippocampus proper and to a lesser extent in dentate granule cells (Figs. 2C and D). At P0, immunocytochemical staining was intense in the strata radiatum and oriens of the hippocampus proper (Figs. 2D and E). In contrast, the upper part of the stratum lacunosum-moleculare and the molecular layer of the

dentate gyrus lacked Nogo-A immunoreactivity (Figs. 2D and E). Numerous immunopositive fibers were seen in the alveus as well as in the fimbria of the hippocampus at E16–P0 (Figs. 2C–E). From P0 to P15, the stratum lacunosum-moleculare gradually decreased the Nogo-A immunoreactivity while the stratum radiatum and the stratum oriens increase neuropil immunostaining (Figs. 2E–G). From P15 upwards, emergent trilaminar immunolabeling was observed in the molecular layer of the dentate gyrus, in which the inner third of the molecular layer was more immunopositive than the outer two-thirds (Figs. 2H–I). Nogo-A immunostaining was also distinguishable in cell bodies and processes of glial cells (most likely oligodendrocytes) in the white matter and in the hippocampal plexiform layers (Fig. 2L).

To analyze the pattern of labeling of Nogo and its mRNA in the adult, we processed horizontal sections of the hippocampal formation. We found a correlation between the distribution of Nogo-A-labeled elements and the topographic projection of hippocampal afferents in the hippocampus proper and dentate gyrus (Figs. 2J–K). 3'-Nogo mRNA and Nogo-A protein levels were higher in the lateral than in the medial entorhinal area (Figs. 2J–K), as observed in layer III cells of the lateral entorhinal cortex (Fig. 2J). Accordingly, high immunoreactivity was found in the stratum lacunosum-moleculare at the subiculum-CA1 border and in CA3 regions, which receive the innervation of the layer III of the lateral entorhinal cortex (Fig. 2K). In contrast, a defined region of the stratum lacunosum-moleculare of the CA1 region close to CA3, innervated by the layer III cells of the medial entorhinal area, lacked relevant Nogo-A immunostaining (Fig. 2K). The same patterns were found in the dentate gyrus, where the outer molecular layer displayed higher levels of Nogo-A than the medial portion, in correlation with the high 3'-Nogo/ α -Nogo-A labeling observed in layer II neurons of the lateral entorhinal area (Fig. 2K). For commissural–associational connections, the stratum radiatum of the CA3 region and the inner molecular layer of the dentate gyrus showed the highest Nogo-A immunolabeling with the stratum radiatum of the CA1 displaying low levels (Fig. 2K). This pattern of immunostaining matches those seen using antibodies against myelin proteins such as myelin basic protein (MBP) or MAG (not shown).

Nogo-A immunoreactivity was also found in principal and local-circuit neurons (Fig. 2L). Positive non-pyramidal cells (Parvalbumin- and Calbindin-positive) with stellate and pyramidal-like shapes were scattered in plexiform layers, the pyramidal and granule cell layers, and the hilus (Fig. 2L). In addition, few small (8 μ m main axis) multipolar cells in the cortical white matter and in the hippocampus and entorhinal cortex were also Nogo-A positive

(Fig. 2L). Double-labeling experiments revealed that these cells corresponded to mature myelinating oligodendrocytes because they co-expressed Nogo-A and MAG, but not NG2 (Figs. 2M–R).

Nogo-A does not inhibit embryonic hippocampal neuronal outgrowth

To address the possible roles of Nogo-A during hippocampal development we performed several *in vitro* assays (Fig. 3; supplementary data 1). To determine whether Nogo-A is inhibitory for embryonic hippocampal neurons we tested different substrates containing or not Nogo-A in a neurite outgrowth assay (Fournier et al., 2001). We first tested if substrates coated with Nogo-A are inhibitory for P4 Cerebellar granule neurons (CGNs) (Figs. 3A, C–F). Neurite length was measured and normalized to the untreated control for each experiment. As reported previously (Fournier et al., 2001), neurite length was clearly reduced in neurons growing over Nogo-A- or Nogo-B-containing substrates when compared with neurons growing over mock or untreated substrates (Fig. 3A). Parallel assays with E15 hippocampal neurons showed that substrates coated with Nogo-A failed to inhibit neurite outgrowth of cultured hippocampal neurons (Fig. 3B). Similar results were obtained for hippocampal neurons growing on Nogo-B- (Fig. 3B) or Nogo-66-treated substrates (not shown).

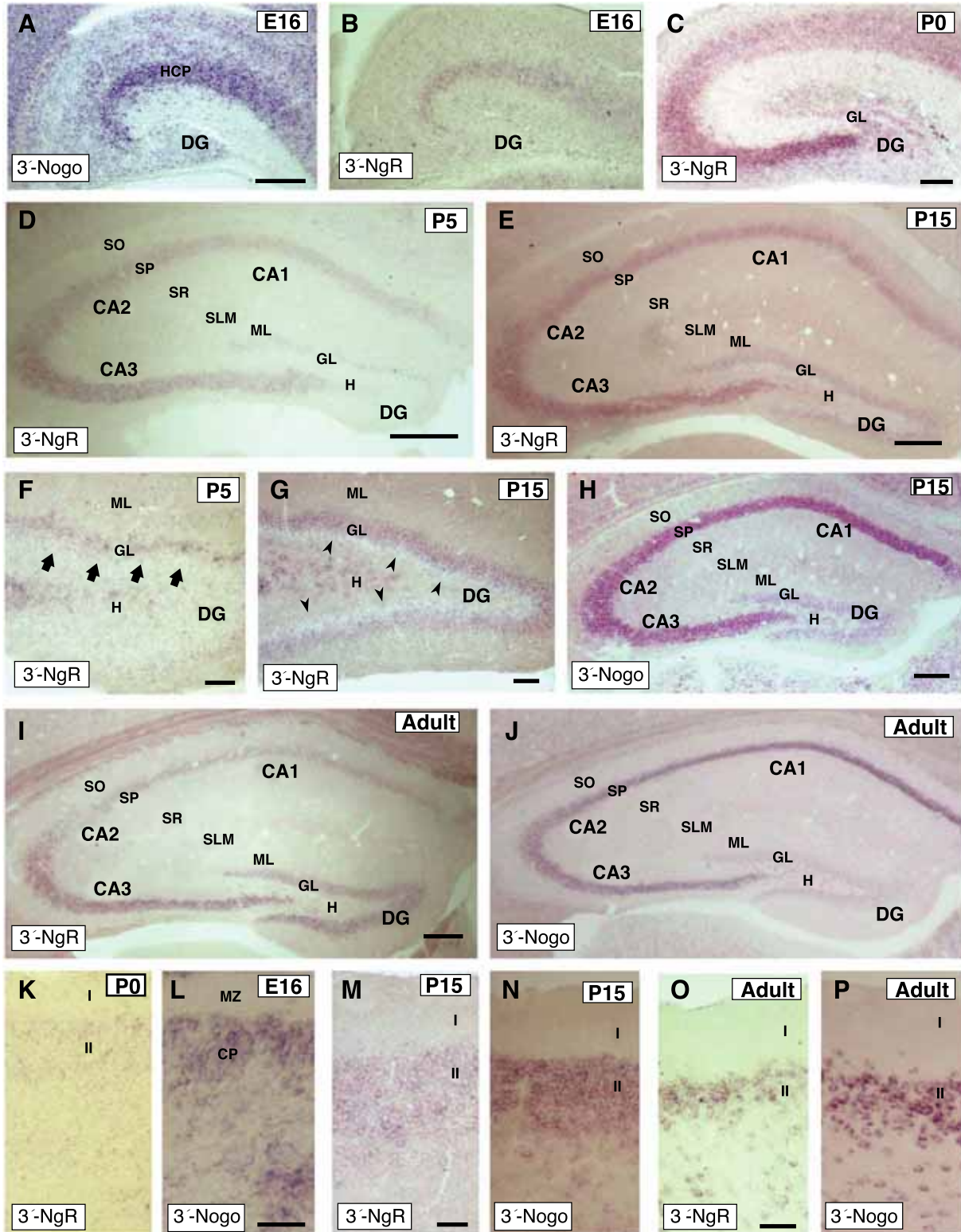
The inhibitory effects of Nogo-A, -B, and Nogo-66 on P4 CGNs were reverted by the addition of the antagonist peptide Nogo-40 (NEP1–40) fused to GST (Fig. 3A). The neurite length of neurons treated with GST was indistinguishable from the controls. Surprisingly, Nogo-A substrates displayed a higher inhibition for granule cell neurites than substrates containing only the Nogo-66 loop. Then, we tried to determine whether this increased inhibition could be due in part to the NiG domain. For that purpose, we treated the coverslips with IN-1 before the addition of the dissociated neurons. The neurite length of neurons growing over Nogo-A-coated substrates was increased, reaching control levels (not shown). However, a similar IN-1 treatment also produced a significant increase in the neurite length of neurons growing over mock or untreated substrates (not shown).

To further corroborate that hippocampal neurons are not inhibited by Nogo-A, we cultured E15 hippocampal explants over coated coverslips or collagen-coated transwells (Figs. 3K, M–P). In both cases, hippocampal neurite length was slightly reduced after 5 days *in vitro* (DIV) in explants growing over Nogo-66 and Nogo-A compared to controls (Fig. 3K). E15 hippocampal explants cultured on coverslips or collagen-I inserts without any treatment displayed a

Fig. 1. Developmental expression of 3'-Nogo and NgR mRNAs in the entorhino-hippocampal region of the mouse. Low power view of the hippocampal region illustrating the distribution of 3'-Nogo and NgR mRNAs. (A) At E16, 3'-Nogo mRNA-labeled cells appeared mainly in the pyramidal layer of the hippocampus. (B) At E16, 3'-NgR mRNA expression is barely detectable in the hippocampus. (C–E) From P0 to P15, 3'-NgR mRNA labeling was distributed at the pyramidal layer of the hippocampus proper, especially in the CA3 region. (F–G) Distribution of 3'-NgR mRNA-labelled cells in the dentate gyrus at P5 (F) and P15 (G). Note that mature granule cells in the suprapyramidal blade of the dentate gyrus at P5 (arrows in F) and in the upper portion of the granule cell layer at P15 (arrowheads in G) are labeled. In addition, increasing numbers of hilar cells are also labeled at P15 compared to P5. (H) At P15, 3'-Nogo mRNA is in the pyramidal layer of the hippocampus proper and, to a lesser extent, in the granule cell layer of the dentate gyrus. (I–J) Low power view of the hippocampal region illustrating the distribution of 3'-NgR (I) and 3'-Nogo (J) in the adult. Both genes are expressed mainly in the pyramidal layer and by hilar cells (I and J). Note that 3'-NgR mRNA signal levels are more intense in the pyramidal layer of the CA3 region and the CA2 region weak hybridization signals in the adult (I). (L, N, and P) Panoramic photomicrographs illustrating the distribution of 3'-Nogo mRNA in the upper layers of the lateral entorhinal cortex at E16 (L), P15 (N), and in the adult (P). 3'-Nogo mRNA signal levels can be seen in projecting neurons through perinatal development until adult stages. (I–K) Photomicrographs illustrating the distribution of 3'-NgR mRNA in the upper layers of the lateral entorhinal cortex at P0 (I), P15 (J), and in the adult (K). 3'-NgR mRNA signal levels were first seen in the entorhinal cortex at P0 with increasing signal levels until the adult. Scale bars: A = 200 μ m pertains to B; C–E = 200 μ m, F–G = 100 μ m; H = 200 μ m; I = 200 μ m pertains to J; K–L = 50 μ m, M = 50 μ m pertains to N; O = 100 μ m pertains to P. Abbreviations: CA1–3, hippocampal fields; DG, dentate gyrus; GL, granular layer; H, hilus; ML, molecular layer; SLM, stratum lacunosum-moleculare; SO, stratum oriens; SP, stratum pyramidale; SR, stratum radiatum; WM, white matter.

radial pattern of axonal outgrowth (Fig. 3M; (supplementary data 1)). This radial outgrowth was also observed in explants growing on substrates containing membrane fractions taken from mock cells (Fig. 3N). However, explants growing on Nogo-66- or Nogo-A-containing substrates displayed a moderate degree of axonal fas-

ciculation (Figs. 3O–P). This degree of fasciculation was scored and was significantly higher when substrates contained Nogo-A (Fig. 3L). To ascertain whether Nogo-A- or Nogo-66-induced effects can be attributed to failure of cells to attach over Nogo-containing substrates, we assessed the cell density of P4 CGNs and



hippocampal neurons shortly after plating (supplementary data 1). Cell counts demonstrated that adherent cell densities were similar in all treatments (supplementary data 1).

Regulation of 3'-Nogo and NgR mRNA expression after intraperitoneal kainic acid administration

In situ hybridization revealed a transient downregulation of both 3'-Nogo and NgR mRNA in the hippocampus after intraperitoneal administration of KA (Fig. 4). Twenty-four hours after KA administration, 3'-Nogo and NgR mRNA were strongly downregulated in dentate granule cells and hippocampal neurons, accompanied by a similar downregulation of NgR mRNA in hilar cells (Figs. 4A–B, D, G, and J). These mRNA levels were partially recovered 72 h after KA administration (Figs. 4C, F, and I). Northern blotting studies employing the same probes further corroborated this transient downregulation (supplementary data 3).

Regulation of 3'-Nogo and NgR mRNA expression in the hippocampus after unilateral entorhinal lesion

We aimed to analyze 3'-Nogo and NgR mRNA expression in the hippocampus after unilateral entorhinal lesion. Three days after lesion, a slight increase in 3'-Nogo mRNA signal levels was observed in the granule cell layer ipsilateral to the axotomy when compared to the contralateral dentate gyrus (Figs. 5A–B). This increase was no longer seen 7 days after lesion (Figs. 5C–D), and 3'-Nogo mRNA signal levels remained constant in both ipsi- and contralateral hippocampus proper (Figs. 5A–B). NgR mRNA levels were increased in the ipsilateral granule cell layer 24 h after lesion and were subsequently downregulated until 15 days postlesion (the longest time analyzed) (Figs. 5E–H). Thus, 15 days after axotomy, the NgR labeling of granule cells ipsilateral to the lesion was lower than the contralateral dentate gyrus (Figs. 5G–H). In contrast to granule cells, pyramidal neurons showed relatively constant signal levels in lesioned and intact hippocampi (Figs. 5E–H).

The regulation of Nogo and NgR in the lesioned hippocampus was corroborated by Western blotting using protein extracts from deafferented hippocampi (Fig. 5I). A densitometric analysis was performed with quantification of the 210–220-kDa Nogo-A and the 80–85-kDa NgR bands (Fig. 5J). A 25% increase in the amount of NgR protein was observed 24 h after lesion, followed by a decrease to 50–75% of the control levels at 7–15 days after lesion (Figs. 5I–J). In contrast, Nogo-A protein levels remained constant after lesion (Figs. 5I–J).

Nogo-A is transiently upregulated by reactive astrocytes in the denervated molecular layer of the fascia dentate after unilateral entorhinal lesion

Following axotomy of the perforant pathway, a slight upregulation of Nogo and α -Nogo-A was observed in cells around the lesion site (not shown). Three days after lesion, increased immunoreactivity for Nogo-A was found in the molecular layer of the ipsilateral dentate gyrus compared to the contralateral hippocampus (Figs. 6A–B). Nogo-A labeling was present in multipolar stellate cells with different intensity of immunoreactivity (Figs. 6C–D). We combined in situ hybridization and immunohistochemistry (ICC) for Nogo with the immunocytochemical detection of the astrocytic marker glial fibrillary acidic protein (GFAP). Sequential multiple channel fluorescence scanning was used for confocal analysis to avoid bleed through (cross talk). Most of the Nogo-A immunoreactive cells were not double-labeled with α -GFAP. However, a subset of cells was double-labeled with α -GFAP antibodies and both 3'-Nogo probe and Nogo-A antibody (Figs. 6E–H). This astrocytic co-localization of Nogo was transient because double-labeled cells were no longer seen 7 and 15 days after lesion, or the ipsilateral molecular layer partially recovered the trilaminar neuropil labeling of Nogo-A (not shown).

Treatment with IN-1 blocking antibodies enhances entorhinal axons regrow after EHP lesion in vitro

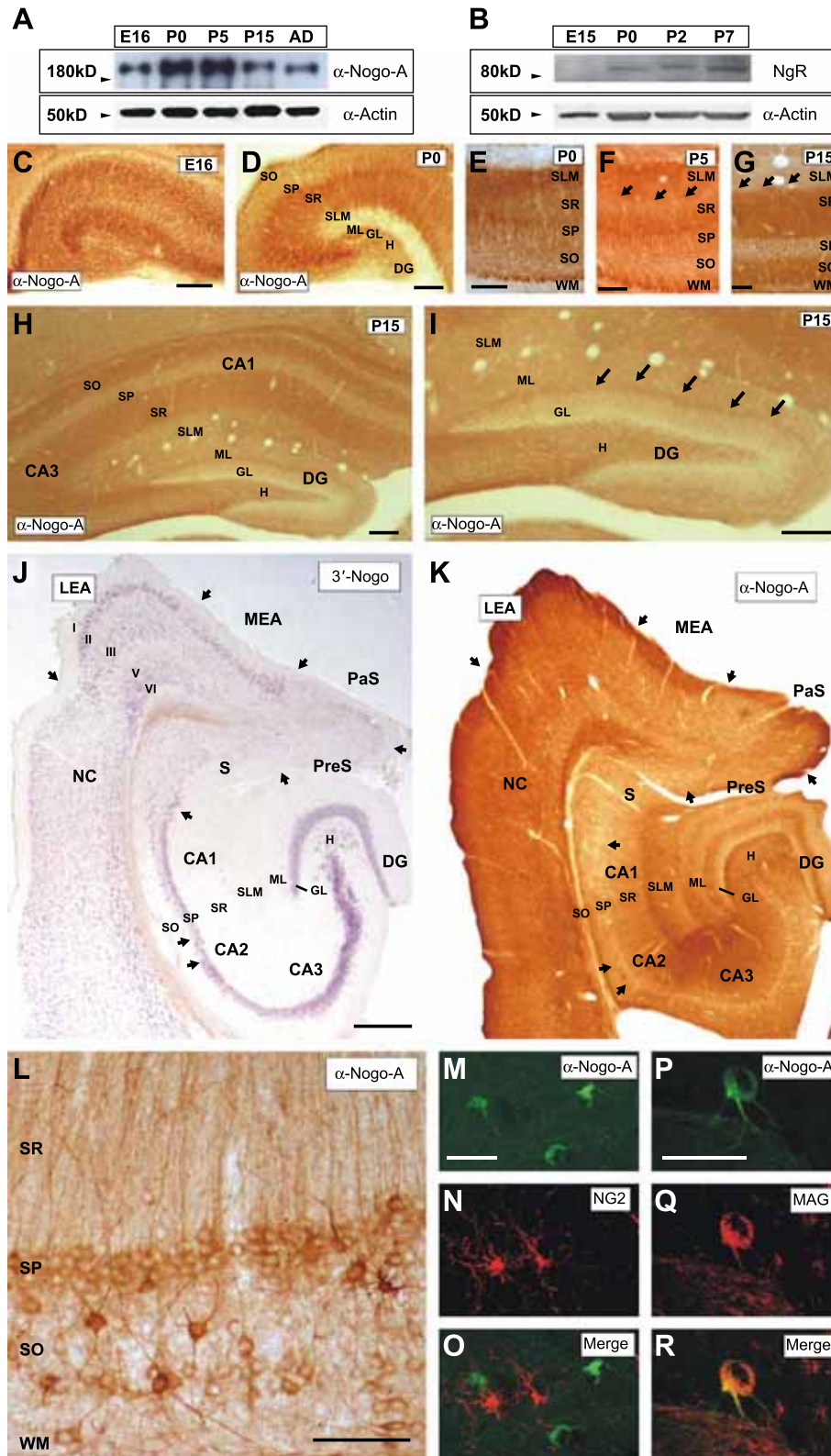
We investigated the potential of the Nogo-A-neutralizing antibody IN-1 to regenerate the perforant pathway after axotomy (Fig. 7). The axotomy was performed in entorhino-hippocampal organotypic cultures after 2 weeks in vitro. In these conditions, axonal regeneration of entorhinal axons does not occur. Western blotting techniques confirmed that Nogo-A is present in organotypic slice cultures after axotomy and throughout the experiments (Fig. 7A).

In control cultures, 7–10 days after lesion of the EHP, axotomized axons ended at the cut edge of the lesion, where no apparent cavitation was observed (not shown). In most control cultures, few entorhinal axons (4.6 ± 1.28 axons per section; mean \pm SD) sprouted within the lesioned hippocampus as ascertained after biocytin labeling (Figs. 7B–C, F). Treatment with IN-1 or IN-1 Fab antibodies increased the number of entorhinal axons growing in the hippocampus (6.72 ± 2.4 axons per section IN-1 treatment and 5.75 ± 2.11 IN-1 Fab treatment) (Figs. 7B, D, E, and G). In

Fig. 2. Developmental expression of Nogo-A and NgR, and topographical distribution of Nogo-A during development and in the adult entorhino-hippocampal formation of the mouse. (A–B) Immunoblot of Nogo-A, NgR, and α -actin in the developing hippocampus. Samples (50 μ g) from mice of the indicated ages were analyzed. The molecular weight standards are indicated in the left. (C–I) Low power view of the hippocampal region illustrating the distribution of Nogo-A-immunoreactive cells. (C–D) At E16 (C) and P0 (D), Nogo-A immunoreactivity appeared at the pyramidal layer of the hippocampus proper as well as in the stratum oriens and radiatum. Nogo-A immunoreactive fibers can also be seen running through the white matter. (E–G) Photomicrographs of the CA1 showing the pattern of Nogo-A immunostaining at P0 (F), P5 (G), and P15 (H). Nogo-A immunostaining decrease in the stratum lacunosum-moleculare between P0 and P15, whereas it increases in the stratum radiatum and oriens. Arrows pointing the interphase radiatum-lacunosum-moleculare. (H–I) Low power view of the hippocampal region illustrating the distribution of Nogo-A immunoreactivity at P15. Nogo-A protein is in the pyramidal layer of the hippocampus proper and, to a lesser extent, in the granule cell layer of the dentate gyrus (H). A conspicuous band of immunoreactivity is in the inner molecular layer of the dentate gyrus (arrows in I). (J–K) Panoramic distribution of 3'-Nogo mRNA and Nogo-A in the entorhino-hippocampal formation of the mouse. See text for details. Anatomical regions are indicated by arrows. (L) High-magnification photomicrographs to illustrate details of Nogo-A-immunoreactivity in the CA1 subiculum. Neurons showed multipolar shapes in the stratum oriens and pyramidal layer. Small immunoreactive cells with multipolar morphologies were also observed in the pyramidal layer. (M–R) Cellular localization of Nogo-A. Sections were processed for α -Nogo-A– α -NG2 (M–O) (using the hamster-raised anti-Nogo-A antibody) and α -Nogo-A– α -MAG (P–R) and examined by confocal microscopy. Note the colocalization of Nogo-A with MAG (R) but not with NG2 (O). Scale bars: C–D = 200 μ m; E–G = 100 μ m; H–I = 200 μ m; J = 100 μ m pertains to K; L = 50 μ m; M–R = 25 μ m. Abbreviations as in Fig. 1.

comparison, cultures treated with control IgM or IgG did not display significant differences in axonal growth from that seen in control untreated cultures (4.5 ± 0.96 axons per section IgM treatment and 4 ± 0.65 IgG) (Fig. 7B). In all the successful cases,

axons ending in growth cone-like structures were not restricted to the stratum lacunosum-moleculare and the dentate molecular layer, and innervated ectopic layers such as the hilus or the stratum radiatum (Figs. 7E and G).



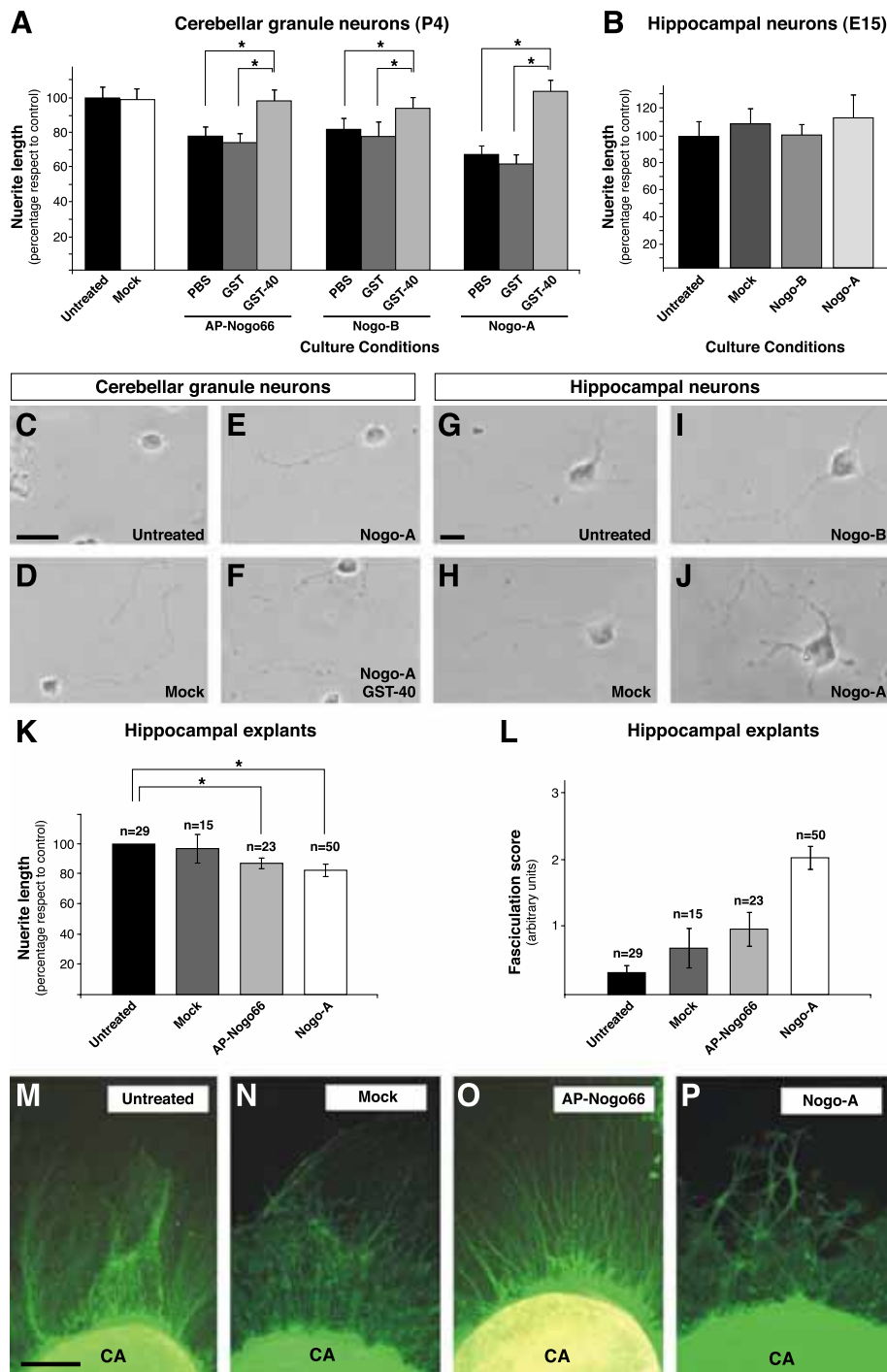


Fig. 3. Analysis of the effects of Nogo-A on hippocampal and cerebellar granule neurons. (A) Quantification of CGN's neurite length on different substrates. AP-Nogo-66, Nogo-B, and -A are inhibitory substrates for postnatal cerebellar granule cells. The inhibitory effects can be prevented by GST-40. Values are represented as mean \pm standard deviation. Asterisk indicates statistical differences between columns ($P < 0.05$; ANOVA test). (B) Quantification of hippocampal cells' neurite length on different substrates. There is no significant difference in the neurite length of cells growing on Nogo-A or -B with respect to control. Values are represented as mean \pm SD. (C–F) Examples of hippocampal neurons growing on different substrates. No difference is observed. (G–J) Examples of CGNs growing on different substrates. On Nogo-A, the neurites length is reduced compared with cells growing on Mock or untreated cultures. Addition of GST-40 to the culture medium prevents Nogo-A inhibition. (K) Quantification of hippocampal explants' neurite length on different substrates. Nogo-A and Nogo-66 loop are inhibitory substrates for embryonic hippocampal explants after 5 days in vitro. Values are expressed as mean \pm SD. (L) Quantification of the axonal fasciculation of hippocampal explants on different substrates (see text for details). Values are represented as mean \pm SD. (M–P) Low-power view of hippocampal explants growing on different substrates. Note the increased fasciculation in explant exposed to Nogo-A (P). Scale bar: C–F = 20 μ m, G–J = 10 μ m; M–P = 100 μ m.

Discussion

A recent study by Meier et al. (2003) described the expression of Nogo and NgR mRNA during the postnatal development of the entorhino-hippocampal formation of the rat and after electrolytic entorhinal lesions by using film autoradiography and densitometric analysis. The present study using digoxigenin-labeled probes and immunocytochemical methods is not only consistent with some of the results of that study, but also extends the observations during the embryonic and postnatal development. In addition, the cellular expression of Nogo-A is analyzed and its putative roles in the outgrowth of embryonic hippocampal axons during development and in limiting axonal regeneration in lesioned organotypic cultures have been examined.

Nogo-A and NgR are expressed by pyramidal and non-pyramidal neurons in the hippocampal formation of the mouse

Although the presence of 3'-Nogo mRNA and Nogo-A protein in neurons and oligodendrocytes in the adult cerebral cortex has been reported (Chen et al., 2000; GrandPre et al., 2000; Jin et al., 2003; Josephson et al., 2001), Taketomi et al. (2002) and more recently Wang et al. (2002) showed exclusive expression of Nogo-A by mature oligodendrocytes. However, Wang et al. (2002), Huber et al. (2002), and the present study report neuropil staining in the hippocampus. Differences in the Nogo-A protein domain recognized by the antibodies and in the immunocytochemical methods employed in these studies are likely to be responsible for such discrepancies. The rabbit antibody α -Nogo-A used recognizes a fragment of the N-terminus of Nogo-A not present in

Nogo-B or -C (Liu et al., 2002). In our experience, the immunolocalization of the neuronal Nogo-A decreases with increasing fixation and strong permeabilization procedures (M. Schwab, unpublished observations), which could explain these differences.

In agreement with Huber et al. (2002), the present paper reports Nogo-A expression by pyramidal neurons and hippocampal interneurons in the hilus of the fascia dentate. Our in situ hybridization study is also consistent with earlier studies describing the expression of NgR by principal and local circuit neurons in the hippocampal formation of adult mice using autoradiographic in situ hybridization (Hunt et al., 2002; Josephson et al., 2001, 2002; Meier et al., 2003) or protein immunolocalization (Wang et al., 2002). Unfortunately, the primary antibody against NgR did not detect it in brain sections and only detects it in Western blotting techniques (Domeniconi et al., 2002). Thus, specific primary antibodies to several epitopes of the NgR molecule would be needed to compare and corroborate the distribution pattern of NgR observed by mRNA in situ hybridization with that of the Nogo isoforms.

Nogo-A does not inhibit embryonic hippocampal neurons outgrowth in vitro

Our study demonstrates that Nogo isoforms, Nogo-A in particular, are widely expressed by neurons in the hippocampus during development. In contrast, NgR levels are hardly significant in the hippocampus before postnatal stages (P0–P5). In this situation, the possibility that Nogo-A is a neurite outgrowth inhibitor seems unlikely. Our in vitro assays demonstrated that E15-dissociated hippocampal neurons are not inhibited by substrate-bound Nogo-66, Nogo-B, or full-length Nogo-A, in contrast to P4 cerebellar

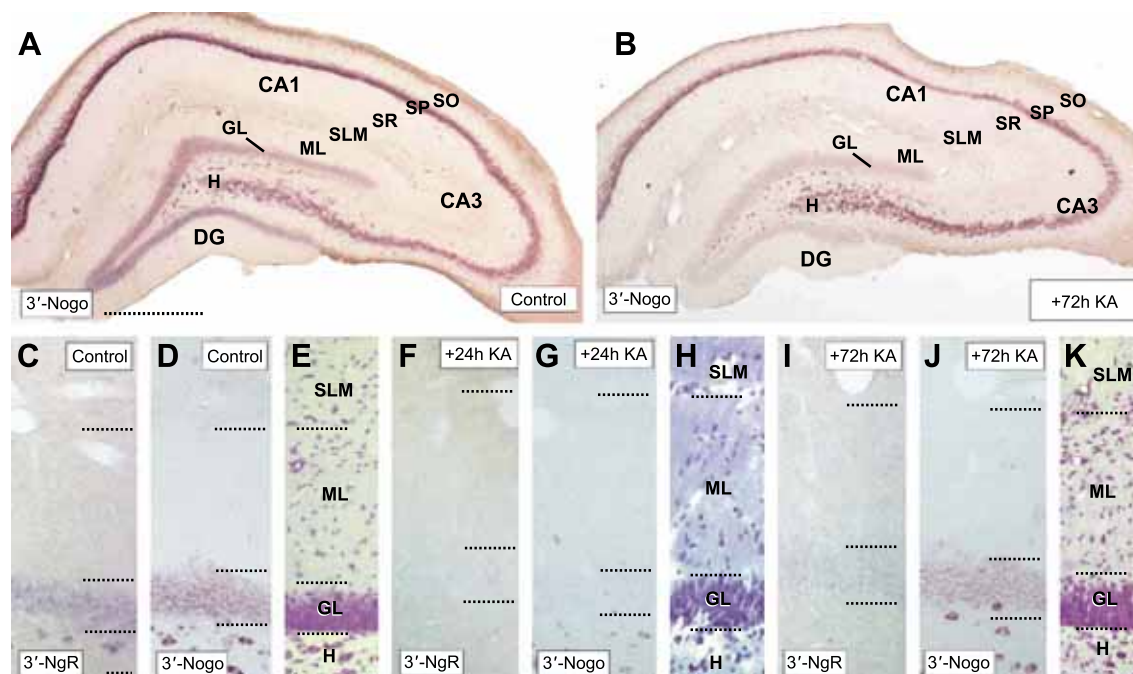


Fig. 4. 3'-Nogo and 3'-NgR mRNA expression pattern in the hippocampus after kainic acid administration. (A–B) Low power photomicrograph of the hippocampus illustrating the distribution of 3'-NgR mRNA in control (A) and 72 h after kainic acid administration (B). Note the overall decrease in 3'-Nogo expression in the pyramidal layer of the hippocampus and especially in the granule cell layer of the dentate gyrus 72 h after lesion. (C–K) Photomicrographs illustrating the time course of 3'-Nogo and 3'-NgR mRNA changes in the dentate gyrus 24 (F–H) and 72 h (I–K) after ip kainic acid injection compared to controls (C–E). Strong downregulation of 3'-Nogo and 3'-NgR mRNAs in the granule cell layer and in the hilus was detectable after 24 h (F and G) followed by partial recovery at 72 h (I and J). Scale bar: A = 1000 μ m pertains to B; C–K = 50 μ m. Abbreviations as in Fig. 1.

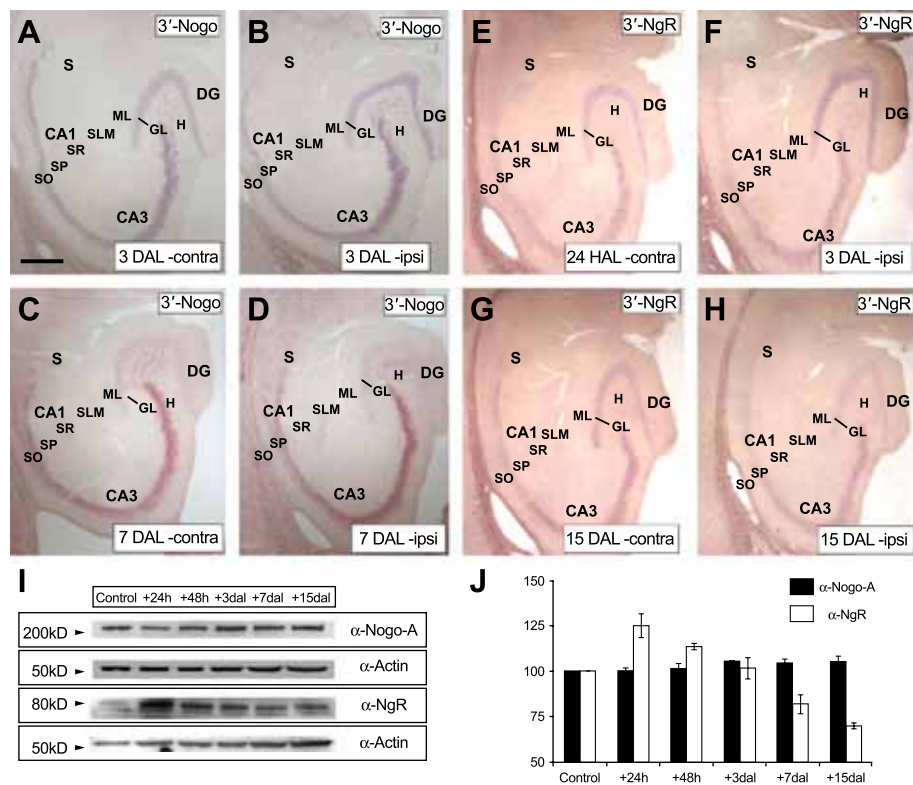


Fig. 5. Pattern of 3'-Nogo and 3'-NgR mRNA expression and protein in the hippocampus after unilateral entorhinal lesion. (A–D) Low-power view of the hippocampus showing the hybridization pattern of the 3'-Nogo mRNA 3 (A–B) and 7 (C–D) days after EHP axotomy. A slight increase in 3'-Nogo hybridization labeling was observed in the granule cell layer ipsilateral to the lesion (B) compared to the contralateral (A) 3 days postlesion. (E–H) Low-power view of the hippocampus showing the hybridization pattern of the 3'-NgR mRNA 3 (E–F) and 15 (G–H) days after EHP axotomy. A transient increase in 3'-NgR mRNA signal levels was observed in the granule cell layer ipsilateral to the lesion 24 h after lesion (F) with decreasing levels 15 days later (H). In contrast, 3'-NgR mRNA labeling remained constant in the contralateral hippocampus at these stages (E and G). (I–J) Immunoblot of Nogo-A and NgR protein levels and quantification in protein extract taken from lesioned hippocampus after several postlesion times. Quantitative data are expressed as the percentage of the mean of the ratio of Nogo-A or NgR protein of the optical density to α -actin with respect to controls. Error bars correspond to the standard deviation of the mean. Scale bar: A = 100 μ m pertains to B–H. Abbreviations as in Fig. 1.

granule cells. CGN's responsiveness to Nogo-66 loop has been reported previously (Fournier et al., 2001), and it is in accordance with their high expression of NgR. However, E15 hippocampal neurons express very low levels of NgR mRNA, and NgR protein is not detected until postnatal stages (Trifunovski et al., 2003; present study). These data, together with our *in vitro* assay, indicate that Nogo-66 and its receptor do not interact during hippocampal development, and that Nogo-A expressed in the embryonic hippocampal neurons may play other roles during development.

We aimed to determine whether NiG was responsible, at least in part, for the inhibition of CGNs, and so we treated the cultures with IN-1 in the substrate or in the culture medium. IN-1 clearly increased the neurite length of CGNs growing on Nogo-A containing substrates, reaching the control outgrowth. However, controls indicated that IN-1 also increased the neurite length of neurons growing on mock or untreated substrates. This effect might be due to the direct interaction between IN-1 and the neuronal Nogo-A, which has been proposed to be enough to produce axonal sprouting (Buffo et al., 2000).

In a second *in vitro* assay, E15 hippocampal explants were cultured on Nogo-A-containing substrates for 5 days. During the culture period, the explants are expected to mature and, after 4 days *in vitro*, to start expressing significant levels of NgR (as detected at

P0 *in vivo* by ISH and Western blotting). Nogo-66 and Nogo-A induced a slight but significant decrease in neurite length, and Nogo-A also increased axonal fasciculation, which cannot be associated with reduced adhesion to the inhibitory substrate because hippocampal and granule cells adhere similarly in controls (untreated and mock-coated) and Nogo-containing substrate. Thus, the increased axonal fasciculation observed in hippocampal explants growing over Nogo-A is not attributable to changes in the adhesive properties of the substrate, but rather a specific effect of Nogo-A, as also suggested by others (Oertle et al., 2003b).

Involvement of Nogo-A and its receptor in the development and maturation of hippocampal connections

NgR protein cannot be detected in the hippocampus before postnatal stages (P0–P5) by Western blotting. As no receptor other than NgR has been suggested for Nogo, it might have a role other than that associated with NgR during the early stages of hippocampal ontogeny (see Hunt et al., 2003 for review). In addition, our outgrowth assay suggests that it may contribute to axon growth and fasciculation. Taken together, our results suggest that molecules other than Nogo–NgR are likely to regulate the ingrowth of entorhinal fibers into the hippocampus (e.g., see Chedotal et al., 1998; Pozas et al., 2001; Skutella and Nitsch, 2001).

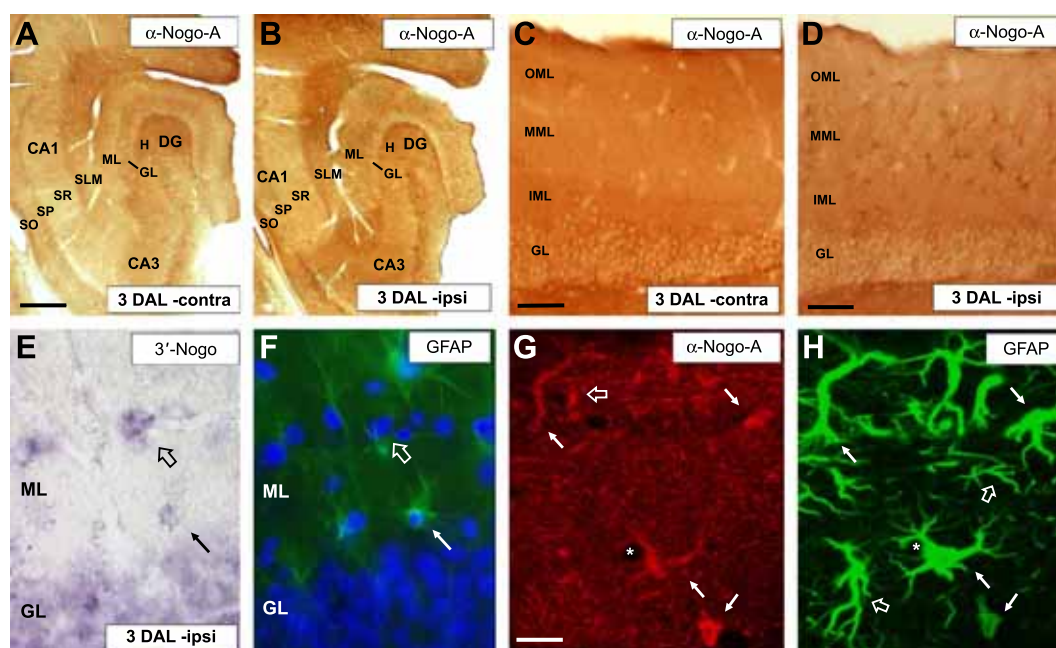


Fig. 6. Upregulation of Nogo-A and 3'-Nogo mRNA by reactive astrocytes after axotomy of the EHP. (A–B) Low-power views of ipsi- and contralateral hippocampus immunoreacted for Nogo-A 3 days after unilateral EHP axotomy. There is an overall increase of immunoreactivity in the lesioned hippocampus accompanied by a loss of the laminar neuropil staining in the dentate molecular layer (B). (C–D) High magnification of the dentate gyrus molecular layer shown in A–B. Note the presence of Nogo-A-immunoreactive glial cells in the denervated molecular layer ipsilateral to the lesion (D). (E–H) Double labeling of 3'-Nogo mRNA (E) or α -Nogo-A (G) with GFAP (F, H). Arrows point to double-labeled cells and the open arrows to labeled non-double-labeled cells. Scale bar: A = 100 μ m pertains to B; C–D = 50 μ m; G = 10 μ m pertains to E–H. Abbreviations as in Fig. 1.

NgR is absent or barely expressed in the developing granular and subgranular zone with proliferating and postmitotic cells. This raises whether NgR is downregulated in proliferating or young postmitotic neurons to facilitate their migration in Nogo-rich areas (e.g., granule cell layer). Another explanation is that this regulation of NgR gene may reflect the fact that NgR is expressed in postmitotic neurons when migration is completed and neurite extension, branch formation, synaptogenesis, and neural activity begin (Ben-Ari et al., 1994; Cherubini et al., 1991).

Nogo and NgR are involved in preventing axon regeneration after axotomy of the EHP in vitro

Axotomized adult entorhinal axons (NgR-positive) regrow into young hippocampal slices (Nogo-A positive) in a layer-specific fashion (Del Rio et al., 2002). Our *in vitro* results show that IN-1 antibodies (culture supernatant and affinity purified IN-1 antibody) induce axonal sprouting and regeneration of axotomized entorhinal axons, but fail to promote lamina-specific entorhino-hippocampal regeneration. Similar administration with IN-1 hybridoma cell culture or the IN-1 Fab *in vivo* has been used to promote long distance axonal regeneration in lesioned corticospinal and optic tracts (e.g. Bregman et al., 1995; Brosamle et al., 2000; Schnell and Schwab, 1990). Thus, the specific inhibition of NiG after lesion may not be enough to induce layer-specific regeneration after axotomy of the EHP. On the other hand, our entorhino-hippocampal culture may have been too inhibitory to reveal stronger effects of the IN-1 treatment and molecules other than Nogo may play a more significant role in inhibiting regeneration of entorhinal axons. In this line, the *in vitro* model displays an injury-like stage during cultivation, with high percentages of reactive glial cells (microglial

as well as astroglial or oligodendroglial cells) (Del Rio et al., 1991; Hailer et al., 1996) and high presence of inhibitory molecules such as sulphated proteoglycans and other myelin inhibitory proteins (Solé et al., in preparation). Further studies are required to ascertain the participation of other molecules in the failure of layer-specific regeneration observed after adult entorhino-hippocampal axotomy. However, our IN-1 blocking experiments indicate that axons of lesioned cortical neurons can regrow after treatment with IN-1.

Are Nogo-A and its receptor involved in the postlesional changes in the hippocampus after axotomy?

Within the first days postlesion, Nogo-A, but not NgR, is upregulated by reactive astrocytes in the outer two-thirds of the molecular layer of the dentate gyrus ipsilateral to the lesion. To our knowledge, the expression of Nogo-A by resting or reactive astrocytes has not been described during neural development or in the adult, unlike other Nogo isoforms such as Nogo-C, which has been described in non-reactive astrocytes in the cerebellum (Woodhams et al., 2001). Nogo-A is also upregulated in a highly reactive glial-derived cell line, the C6 glioblastoma (supplementary data 2; see also Michel et al., 1999). Previous reports have indicated that reactive astrocytes in the mature brain overexpress proteins characteristic of immaturity shortly after lesion, including cytoskeletal elements, adhesion molecules, and extracellular matrix proteins (Horner and Gage, 2000). Some of these molecules (e.g., proteoglycans) influence the proliferation and migration of reactive astroglial cells in the hippocampus (e.g., Haas et al., 1999). Thus, the early expression of Nogo-A in reactive astroglia after lesion could play a role in regulating the proliferation or the migration of reactive astroglia in conjunction with other upregulated gene products.

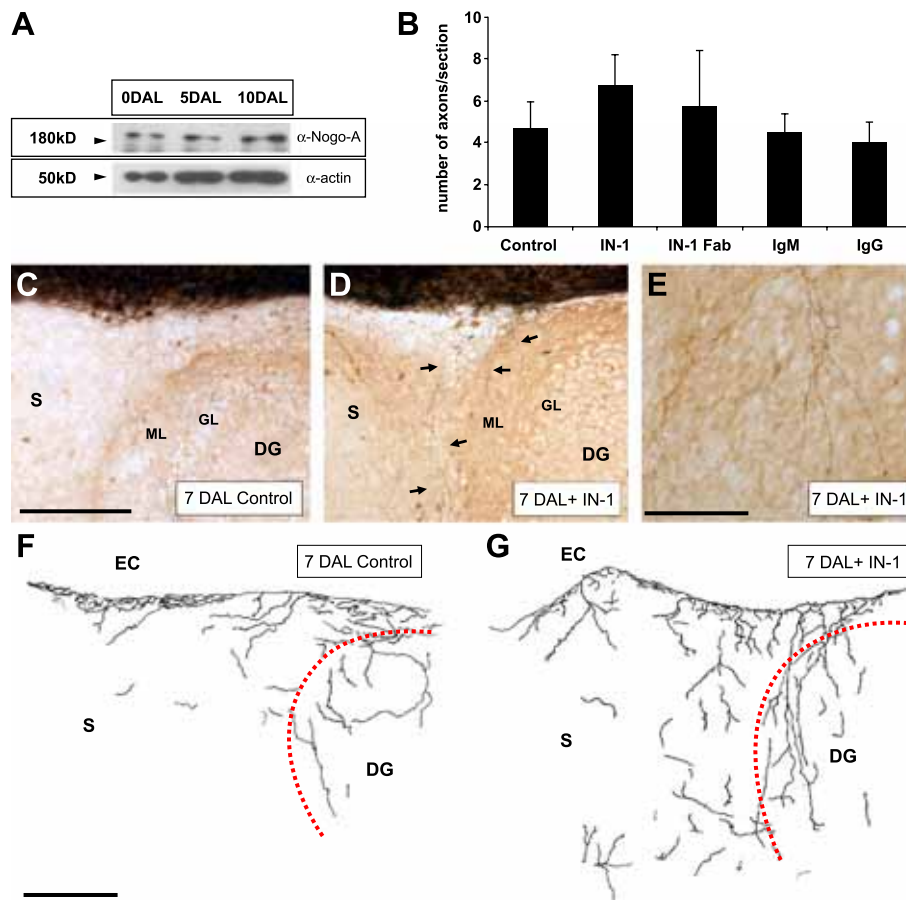


Fig. 7. Treatment with IN-1 or IN-1 Fab monoclonal antibodies promotes axonal sprouting in axotomized organotypic cultures. (A) Immunoblot of Nogo-A and α -actin in control unlesioned entorhino-hippocampal co-cultures and 5 and 10 days after axotomy of the EHP. Samples (20 μ g) at each case were analyzed. The molecular weight standards are indicated in the left. (B) The sprouting density of biocytin-labeled fibers in the deafferented hippocampus is illustrated after treatment with the IN-1 supernatant, the IN-1-Fab monoclonal antibody, control mouse IgM and goat IgGs. Means \pm SEM are reported in each case. (C–D) Biocytin-labeled fibers visualized in horizontal sections in control (C) and IN-1 (D–E)-treated cultures after biocytin tracing 7 days postlesion. IN-1-treated cultures showed increased axonal sprouting after treatment (arrows in D) compared to controls (C). (F–G) Camera lucida drawings of control and IN-1-treated cultures. The hippocampal fissure is indicated by the red dashed line. Most regenerating fibers do not show a layer-specific pattern of regeneration and innervate layers other than the stratum lacunosum-moleculare. Scale bar: C = 50 μ m pertains to D; E = 25 μ m; F = 50 μ m pertains to G. Abbreviations as in Fig. 1.

In addition, the downregulation of NgR mRNA observed in granule and hilar cells 15 days after lesion could play a role in the delayed translaminal sprouting of commissural–associational fibers after entorhinal cortex lesion (Deller and Frotscher, 1997). It is interesting to note that the adult blockage of Nogo-A by the IN-1 neutralizing antibody allows axonal sprouting and the formation of new synaptic contacts by intact neurons (Zagrebelsky et al., 1998), which indicates a role for Nogo-A in the stabilization of synaptic contacts (Fournier and Strittmatter, 2001; He et al., 2003).

Are Nogo-A and its receptor regulated in the hippocampus by neuronal activity?

Nogo-A and its receptor are expressed in cortical brain regions that are strongly involved in neuronal plasticity (Hunt et al., 2003). Here we have reported by in situ hybridization and Northern blotting techniques that Nogo and NgR gene activity are transiently downregulated in the hippocampus by granule cells after kainic acid administration. There is some disparity between our findings and previous studies. Josephson et al. (2001) reported no regulation

of Nogo mRNA in the hippocampal formation of kainate-treated rats, although Josephson et al. (2003) found downregulation in response to kainate or wheel-running. Meier et al. (2003) showed no change in Nogo mRNA at 24 h but upregulation by 5 days after kainic acid administration. These differences may be due to technical considerations, such as the concentration of kainic acid or differences in the antisense probes or the in situ hybridization procedure. Neuronal cell death is unlikely to be responsible for the different findings because pyknotic cells were not observed in the granule cell layer in parallel sections stained with cresyl violet (Figs. 4E, H, and K). The mossy fiber pathway in the dentate gyrus undergoes fast sprouting and synaptic reorganization in response to kainic acid (Ben-Ari and Represa, 1990). Regulation of 3'-Nogo and NgR gene expression after KA treatment by granule cells suggests that their regulation could contribute to the synaptic reorganization observed in mossy fibers after injury of the mature brain. This is also consistent with the fast reactive sprouting (48 h after injection of IN-1 antibody) and active synaptogenesis observed in other CNS neurons when IN-1 antibodies are used to block Nogo-A-specific domain activity (Buffo et al., 2000).

Experimental methods

All procedures were carried out in accordance with the guidelines approved by the Spanish Ministry of Science and Technology, following European standards.

Antibodies and peptides

Rabbit polyclonal (diluted 1:2000, Dakopatts, Glostrup, Denmark) and mouse monoclonal (diluted 1:500, Roche Applied Science, Basel, Switzerland) antibodies against glial fibrillary acidic protein (GFAP) were used to label astrocytes. NG2 antibody (diluted 1:500, Chemicon, Temecula, USA) was used to label oligodendrocyte precursor cells. Mouse monoclonal antibody against MAG (diluted 1:1000, Chemicon) was used to detect mature oligodendrocytes. Several antibodies against Nogo-A were used: a rabbit-raised polyclonal antibody against the 223–399 aa of human Nogo-A (GenBank accession no. KIAA0886, diluted 1:1000, Liu et al., 2002) (unless specified this was the anti-Nogo-A antibody used for ICC and Western blotting, and will be designated as α -Nogo-A), a hamster-raised monoclonal antibody against an internal region of Nogo-A (cDNA clone #4-1D9 Δ C from GenBank Accession No. AB0732672, diluted 1:20, kindly provided by T. Hirata, Tozaki et al., 2002) (this antibody was used for double immunocytochemical techniques), and a goat polyclonal antibody against Nogo, N-18 (which recognizes Nogo-A–B, diluted 1:250) purchased from Santa Cruz Biotechnology (Santa Cruz, USA) (used for Western blotting). A goat polyclonal antibody against NgR (N-20, diluted 1:250; Santa Cruz Biotechnology) was also used. Monoclonal antibodies against α -actin (diluted 1:10,000; Chemicon) and β III-tubulin isoform (TUBJ-1, diluted 1:3000; Babco, Richmond, USA) were used to identify the cytoskeletal protein.

To generate GST-Nogo40, the DNA fragment corresponding to the first 40 amino acids of Nogo-66 was cloned into *Eco*RI and *Xho*I sites of the pGex4T-1 vector (Amersham Biosciences, Buckinghamshire, UK). The primers used were forward: 5' CGG GAA TTC AGG ATA TAC AAG GGT GTG ATC CAA GC 3' and reverse: 5' C CCG CTC GAG TCA AGA ATT ACT GTA CTT CTG AAC C 3'. Fusion protein expression in DH5- α *Escherichia coli* strain was induced by IPTG (0.1 mM, 37°C for 3 h) and the GST-Nogo40 fusion protein was purified using glutathione-agarose affinity purification.

Animals and tissue collection for developmental studies

A total of 15 pregnant OF1 mice (Iffa Credo, Lyon, France) were used. Animals were killed at the following stages: E16, P0, P5, P15, and adult. Three to six animals (30 in total) from at least two different litters were processed for immunohistochemistry (ICC) or in situ hybridization (ISH) at each of the stages analyzed. Mutant mice carrying a tau-tagged green fluorescent protein (Tau-GFP) under the actin promoter were used for in vitro assays (Pratt et al., 2000).

Fetuses were removed by cesarean section after deep anesthesia of the mother with chloral hydrate (3.5 mg/kg ip injection). Postnatal mice were anesthetized with ether unless otherwise specified. After preliminary experiments with various fixative solutions, all animals were transcardially perfused with 2% (ICC) or 4% (ISH) paraformaldehyde dissolved in phosphate buffer 0.12 M (pH 7.2–7.4). After perfusion, the brains were

removed from the skull and postfixed in the same solution for a further 12 h (ICC) or 2 days (ISH), cryoprotected in 30% sucrose, and coronally sectioned on a freezing microtome (30 μ m thick). Free-floating sections were further processed for ICC or ISH.

In vitro experiments

Nogo-A-containing membranes were prepared according to Jin et al. (2003). COS1 cells at 70–80% confluence were transfected with Nogo-A (pCAGGS-HA-RTN-xL), Mock (pCAGGS-HA), and Nogo-B (pCMV-ASY) using LipofectAMINE-Plus reagents (GIBCO Life Technologies, Merelbeke, Belgium). Forty-eight hours after transfection, cells were scraped into 0.1 M phosphate-buffered saline (PBS), centrifuged, and homogenized with a 1.5 ml tube Eppendorf pestle (Sigma, Poole, Dorset, UK) for 1 min in homogenization buffer (0.32 M sucrose, 5 mM HEPES-NaOH (pH 7.4), 0.2 mM CaCl₂ and 1x protease inhibitors, Sigma). The homogenate was centrifuged at 1000 \times g for 10 min at 4°C to discard nuclei. The supernatant was further centrifuged at 9800 \times g for 20 min to obtain a membrane-enriched pellet and a cytosolic supernatant. After resuspension, the membrane concentration was adjusted to contain about 100–200 μ g protein/ml (final volume: 100–150 μ l; Walter et al., 1987). Aliquots (5 μ l) of the membrane fractions were boiled in Laemmli sample buffer and the presence of Nogo-A in these fractions was further confirmed by Western blot using ECL-plus peroxidase Western kit (Amersham Biosciences). To obtain AP-Nogo-66, COS1 cells were transfected with the vector pAPtag-5-Nogo-66 and cultured in OPTIMEM medium. After 48 h, the supernatant containing AP-Nogo-66 was concentrated 10-fold using Amicon Ultra-4 centrifugal filter devices 30,000 NMWL (Millipore, Bedford, MA, USA).

Glass coverslips were coated essentially as described (Fournier et al., 2001). Briefly, coverslips were precoated with poly-L-ornithine 0.1 mg/ml dissolved in PBS and washed. Then, coverslips were incubated with 15 μ l of PBS containing membrane extract from Nogo-A, Nogo-B, and Mock-transfected COS cells, PBS alone (untreated control), or concentrated supernatant containing AP-Nogo-66, and allowed to dry. After washing, coverslips were coated with poly-L-lysine, dried, and washed. Some of the coated coverslips were incubated with IN-1 (hybridoma supernatant) at 37°C for 30 min and then washed in PBS.

Cerebellar granule neurons (CGNs) from postnatal day 4 (P4) mouse pups were dissociated by combined trypsinization as described previously (Niederost et al., 2002). Cells were planted in 24-well tissue culture dishes (Nunc, Roskilde, Denmark) on coated coverslips and grown for 36 h in DMEM medium supplemented with N2 and B27. Where indicated, the antagonist fusion peptide GST-40 (at a concentration equivalent to 1 μ M of NEP1–40 (Fournier et al., 2002)), or GST, was added to the culture medium. After culture, cells were fixed with 2% paraformaldehyde in PBS 0.1 M. Neurite length was assessed in a phase contrast inverted microscope using a 40 \times objective and a micrometric eyepiece. Hippocampal cells from embryonic day 15 (E15) mouse pups were dissociated as described for CGNs, and a similar neurite outgrowth assay was performed.

In a subsequent experiment, hippocampal explants obtained from tau-GFP mice were cultured in 24-well collagen-I coated inserts (0.45 μ \varnothing ; Biocoat cell environment, Becton Dickinson,

Bedford, USA) previously treated with membrane fractions (25 μ l/insert, 25–50 μ g total protein) for 2 h at 37°C, or in 10 mm \varnothing glass coverslips coated as above. Explants were cultured at 37°C in 5% CO₂ with a relative humidity of 95% for 5 days. The presence of Nogo-A in the coated insert after 5 days in culture was confirmed by sectioning a small portion of the transwell membrane and performing Western blotting. Cultures were photodocumented in a fluorescence inverted microscope (Leica). The overall extent of hippocampal axons, defined as the distance between the border of the explants and their distal tips, was measured with an ocular micrometer. Fasciculation scores were assigned as follows: score 0 = explants growing in a radial pattern without bundles of neurites; score 1 = bundles of neurites in less than 20% of the explant surface; score 2 = fasciculation of half of the neurites' length with some radial zones; score 3 = bundles of neurites around the whole explant, few processes are not fasciculated; score 4 = the whole explant is fasciculated.

Surgical procedures and sample collection

Adult mice ($n = 43$, 3 months old) were subjected to knife-lesioning of the perforant pathway by using a wire-knife (Kopf instruments, Consultants GmbH, Düsseldorf, Germany) essentially as described by Jensen et al. (1997). Briefly, animals were placed in a stereotaxic apparatus after pentobarbital anesthesia (50 mg/kg, bw) and drilled at 1 mm posterior and 3 mm lateral from lambda. A closed wire-knife was then inserted at an angle of 15° anterior and 15° lateral. Four millimeters ventral to dura the wire was unfolded (1.5 mm) and the perforant pathway was sectioned by retracting the knife 3 mm. After different survival times (24 h, 48 h, 3, 7, 15 days), some lesioned ($n = 10$) and sham-operated ($n = 2$) mice were anesthetized and their brains were dissected out. After washing in cold PBS, the hippocampi ipsilateral and contralateral to the lesion were dissected out and homogenized on ice in homogenization buffer containing 150 mM NaCl, 1 mM EDTA, 10% glycerol, 1% Triton X-100, and 1 \times protease inhibitor cocktail. After measurement, protein aliquots containing 30–50 μ g/ml were stored at –80°C until use. The remaining mice (33 lesioned and 10 sham operated) were anesthetized and transcardially perfused with 4% paraformaldehyde in 0.1 phosphate buffer pH 7.3, and their brains were cryoprotected and sectioned (30 μ m thick).

Kainic acid administration

Kainic acid (KA) (12–15 mg/kg bw) was administered ip in six adult (250 g bw) Sprague–Dawley rats (Calbet et al., 1999; Przewlocki et al., 1995). Animals were perfusion fixed with 4% paraformaldehyde dissolved in 0.1 M phosphate buffer (pH 7.3) 24 and 72 h after the KA injections (three animals each case). After fixation, animals injected with saline (three animals) or KA were processed for in situ hybridization using 3'-Nogo and 3'-NgR antisense probes (see below).

Northern-blot analysis

For Northern analysis, 10 μ g of total RNA extracted from the neocortex and hippocampus was run per lane through a formaldehyde gel electrophoresis according to Sambrook et al. (1989) (section 7.43–7.45) and transferred to a nitrocellulose membrane

(Schleicher and Schuell, Dassel, Germany) overnight using 20 \times standard saline citrate (SSC). The filter was probed with a random-primed (GIBCO) α -³²P-ATP-labelled probe corresponding to Nogo, Nogo receptor, and GAPDH. Hybridization was performed overnight in 6 \times SSC, 50% formamide, 5 \times Denhardt's, 1% SDS, and 100 μ g/ml denatured herring sperm DNA at 42°C with a minimum of 10⁶ cpm of labeled probe per milliliter and a prehybridization period of 4 h with the same solution without labeled probe. The blot was washed with 1 \times SSC, 1% SDS for 1 h at 42°C; 0.5 \times SSC, 0.1% SDS for 1 h at 45°C; 0.2 \times SSC, 0.1% SDS for 1 h at 48°C; and 0.1 \times SSC, 0.1% SDS for 1 h at 52°C before autoradiography or phosphor Imager analysis (Applied Biosystems).

Immunocytochemical methods

Sections were permeabilized with phosphate-buffered saline (PBS) containing 0.75% Triton X-100 and blocked with 10% normal goat serum containing anti-mouse or anti-rabbit Fab fragments (diluted 1:50; Jackson Immunocytochemical, Westgrove, USA) to avoid unwanted cross-reactivity and incubated with primary antibodies for 2 days at 4°C. Tissue-bound primary antibodies were detected using the avidin–biotin peroxidase complex (ABC) as indicated by the manufacturer (Vector Labs). Immunoreagents were diluted in PBS containing 0.5% Triton X-100, 0.2% gelatin, and 5% pre-immune serum. After development with 0.05–0.07% diaminobenzidine (DAB) and 0.01% H₂O₂, sections were mounted onto gelatinized slides, dehydrated in ethanol, and coverslipped with Eukitt (Merck, Darmstadt, Germany). Immunocytochemical controls, including omission of the primary antibody or its substitution by normal serum, prevented immunostaining. In parallel, sections were stained with cresyl violet or processed for the double immunofluorescence detection of Nogo and GFAP, MAG and NG2 by using Alexa-Fluor 488- and Alexa-Fluor 5868-tagged secondary antibodies (Molecular Probes, Eugene, USA).

Generation of digoxigenin-labeled riboprobes against 3'-Nogo and 3'-NgR and in situ hybridization

The 3' segment of the mouse Nogo receptor (GenBank accession no. AF283462) and the 3' region of rat Nogo-A (GenBank accession no. AJ242961) were subcloned in pSP72 between *Xho*I and *Hind*III sites (Hunt et al., 2002). Nogo and NgR antisense probes were generated by linearization with *Xho*I followed by in vitro transcription with T7 RNA polymerase. Conversely, Nogo and NgR sense probes were generated by linearization with *Hind*III and *Bam*HI followed by SP6 and T7 RNA polymerase transcription, respectively. Both sense and antisense riboprobes were labeled with digoxigenin according to the manufacturer's recommendation (Roche Applied Science). In situ hybridization was carried out essentially as described by De Lecea et al. (1994), Alcántara et al. (2000), and Hunt et al. (2002). Sections taken from different survival times after lesion were processed in the same vial for in situ hybridization. After washing in PBS, free floating sections were treated with 0.2 N HCl, incubated with 0.1M triethanolamine containing 0.25% acetic anhydride, and dehydrated in an ascending series of ethanol. Afterwards, sections were prehybridized with 50% formamide, 25 mM ethylenediaminetetraacetic acid (EDTA), 50 mM Tris–HCl pH 7.6, 2.5 \times Denhardt's solution, 0.25 mg/ml tRNA (Roche Applied Science), and 20 mM NaCl for 4 h at 60°C. This was followed by hybridization with labeled riboprobes (750

ng/ml, overnight at 62°C) dissolved in 50% formamide, 20 mM Tris–HCl (pH, 7.5), 1mM EDTA, 1× Denhardt's solution, 0.5 mg/ml tRNA, 0.1 mg/ml poly(A) RNA, 0.1 M DTT, and 10% dextran sulfate. The next day, sections were washed in 0.2× standard saline citrate (SSC, containing 30 mM NaCl and 3 mM Na-citrate, pH 7.0) and then in 0.1× SSC/50% formamide at 50°C. After rinsing, sections were blocked with 2% bovine serum albumin (BSA, fraction V) and incubated with alkaline phosphatase-tagged antibodies against digoxigenin for 48 h at 4°C (diluted 1:1500, Roche Applied Science). Sections were developed with 0.34 mg/ml of 4-nitroblue tetrazolium chloride, 0.175 mg/ml 5-bromo-4-chloro-3-indolylphosphate, and 0.25 mg/ml levamisole (all from Sigma). After rinsing, sections were mounted onto gelatinized slides and coverslipped with Mowiol.

Entorhino-hippocampal organotypic slice co-cultures

Entorhino-hippocampal slice co-cultures were prepared from newborn OF1 mice as described (Del Rio et al., 1997; Stoppini et al., 1991). P0–P1 animals were anesthetized by hypothermia, and the hippocampus and entorhinal cortex were dissected out. Horizontal sections (300–350 µm thick) were obtained in a McIlwain tissue chopper (Mickle Laboratory Eng). Slices were maintained in Minimum Essential Medium (MEM) supplemented with glutamine (2 mM) for 45 min at 4°C (MEM dissecting salt solution). Thereafter, slices were laid down on a porous Millicell CM-membrane (Millipore) and incubated using the interface culture technique (Stoppini et al., 1991). Incubation medium was 50% MEM, 25% horse serum, 25% Hank's balanced salts, supplemented with L-glutamine (2 mM) (all reagents were purchased from GIBCO). The medium was changed after 24 h and thereafter every 48 h until the tissue was examined.

Axotomy of the entorhino-hippocampal projections in vitro and IN-1 antibodies treatment

After 15 days in vitro (DIV), the entorhino-hippocampal connections were axotomized by cutting the co-cultures from the rhinal fissure to the ventricular side along the entire entorhino-hippocampal interface using a tungsten knife (Del Rio et al., 2002). IN-1 monoclonal antibody (hybridoma supernatant; Schnell and Schwab, 1990) or the humanized IN-1 Fab antibody (Brosamle et al., 2000), both kindly provided by M.E. Schwab, was added daily at a final concentration of 1:50 diluted in the culture media (IN-1 culture supernatant) or 4 µg/µl added to each lesioned culture (6 µl final volume/culture). After 7–10 days of treatment, control ($n = 18$) and treated (IN-1, supernatant $n = 6$, and IN-1 Fab, $n = 6$) co-cultures were processed for biocytin tracing of entorhinal afferents to monitor axonal regeneration and counterstained with cresyl violet. Alternatively, biocytin-labelled cultures were also processed for calretinin as described by Del Rio et al. (1996) and Del Rio et al. (1997). Controls included omission of the IN-1 antibody, replacing the specific antibody with the equivalent concentration of normal mouse IgM (Sigma), and incubation with normal serum. The presence of Nogo-A was determined by immunoblotting in parallel axotomized cultures that had not been treated with the IN-1 antibodies. For quantification, the mean number of biocytin-labeled fibers that crossed a 400-µm segment located at a distance of 75–80 µm in the hippocampus parallel to the lesion interphase of consecutive sections from each culture (40× oil immersion objective) was counted.

Acknowledgments

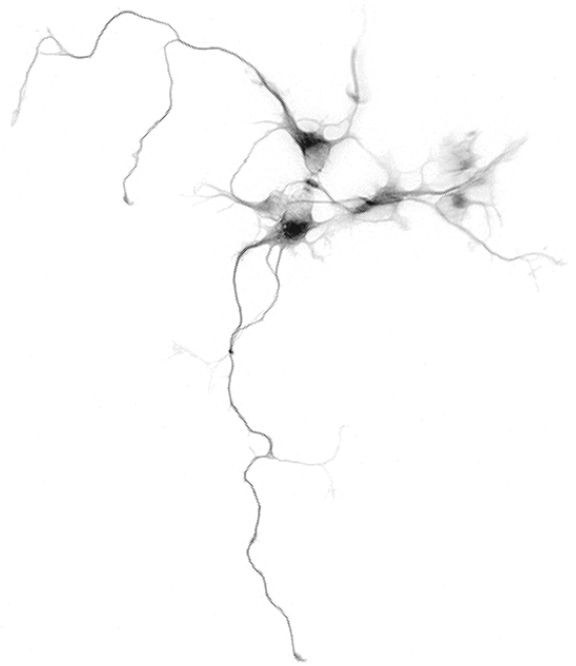
We thank Prof. Y. Tsujimoto (Department of Medical Genetics, Osaka University Graduate School of Medicine, Osaka, Japan) for providing the HA-tagged Nogo-A expression vector, Dr. Z. He (Harvard Medical School, Longwood Avenue, MA, USA) for providing the AP-Nogo-66 construction, and Dr. M. Yutsudo (Research Institute for Microbial Diseases, Osaka University, Osaka, Japan) for providing the Nogo-B cDNA. The authors also thank Tatsumi Hirata (National Institute of Genetics, Graduate University for Advanced Studies, Mishima, Japan) for the gift of the NG1 antibody and Nathalia Vitreireira and Anna La Torre for their technical advice on the non-radioactive in situ hybridization and preparation of the mRNA probes. The authors are also grateful to Susana Maqueda for her technical assistance and Robin Rycroft for linguistic advice. This study was supported by grants from the Spanish Ministry of Science and Technology (MCYT) (EET2003-05149 and BFI2003-03594), FISS (FIS01-0895) and The Caixa Foundation (2004–2007) to JADR, and MCYT (SAF2001-3290) to E.S. Ana Mingorance is a fellow of the Universitat de Barcelona and Xavier Fontana is supplied by fellows from the Fundació Agustí Pedro i Pons (2001–2002) and the Spanish Ministry of Education and Culture (2003).

References

- Alcántara, S., Ruiz, M., De Castro, F., Soriano, E., Sotelo, C., 2000. Netrin 1 acts as an attractive or as a repulsive cue for distinct migrating neurons during the development of the cerebellar system. *Development* 127, 1359–1372.
- Amaral, D.G., Witter, M.P., 1995. Hippocampal formation. In: Paxinos, G. (Ed.), *The Rat Nervous System*. Academic Press, San Diego, pp. 443–493.
- Ben-Ari, Y., Represa, A., 1990. Brief seizure episodes induce long-term potentiation and mossy fibre sprouting in the hippocampus. *Trends Neurosci.* 13, 312–318.
- Ben-Ari, Y., Tseeb, V., Raggozzino, D., Khazipov, R., Gaiarsa, J.L., 1994. Gamma-aminobutyric acid (GABA): a fast excitatory transmitter which may regulate the development of hippocampal neurones in early postnatal life. *Prog. Brain Res.* 102, 261–273.
- Bovolenta, P., Wandosell, F., Nieto-Sampedro, M., 1993. Neurite outgrowth inhibitors associated with glial cells and glial cell lines. *Neuro-Report* 5, 345–348.
- Bregman, B.S., Kunkel-Bagden, E., Schnell, L., Dai, H.N., Gao, D., Schwab, M.E., 1995. Recovery from spinal cord injury mediated by antibodies to neurite growth inhibitors. *Nature* 378, 498–501.
- Brosamle, C., Huber, A.B., Fiedler, M., Skerra, A., Schwab, M.E., 2000. Regeneration of lesioned corticospinal tract fibers in the adult rat induced by a recombinant, humanized IN-1 antibody fragment. *J. Neurosci.* 20, 8061–8068.
- Buffo, A., Zagrebelsky, M., Huber, A.B., Skerra, A., Schwab, M.E., Strata, P., Rossi, F., 2000. Application of neutralizing antibodies against NI-35/250 myelin-associated neurite growth inhibitory proteins to the adult rat cerebellum induces sprouting of uninjured Purkinje cell axons. *J. Neurosci.* 20, 2275–2286.
- Calbet, M., Guadano-Ferraz, A., Spier, A.D., Maj, M., Sutcliffe, J.G., Przewlocki, R., de Lecea, L., 1999. Cortistatin and somatostatin mRNAs are differentially regulated in response to kainate. *Brain Res. Mol. Brain Res.* 72, 55–64.
- Chedotal, A., Del Rio, J.A., Ruiz, M., He, Z., Borrell, V., de Castro, F., Ezan, F., Goodman, C.S., Tessier-Lavigne, M., Sotelo, C., Soriano, E., 1998. Semaphorins III and IV repel hippocampal axons via two distinct receptors. *Development* 125, 4313–4323.

- Chen, M.S., Huber, A.B., van der Haar, M.E., Frank, M., Schnell, L., Spillmann, A.A., Christ, F., Schwab, M.E., 2000. Nogo-A is a myelin-associated neurite outgrowth inhibitor and an antigen for monoclonal antibody IN-1. *Nature* 403, 434–439.
- Cherubini, E., Gaiarsa, J.L., Ben-Ari, Y., 1991. GABA: an excitatory transmitter in early postnatal life. *Trends Neurosci.* 14, 515–519.
- De Lecea, L., Soriano, E., Criado, J.R., Steffensen, S.C., Henriksen, S.J., Sutcliffe, J.G., 1994. Transcripts encoding a neural membrane CD26 peptidase-like protein are stimulated by synaptic activity. *Brain Res. Mol. Brain Res.* 25, 286–296.
- Del Rio, J.A., Heimrich, B., Soriano, E., Schwegler, H., Frotscher, M., 1991. Proliferation and differentiation of glial fibrillary acidic protein-immunoreactive glial cells in organotypic slice cultures of rat hippocampus. *Neuroscience* 43, 335–347.
- Del Rio, J.A., Heimrich, B., Super, H., Borrell, V., Frotscher, M., Soriano, E., 1996. Differential survival of Cajal–Retzius cells in organotypic cultures of hippocampus and neocortex. *J. Neurosci.* 16, 6896–6907.
- Del Rio, J.A., Heimrich, B., Borrell, V., Forster, E., Drakew, A., Alcantara, S., Nakajima, K., Miyata, T., Ogawa, M., Mikoshiba, K., Derer, P., Frotscher, M., Soriano, E., 1997. A role for Cajal–Retzius cells and reelin in the development of hippocampal connections. *Nature* 385, 70–74.
- Del Rio, J.A., Sole, M., Borrell, V., Martinez, A., Soriano, E., 2002. Involvement of Cajal–Retzius cells in robust and layer-specific regeneration of the entorhino-hippocampal pathways. *Eur. J. Neurosci.* 15, 1881–1890.
- Deller, T., Frotscher, M., 1997. Lesion-induced plasticity of central neurons: sprouting of single fibres in the rat hippocampus after unilateral entorhinal cortex lesion. *Prog. Neurobiol.* 53, 687–727.
- Domeniconi, M., Cao, Z., Spencer, T., Sivasankaran, R., Wang, K., Nikulina, E., Kimura, N., Cai, H., Deng, K., Gao, Y., He, Z., Filbin, M., 2002. Myelin-associated glycoprotein interacts with the Nogo66 receptor to inhibit neurite outgrowth. *Neuron* 35, 283–290.
- Fagan, A.M., Gage, F.H., 1990. Cholinergic sprouting in the hippocampus, a proposed role for IL-1. *Exp. Neurol.* 110, 105–120.
- Fournier, A.E., Strittmatter, S.M., 2001. Repulsive factors and axon regeneration in the CNS. *Curr. Opin. Neurobiol.* 11, 89–94.
- Fournier, A.E., GrandPre, T., Strittmatter, S.M., 2001. Identification of a receptor mediating Nogo-66 inhibition of axonal regeneration. *Nature* 409, 341–346.
- Fournier, A.E., Gould, G.C., Liu, B.P., Strittmatter, S.M., 2002. Truncated soluble Nogo receptor binds Nogo-66 and blocks inhibition of axon growth by myelin. *J. Neurosci.* 22, 8876–8883.
- GrandPre, T., Nakamura, F., Vartanian, T., Strittmatter, S.M., 2000. Identification of the Nogo inhibitor of axon regeneration as a reticulon protein. *Nature* 403, 439–444.
- GrandPre, T., Li, S., Strittmatter, S.M., 2002. Nogo-66 receptor antagonist peptide promotes axonal regeneration. *Nature* 417, 547–551.
- Hass, C.A., Rauch, U., Thon, N., Merten, T., Deller, T., 1999. Entorhinal cortex lesion in adult rats induces the expression of the neuronal chondroitin sulfate proteoglycan neurocan in reactive astrocytes. *J. Neurosci.* 19, 9953–9963.
- Hailer, N.P., Jarhult, J.D., Nitsch, R., 1996. Resting microglial cells in vitro: analysis of morphology and adhesion molecule expression in organotypic hippocampal slice cultures. *Glia* 18, 319–331.
- He, X.L., Bazan, J.F., McDermott, G., Park, J.B., Wang, K., Tessier-Lavigne, M., He, Z., Garcia, K.C., 2003. Structure of the nogo receptor ectodomain. A recognition module implicated in myelin inhibition. *Neuron* 38, 177–185.
- Hjorth-Simonsen, A., Jeune, B., 1972. Origin and termination of the hippocampal perforant path in the rat studied by silver impregnation. *J. Comp. Neurol.* 144, 215–232.
- Horner, P.J., Gage, F.H., 2000. Regenerating the damaged central nervous system. *Nature* 407, 963–970.
- Hu, W.H., Hausmann, O.N., Yan, M.S., Walters, W.M., Wong, P.K., Bethea, J.R., 2002. Identification and characterization of a novel Nogo-interacting mitochondrial protein (NIMP). *J. Neurochem.* 81, 36–45.
- Huber, A.B., Weinmann, O., Brosamle, C., Oertle, T., Schwab, M.E., 2002. Patterns of Nogo mRNA and protein expression in the developing and adult rat and after CNS lesions. *J. Neurosci.* 9, 3553–3567.
- Hunt, D., Mason, M.R., Campbell, G., Coffin, R., Anderson, P.N., 2002. Nogo receptor mRNA expression in intact and regenerating CNS neurons. *Mol. Cell. Neurosci.* 20, 537–552.
- Hunt, D., Coffin, R.S., Anderson, P.N., 2003. The Nogo receptor, its ligands and axonal regeneration in the spinal cord; a review. *J. Neurocytol.* 31, 93–120.
- Jessen, M.B., Finsen, B., Zimmer, J., 1997. Morphological and microglial changes in the denervated fascia dentata: correlation with blood–brain-barrier damage and astroglial reactions. *Exp. Neurol.* 143, 103–116.
- Jin, W.L., Liu, Y.Y., Liu, H.L., Yang, H., Wang, Y., Jiao, X.Y., Ju, G., 2003. Intraneuronal localization of Nogo-A in the rat. *J. Comp. Neurol.* 458, 1–10.
- Josephon, A., Widenfalk, J., Widmer, H.W., Olson, L., Spenger, C., 2001. Nogo mRNA expression in adult and fetal human and rat nervous tissue and in weight drop injury. *Exp. Neurol.* 169, 319–328.
- Josephon, A., Trifunovski, A., Widmer, H.R., Widenfalk, J., Olson, L., Spenger, C., 2002. Nogo-receptor gene activity: cellular localization and developmental regulation of mRNA in mice and humans. *J. Comp. Neurol.* 453, 292–304.
- Josephon, A., Trifunovski, A., Scheele, C., Widenfalk, J., Wahlestedt, C., Brene, S., Olson, L., Spenger, C., 2003. Activity-induced and developmental downregulation of the Nogo receptor. *Cell Tissue Res.* 311, 333–342.
- Kottis, V., Thibault, P., Mikol, D., Xiao, Z.C., Zhang, R., Dergham, P., Braun, P.E., 2002. Oligodendrocyte-myelin glycoprotein (OMgp) is an inhibitor of neurite outgrowth. *J. Neurochem.* 6, 1566–1569.
- Li, D., Field, P.M., Raisman, G., 1995. Failure of axon regeneration in postnatal rat entorhinohippocampal slice coculture is due to maturation of the axon, not that of the pathway or target. *Eur. J. Neurosci.* 7, 1164–1171.
- Li, Q., Qi, B., Oka, K., Shimakage, M., Yoshioka, N., Inoue, H., Hakura, A., Kodama, K., Stanbridge, E.J., Yutsudo, M., 2001. Link of a new type of apoptosis-inducing gene ASYNogo-B to human cancer. *Oncogene* 20, 3929–3936.
- Li, Q., Ng, C.E., Tang, B.L., 2002. Nogo-A expression in mouse central nervous system neurons. *Neurosci. Lett.* 328, 257–260.
- McKerracher, L., David, S., Jackson, D.L., Kottis, V., Dunn, R.J., Braun, P.E., 1994. Identification of myelin-associated glycoprotein as a major myelin-derived inhibitor of neurite growth. *Neuron* 4, 805–811.
- Meier, S., Brauer, A.U., Heimrich, B., Schwab, M.E., Nitsch, R., Savaskan, N.E., 2003. Molecular analysis of Nogo expression in the hippocampus during development and following lesion and seizure. *FASEB J.* 17, 1153–1155.
- Michel, A., Fischer, U., Meese, E., 1999. Novel glioma expressed antigen immunogenic in glioblastoma and pilocytic astrocytoma. *Electron. J. Pathol. Histol.* 5, 993–997.
- Mukhopadhyay, G., Doherty, P., Walsh, F.S., Crocker, P.R., Filbin, M.T., 1994. A novel role for myelin-associated glycoprotein as an inhibitor of axonal regeneration. *Neuron* 13, 757–767.
- Niederost, B., Oertle, T., Fritsche, J., McKinney, R.A., Bandtlow, C.E., 2002. Nogo-A and myelin-associated glycoprotein mediate neurite growth inhibition by antagonistic regulation of RhoA and Rac1. *J. Neurosci.* 22, 10368–10376.
- Oertle, T., Schwab, M.E., 2003. Nogo and its pARTNers. *Trends Cell Biol.* 4, 187–194.
- Oertle, T., Merkler, D., Schwab, M.E., 2003a. Do cancer cells die because of Nogo-B? *Oncogene* 22, 1390–1399.
- Oertle, T., van der Haar, M.E., Bandtlow, C.E., Robeva, A., Burfeind, P., Buss, A., Huber, A.B., Simonen, M., Schnell, L., Brosamle, C., Kaupmann, K., Vallon, R., Schwab, M.E., 2003b. Nogo-A inhibits neurite outgrowth and cell spreading with three discrete regions. *J. Neurosci.* 23, 5393–5406.
- Pozas, E., Pascual, M., Nguyen Ba-Charvet, K.T., Guijarro, P., Sotelo, C., Chedotal, A., Del Rio, J.A., Soriano, E., 2001. Age-dependent effects of

- secreted Semaphorins 3A, 3F, and 3E on developing hippocampal axons, in vitro effects and phenotype of Semaphorin 3A (–) mice. *Mol. Cell. Neurosci.* 18, 26–43.
- Prang, P., Del Turco, D., Kapfhammer, J.P., 2001. Regeneration of entorhinal fibers in mouse slice cultures is age dependent and can be stimulated by NT-4, GDNF, and modulators of G-proteins and protein kinase C. *Exp. Neurol.* 169, 135–147.
- Pratt, T., Sharp, L., Nichols, J., Price, D.J., Mason, J.O., 2000. Embryonic stem cells and transgenic mice ubiquitously expressing a tau-tagged green fluorescent protein. *Dev. Biol.* 228, 19–28.
- Prinjha, R., Moore, S.E., Vinson, M., Blake, S., Morrow, R., Christie, G., Michalovich, D., Simmons, D.L., Walsh, F.S., 2000. Inhibitor of neurite outgrowth in humans. *Nature* 403, 383–384.
- Przewlocki, R., Kaminska, B., Lukasiuk, K., Nowicka, D.Z., Przewlocka, B., Kaczmarek, L., Lason, W., 1995. Seizure related changes in the regulation of opioid genes and transcription factors in the dentate gyrus of rat hippocampus. *Neuroscience* 68, 73–81.
- Sambrook, J., Fritsch, E.F., Maniatis, T., 1989. *Molecular Cloning: A Laboratory Manual*, second ed. Cold Spring Harbor Laboratory Press, Cold Spring Harbor, NY.
- Savaskan, N.E., Plaschke, M., Ninnemann, O., Spillmann, A.A., Schwab, M.E., Nitsch, R., Skutella, T., 1999. Myelin does not influence the choice behaviour of entorhinal axons but strongly inhibits their outgrowth length in vitro. *Eur. J. Neurosci.* 11, 316–326.
- Schnell, L., Schwab, M.E., 1990. Axonal regeneration in the rat spinal cord produced by an antibody against myelin-associated neurite growth inhibitors. *Nature* 343, 269–272.
- Schwab, M.E., Bartholdi, D., 1996. Degeneration and regeneration of axons in the lesioned spinal cord. *Physiol. Rev.* 76, 319–370.
- Skutella, T., Nitsch, R., 2001. New molecules for hippocampal development. *Trends Neurosci.* 24, 107–113.
- Stoppini, L., Buchs, P.A., Muller, D., 1991. A simple method for organotypic cultures of nervous tissue. *J. Neurosci. Methods* 37, 173–182.
- Taketomi, M., Kinoshita, N., Kimura, K., Kitada, M., Noda, T., Asou, H., Nakamura, T., Ide, C., 2002. Nogo-A expression in mature oligodendrocytes of rat spinal cord in association with specific molecules. *Neurosci. Lett.* 332, 37–40.
- Tang, B.L., 2003. Inhibitors of neuronal regeneration: mediators and signaling mechanisms. *Neurochem. Int.* 42, 189–203.
- Thallmair, M., Metz, G.A., Z'Graggen, W.J., Raineteau, O., Kärtje, G.L., Schwab, M.E., 1998. Neurite growth inhibitors restrict plasticity and functional recovery following corticospinal tract lesions. *Nat. Neurosci.* 1, 124–131.
- Tozaki, H., Kawasaki, T., Takagi, Y., Hirata, T., 2002. Expression of Nogo protein by growing axons in the developing nervous system. *Brain Res. Mol. Brain Res.* 104, 111–119.
- Trifunovski, A., Galter, D., Josephson, A., Widmer, H.R., Olson, L., Spenger, C., 2003. Nogo-receptor in developing and adult rat and human brain and spinal cord 2003 Abstract Viewer/Itinerary Planner. Society for Neuroscience, Washington, DC (Program No. 358.14. Online).
- Turner, D.A., Buhl, E.H., Hailer, N.P., Nitsch, R., 1998. Morphological features of the entorhinal-hippocampal connection. *Prog. Neurobiol.* 55, 537–562.
- Walter, J., Kern-Veits, B., Huf, J., Stolze, B., Bonhoeffer, F., 1987. Recognition of position-specific properties of tectal cell membranes by retinal axons in vitro. *Development* 101, 685–696.
- Wang, X., Chun, S.J., Treloar, H., Vartanian, T., Greer, C.A., Strittmatter, S.M., 2002. Localization of Nogo-A and Nogo-66 receptor proteins at sites of axon-myelin and synaptic contact. *J. Neurosci.* 22, 5505–5515.
- Watari, A., Yutsudo, M., 2003. Multi-functional gene ASYNogoRTN-XRTN4: apoptosis, tumor suppression, and inhibition of neuronal regeneration. *Apoptosis* 1, 5–9.
- Wong, S.T., Henley, J.R., Kanning, K.C., Huang, K.H., Bothwell, M., Poo, M.M., 2002. A p75(NTR) and Nogo receptor complex mediates repulsive signaling by myelin-associated glycoprotein. *Nat. Neurosci.* 5, 1302–1308.
- Woodhams, P.L., Prinjha, R., Moore, S.E., Walsh, F.S., 2001. Differential distribution of Nogo isoforms in the rat central nervous system. *Soc. Neurosci. Abstr.* 27, 670.
- Zagrebelsky, M., Buffo, A., Skerra, A., Schwab, M.E., Strata, P., Rossi, F., 1998. Retrograde regulation of growth-associated gene expression in adult rat Purkinje cells by myelin-associated neurite growth inhibitory proteins. *J. Neurosci.* 18, 7912–7929.



Results

Chapter II

Overexpression of Myelin-Associated Glycoprotein after axotomy of the perforant pathway

Ana Mingorance, Xavier Fontana, Eduardo Soriano and José A. del Río.

Molecular and Cellular Neuroscience (2005) 29: 471-483

Overexpression of myelin-associated glycoprotein after axotomy of the perforant pathway

Ana Mingorance, Xavier Fontana, Eduardo Soriano, and José A. del Río*

Development and Regeneration of the CNS, Cellular Biology Department, Barcelona Science Park-IRB, University of Barcelona, Josep Samitier 1-5, 08028 Barcelona, Spain

Received 24 January 2005; revised 24 January 2005; accepted 30 March 2005
Available online 17 May 2005

Myelin-associated glycoprotein (MAG) contributes to the prevention of axonal regeneration in the adult central nervous system (CNS). However, changes in MAG expression following lesions and the involvement of MAG in the failure of cortical connections to regenerate are still poorly understood. Here, we show that MAG expression is differently regulated in the entorhinal cortex (EC) and the hippocampus in response to axotomy of the perforant pathway. In the EC, MAG mRNA is transiently overexpressed by mature oligodendrocytes after lesion. In the hippocampus, MAG overexpression is accompanied by an increase in the number of MAG-expressing cells. Lastly, the participation of MAG in preventing axonal regeneration was tested *in vitro*, where neuraminidase treatment of axotomized entorhino-hippocampal cultures potentiates axonal regeneration. These results demonstrate that MAG expression is regulated in response to cortical axotomy, and indicate that it may limit axonal regeneration after CNS injury.

© 2005 Elsevier Inc. All rights reserved.

Introduction

Axons of the adult central nervous system (CNS) do not regenerate after injury, which is largely due to the presence of growth inhibitory molecules in the glial scar and in CNS myelin (Cadelli and Schwab, 1991; Fawcett and Asher, 1999; Sandvig et al., 2004). Mature oligodendrocytes express at least three proteins in association with myelin that are inhibitory for axonal growth: myelin-associated glycoprotein (MAG), Nogo-A, and oligodendrocyte-myelin glycoprotein (OMgp) (Chen et al., 2000; GrandPre et al., 2000; Kottis et al., 2002; McKerracher et al., 1994; Mukhopadhyay et al., 1994). Interestingly, they all bind to the same neuronal receptor, the Nogo-66 receptor (NgR) (Fournier et al., 2001). So far, most work has focused on Nogo-A. Studies using the IN-1 antibody or the antagonist peptide NEP1–40 have shown that inhibition of Nogo-A function induces axonal regeneration both in

vitro and *in vivo* (GrandPre et al., 2002; Hunt et al., 2003; Josephson et al., 2001; Meier et al., 2003; Mingorance et al., 2004; Schwab, 2004). However, data obtained from analysis of the Nogo-A knockout mice are not conclusive (Woolf, 2003), and the characterization of the other myelin-associated inhibitors is essential to understand the bases of axonal regeneration failure. Here we have focused on MAG.

MAG is a transmembrane protein of the immunoglobulin superfamily that is expressed by both mature oligodendrocytes and Schwann cells, and is involved in the formation and maintenance of the myelin sheath (Schachner and Bartsch, 2000). In addition, MAG prevents axonal growth of postnatal neurons *in vitro*, and its inactivation promotes axonal regeneration both *in vitro* and *in vivo* (McKerracher et al., 1994; Mukhopadhyay et al., 1994; Wong et al., 2003). There are two MAG isoforms, S-MAG and L-MAG, which differ only in the carboxy-terminal portion of their cytoplasmic domain (Tropak et al., 1988). Since both isoforms share the extracellular domain, they may potentially bind to the same receptors, and thereby inhibit neurite outgrowth (see below). MAG is a Sialoadhesin (Kelm et al., 1994) and binds to sialic acid residues on the surface of gangliosides and proteins (Tang et al., 1997a,b; Vinson et al., 2001; Vyas et al., 2002). The gangliosides GD1a and GT1b have been proposed as neuronal receptors for MAG (Vinson et al., 2001; Vyas et al., 2002), and the removal of sialic acid residues with neuraminidase (NANase) reduces the inhibitory effect of MAG on neurite outgrowth *in vitro* (DeBellard et al., 1996; Tang et al., 1997b; Vinson et al., 2001). In addition to gangliosides, MAG binds to NgR in a sialic acid-independent fashion (Domeniconi et al., 2002; Liu et al., 2002), although this interaction seems not to be essential for mediating inhibition from myelin (Zheng et al., 2005). Importantly, a soluble form of MAG (named dMAG), comprising the entire extracellular domain, is released from myelin *in vivo* and inhibits axonal regeneration (Tang et al., 1997a,b, 2001). Since neither Nogo-A nor OMgp have been found in soluble form, the diffusion of dMAG into the neuronal tissue may play an important role in preventing axonal regeneration away from the glial scar.

In a previous study, we analyzed the regulation of Nogo-A and NgR after axotomy of the entorhino-hippocampal pathway (EHP)

* Corresponding author. Fax: +34 934037116.

E-mail address: jario@pcb.ub.es (J.A. del Río).

Available online on ScienceDirect (www.sciencedirect.com).

(Mingorance et al., 2004). EHP lesions lead to alterations in both the deafferented hippocampus and the entorhinal cortex (EC), such as the activation of glial cells, overexpression of extracellular matrix proteins, infiltration of serum-derived elements, and changes in myelin basic protein (MBP) expression (Bechmann and Nitsch, 2000; Drojdahl et al., 2004; Jensen et al., 2000). Among these changes, NgR is strongly upregulated shortly after axotomy, suggesting a role for myelin-associated inhibitors after lesion (Meier et al., 2003; Mingorance et al., 2004). In contrast to Nogo-A, which shows limited expression at the oligodendrocyte surface (Chen et al., 2000), MAG is one of the major proteins of the periaxonal myelin sheath (Quarles et al., 1973). However, little information is available on the regulation of MAG after CNS lesions.

In this study, we use *in situ* hybridization to analyze the regulation of MAG mRNA in hippocampal formation after axotomy of the EHP *in vivo*. We demonstrate that MAG expression is regulated in both the EC and the hippocampus in response to axotomy. MAG overexpression in the EC is part of a reactive response of pre-existing mature oligodendrocytes to cortical axotomy and does not involve proliferation of oligodendrocyte progenitors. In the hippocampus, the overexpression of MAG by mature oligodendrocytes is combined with a reactive response of oligodendrocyte progenitor cells to axotomy, leading to an increase in the number of MAG-expressing cells. In addition, myelin debris containing MAG are observed in the deafferented hippocampal layers and around the glial scar. Moreover, treatment of entorhino-hippocampal organotypic cultures with NANase, which reduces MAG inhibition, promotes axonal regeneration after lesion. Taken together, these results demonstrate that overexpression of MAG forms part of the early response of oligodendrocyte progenitors and mature oligodendrocytes to axotomy, and indicate that MAG may play an important role in the inhibition of axonal regeneration.

Results

Developmental expression of MAG mRNA in the mouse hippocampus

To analyze myelin-associated glycoprotein (MAG) expression in the lesioned and unlesioned entorhino-hippocampal formation, we generated an RNA probe to the region of the MAG mRNA encoding the extracellular portion of the protein (Fig. 1; see Experimental methods for details). The specificity of the MAG probe was assessed by comparison of MAG immunostaining with *in situ* hybridization pattern in equivalent sections of adult brain (Figs. 1F–I). To study the temporal patterns of MAG mRNA in the hippocampal formation, we performed *in situ* hybridization in mouse postnatal animals until adulthood. No hybridization signal was observed at any developmental stage when digoxigenin-labeled sense probes were used (data not shown). In contrast, MAG mRNA signal levels using antisense probes were first observed in the cortical white matter at P5 (Fig. 1B). There was an overall increase in the hybridization signal in all cortical layers except layer I as well as in the white matter between P5 and adult (Figs. 1B–F). In the hippocampus, the first MAG mRNA-expressing oligodendrocytes were seen at P10 (Fig. 1C) and their number increased until adulthood (Fig. 1F). This temporal pattern of MAG mRNA expression follows the onset of myelination in the hippocampal formation (Savaskan et al., 1999). In agreement with

the presence of MAG in myelin, myelinated fiber tracts were labeled with anti-MAG antibodies in the adult (Fig. 1G). Together with the hippocampal white matter and the fimbria, the entorhino-hippocampal pathway (EHP) was intensely labeled, including numerous fibers in the SLM (Fig. 1G). In addition, high immunoreactivity was found in the CA3 stratum radiatum, in contrast to other hippocampal areas (Fig. 1G). The overall cellular distribution of MAG mRNA correlated with that observed with the anti-MAG antibody (Fig. 1F). Thus, MAG mRNA-positive cells were abundant in the CA3 pyramidal layer and scattered cells were seen in the plexiform hippocampal layers (i.e., SLM, stratum radiatum, and stratum oriens; Fig. 1F). In addition, MAG-positive cells were numerous throughout the EC and in the white matter (Figs. 1F and 2). Most cells labeled with MAG mRNA were small and exhibited moderate perinuclear staining. In contrast, some cells, mainly in the CA3 region and white matter, were larger and exhibited stronger signal for MAG mRNA (Fig. 1I). These cells were also observed using MAG antibodies, and in the CA3 area displayed a characteristic chandelier-like morphology (Fig. 1H).

MAG mRNA expression changes in the entorhinal cortex after lesion

To analyze the changes in MAG mRNA expression after *in vivo* axotomy of the EHP, we examined the levels of MAG mRNA in the EC (Figs. 2 and 3) and hippocampus (Fig. 4) from 24 h to 15 days post-lesion (dpl). *In situ* hybridization showed that MAG mRNA expression was strongly upregulated in the lesioned EC (Fig. 2). MAG-overexpressing cells were observed as early as 24 h after lesion (the first time point analyzed) and peaked at 3 dpl (Figs. 2B and D). The upregulation of MAG mRNA was still visible at 7 dpl and returned to control levels by 14 dpl (Fig. 2F and data not shown). A moderate increase in MAG expression levels was also observed in the contralateral EC at 3 dpl (Fig. 2E). This upregulation of MAG expression in the EC was confirmed using anti-MAG antibodies, with which a general increase in MAG immunostaining was observed in the EC, together with the labeling of individual cells, in contrast to the contralateral side (Supplementary Figs. 1A–B). Consistent with results from *in situ* hybridization, we differentiated two populations of MAG-positive cells in the EC: the moderately labeled cells, and the strongly labeled cells, which in addition were larger in size (Figs. 2H–I). We refer to the strongly labeled cells as MAG-overexpressing cells. Cell counts demonstrated that there was no significant change in the total number of MAG-positive cells between contralateral and ipsilateral EC after unilateral EHP axotomy (Fig. 2J). However, the relative percentage of MAG-overexpressing cells increased shortly after axotomy (57% of total MAG-expressing cells 24 h after lesion) and peaked at 3 dpl (65% of total MAG-expressing cells). Subsequently, the percentage of MAG-overexpressing cells decreased, and control levels were recovered after 2 weeks (Fig. 2K). These observations suggest that a subset of MAG-expressing oligodendrocytes transiently overexpress MAG in the EC after EHP axotomy.

MAG-overexpressing oligodendrocytes do not undergo cell proliferation or cell death in the EC after axotomy of the perforant pathway

After axotomy of the perforant pathway, reactive astrocytes transiently express Nogo-A (Mingorance et al., 2004). It has also

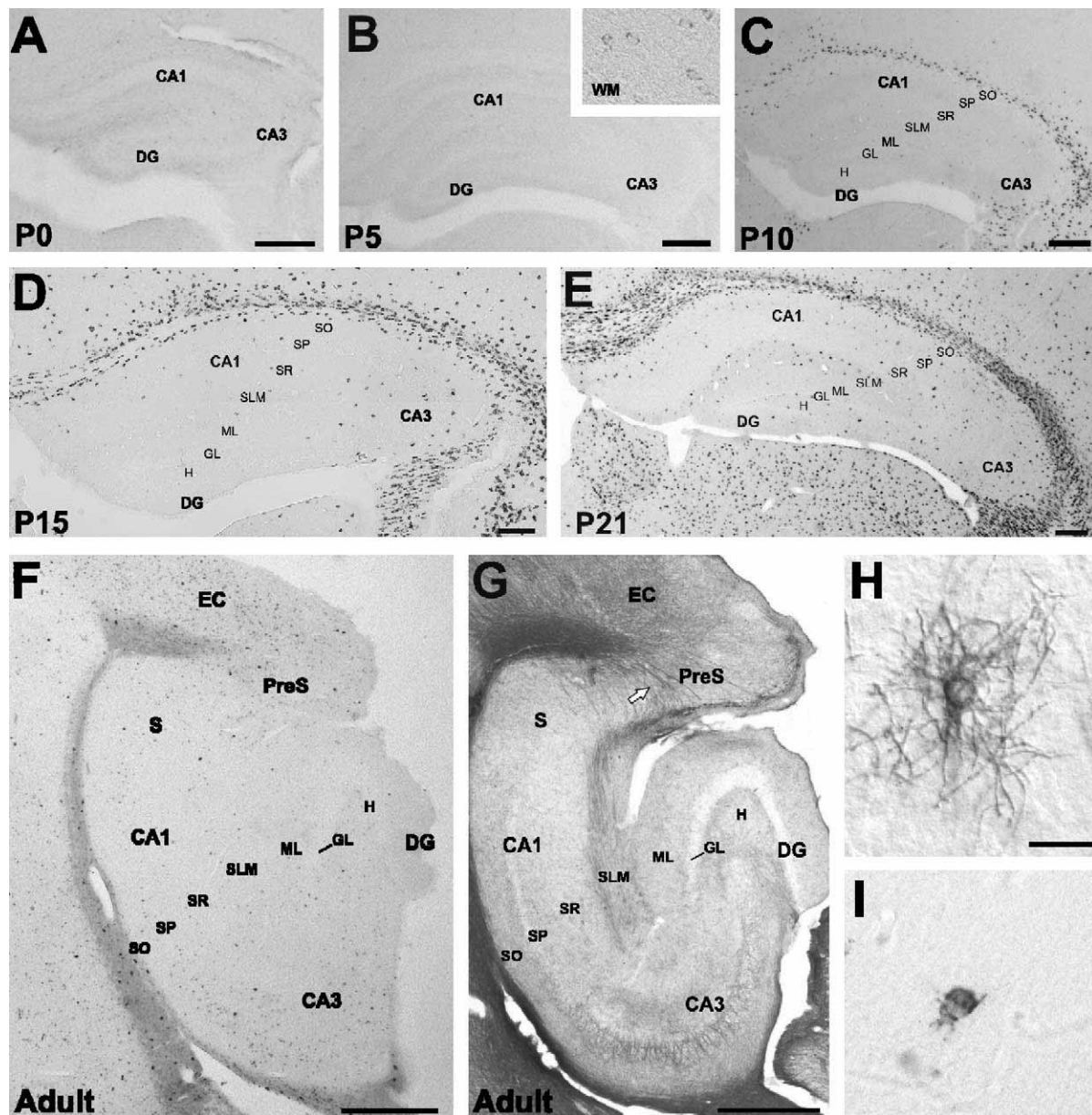


Fig. 1. MAG mRNA expression during the development of the hippocampus. (A) At P0 there is no expression of MAG in the CNS. (B) At P5 MAG mRNA-labeled cells appeared in the cortical white matter but are not detected in the hippocampus. Insert in B shows MAG-expressing cells in the cortical white matter at higher magnification. (C–E) MAG mRNA-labeled cells can be first detected in the hippocampus at P10 from which the number of MAG-expressing cells increases until P21. (F–G) Horizontal sections of the adult hippocampus showing in situ hybridization (F) and immunohistochemistry (G) for MAG. Note the strong myelination of fibers in the entorhinal cortex, the perforant pathway (white arrow in G), and the CA3. (H–I) High magnification view of oligodendrocytes that overexpress MAG in the CA3 area revealed by immunohistochemistry (H) and in situ hybridization (I). Abbreviations: CA1–CA3, hippocampal fields (cornu ammonis); DG, dentate gyrus; dpl, days post-lesion; EC, entorhinal cortex; GL, granule layer; H, hylus; ML, molecular layer; PreS, pre-subiculum; SLM, stratum lacunosum-moleculare; SO, stratum oriens; SP, stratum pyramidale; SR, stratum radiatum; WM, white matter. Scale bars: A–E = 200 μ m; F–G = 500 μ m; H–I = 25 μ m.

been reported that NG2⁺ oligodendrocyte precursor cells (OPCs) proliferate after lesion and differentiate into mature myelinating oligodendrocytes (Levine et al., 2001). We wanted to determine whether these reactive populations contribute to the overexpression of MAG mRNA after lesion. Double-labeling analyses showed no colocalization of MAG mRNA with NG2 or GFAP in the EC at any time point after lesion (Figs. 3A–F). Furthermore, the transection site, characterized by the presence of strongly labeled GFAP-positive cells, was devoid of MAG mRNA (Figs. 3E–F). In

addition, there was no colocalization of MAG with the neuronal marker NeuN (data not shown). These observations suggest that MAG mRNA is only overexpressed by mature oligodendrocytes after axotomy.

It has been shown that mature oligodendrocytes can proliferate in response to damage (Ludwin, 1984). To determine whether mature oligodendrocytes proliferate after EHP axotomy, we combined in situ hybridization for MAG with immunohistochemical detection of the Ki67 antigen, present in proliferating cells, and

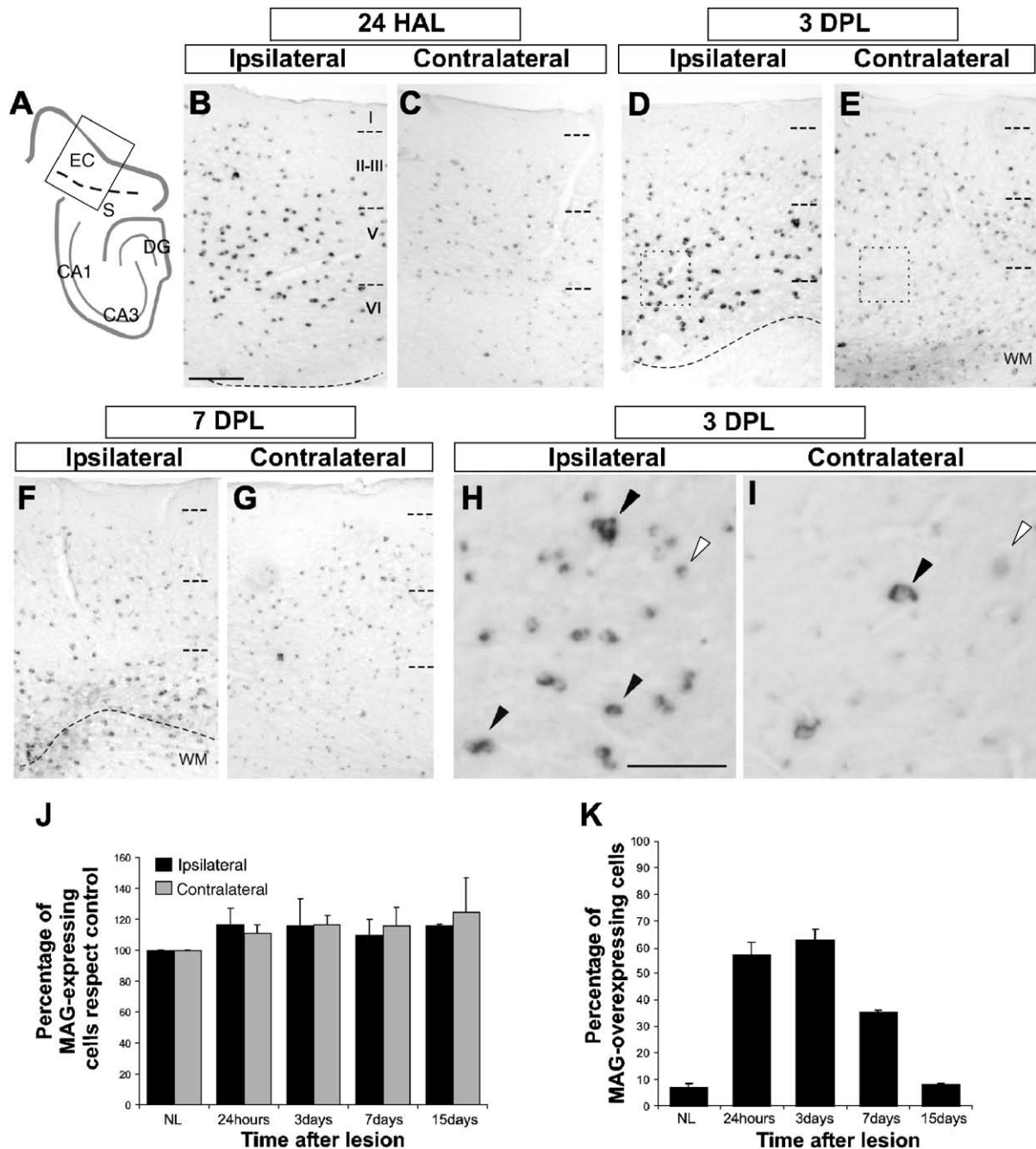


Fig. 2. Overexpression of MAG in the entorhinal cortex after EHP axotomy. (A) Schematic drawing of the entorhino-hippocampal system showing the localization of the transection site and the entorhinal area compared in B–G. (B–G) Photomicrographs illustrating the time course of the changes in MAG mRNA expression after perforant pathway lesion (dotted line in photographs). Entorhinal cortex layers are indicated. MAG mRNA is upregulated in the ipsilateral EC as early as 24 h after lesion (B) and reaches a maximum 3 dpl (D). Seven days after axotomy, MAG upregulation has decreased (F). In the contralateral EC (C, E, G), a slight upregulation is observed at 3 dpl (E). (H–I) Two populations of MAG-expressing cells could be distinguished according to their MAG expression levels: moderately labeled cells, widely distributed throughout unlesioned EC (white arrowheads, H–I), and intensely labeled cells, which overexpress MAG and were abundant in the lesioned entorhinal cortex (black arrowheads in H and I). (J) Quantification of the number of MAG-expressing cells in the EC in non-lesioned animals (NL) and at several post-lesion time points. Data are expressed as percentages with respect to control unlesioned cortex. (K) Relative percentage of MAG-overexpressing cells for the same areas after axotomy. Although there were no changes in the total number of cells expressing MAG (J), there was a strong increase in the percentage of those cells that overexpressed MAG after lesioning (K). Abbreviations as in Fig. 1. Scale bars: B–G = 100 μ m; H–I = 50 μ m.

compared it with NG2 staining (Figs. 3G–I). Three days after EHP axotomy, we observed an increase in the number of NG2+ cells (some of which were double labeled with Ki67) in the glial scar and surrounding areas (Figs. 3H–I). However, no MAG-positive

cell was double labeled with Ki67, indicating that mature oligodendrocytes do not proliferate after EHP axotomy (Fig. 3I).

MAG-overexpressing oligodendrocytes could correspond to new mature oligodendrocytes generated from OPCs in response

to axotomy. To address this issue, we labeled the cycling population of proliferating cells in adult cortex and hippocampus proper (mainly NG2+ progenitors; XF and JADR, unpublished observations; Dawson et al., 2003) with a cumulative pulse of BrdU of 4 days followed by axotomy of the perforant pathway. At 4 dpl, the number of BrdU+ cells located at different distances from the lesion site was compared with the distribution of MAG-overexpressing cells in different sections (Figs. 3J–K; see Experimental methods for details). While BrdU+ cells were mainly located close to the transection (Fig. 3J), MAG-overexpressing cells were almost absent in this zone. Further away from the lesion, the number of BrdU+ cells decreased dramatically, whereas the number of MAG-expressing cells increased, reaching a maximum between 150 and 300 μ m from the lesion (Fig. 3K). The radial distribution of BrdU+ cells around the lesion and the localization of MAG-overexpressing cells were conserved at 7 dpl, although the number of BrdU-labeled cells had decreased (not shown). In addition, the distribution of MAG-overexpressing oligodendrocytes correlated with an increase in the immunoreactivity of MBP, another myelin-related protein, in the upper layers of the lesioned EC at 4 dpl (Supplementary Fig. 1). Taken together, these data indicate that MAG-overexpressing cells do not arise from cell proliferation, but rather, correspond to pre-existing mature oligodendrocytes that react to axotomy by overexpressing myelin-related proteins.

It has been described that some mature oligodendrocytes die following lesion and are replaced by new oligodendrocytes (Keirstead and Blakemore, 1999; McTigue et al., 2001). To determine whether part of MAG-expressing oligodendrocytes undergo cell death after EHP axotomy, we combined *in situ* hybridization for MAG with Hoechst staining and immunodetection of cleaved Caspase-3 and NeuN, markers of apoptosis and neuronal identity, respectively (Figs. 3L–Q). Cleaved Caspase-3 labeling was absent in controls as well as in the contralateral hippocampus and EC (data not shown). In contrast, we observed strong Caspase-3 labeling around the lesion, where no MAG+ cell was recognized (Figs. 3F–G), and cells double-labeled with NeuN and Caspase-3 in the layers II–III of the lesioned EC (Figs. 3L–N). No Caspase-3/MAG+ cells were observed in the EC after lesion (not shown). To further analyze the presence of cell death markers in oligodendrocytes, we performed Hoechst staining of the hybridized sections: no MAG-expressing cells displayed pyknotic nuclei (Figs. 3O–Q). In addition, aberrant MAG+ oligodendrocyte cell bodies were not observed. These results indicate that besides the retrograde degeneration of entorhinal neurons (Fig. 4N), MAG+ oligodendrocytes do not show evidence of cell death in the EC after EHP axotomy.

MAG mRNA expression changes in the hippocampus after lesion

EHP lesion also induced a transient overexpression of MAG mRNA in the deafferented SLM of the hippocampus (Fig. 4). Cell counts demonstrated a 3-fold increase in the number of cells expressing MAG mRNA in the deafferented SLM at 24 h after lesion, which was accompanied by a lower increase in the contralateral SLM (Figs. 4B–E). In addition, an overexpression of MAG mRNA by individual oligodendrocytes could be observed in the deafferented SLM at 3 dpl, but not on the contralateral side (Figs. 4B–D). In contrast to the SLM, the

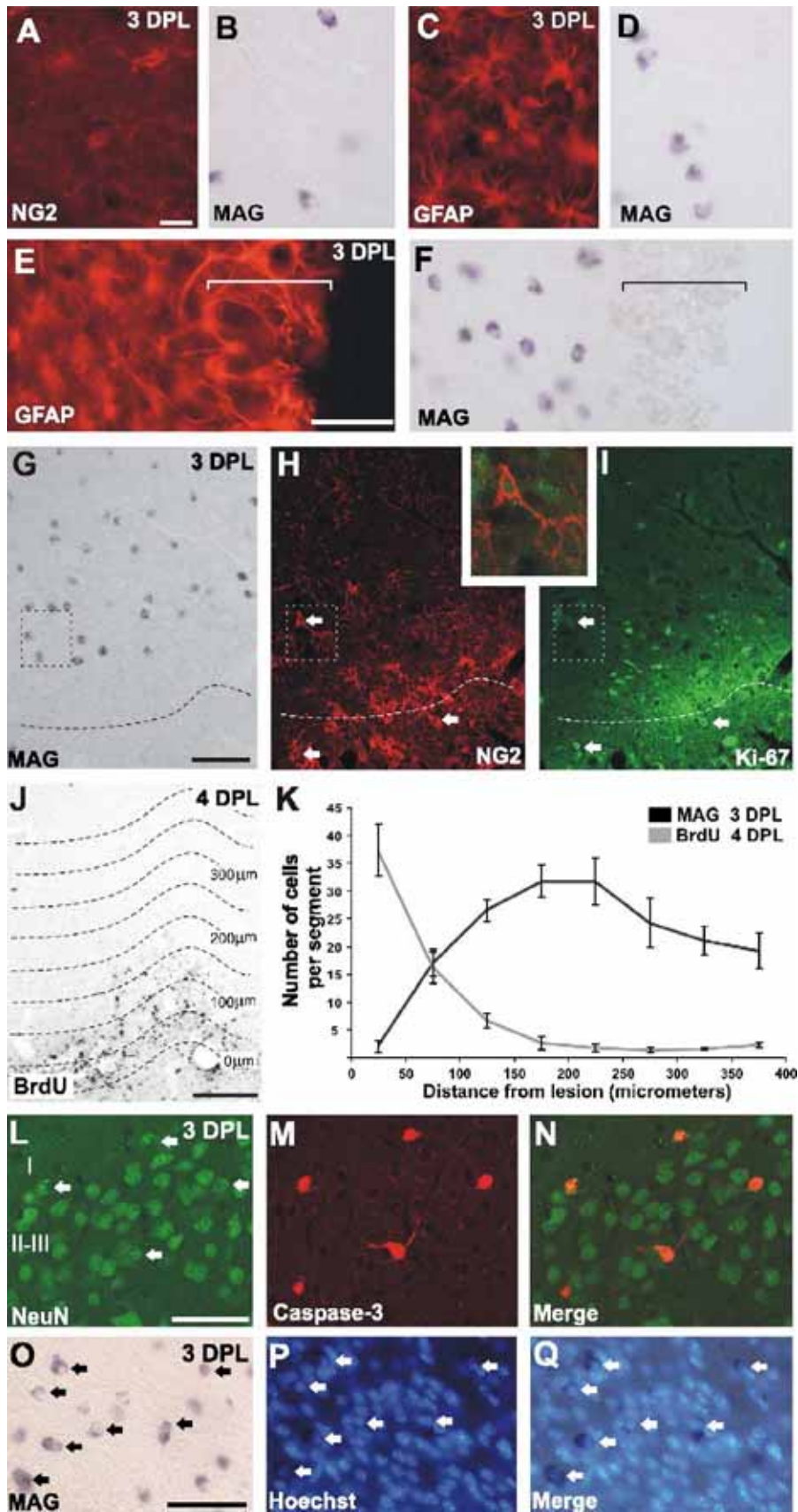
other hippocampal fields (such as the CA3 region) displayed relatively constant MAG mRNA expression levels after EHP axotomy.

Double-labeling analysis demonstrated that, as observed in the EC, there was no colocalization of MAG mRNA with GFAP, NG2, or neuronal markers (data not shown), and MAG-expressing cells correspond to mature oligodendrocytes. Thus, the increase in the number of MAG-expressing cells suggests that new mature oligodendrocytes are generated in the SLM in response to EHP axotomy. There are two potential sources or myelinating oligodendrocytes: progenitors and mature oligodendrocytes. To determine whether the increase in the number of MAG-expressing oligodendrocytes is a result of cell proliferation (most probably proliferation of OPCs), we compared the temporal evolution of MAG+ and BrdU+ cells in the SLM and analyzed the colocalization of MAG mRNA and the Ki67 antigen (Figs. 4F–I). An increase in the number of BrdU+ cells was observed in both the ipsilateral and the contralateral SLM at 4 dpl (4.7- and 2.8-fold increase, respectively, data not shown), coinciding with the increased number of MAG-expressing cells (Figs. 4B–D). In addition, many NG2-expressing cells were double labeled with Ki67 (Figs. 4G–I), in contrast to MAG+ cells, which never colocalized with Ki67 at 3 dpl (Figs. 4F and H). These results suggest that in response to axotomy of the EHP, OPCs (BrdU prelesion-positive cells) proliferate in the deafferented SLM, probably contributing to the increase in the number of MAG+ oligodendrocytes, and at the same time mature oligodendrocytes overexpress MAG transiently after axotomy, as observed in the EC.

Reduction of MAG inhibition promotes axonal regeneration in organotypic cultures after perforant-pathway lesion

Axotomy of the perforant pathway *in vivo* resulted in an accumulation of myelin debris in the lesion (Supplementary Fig. 1; Meier et al., 2004) and in the denervated hippocampal fields (Drojdahl et al., 2004; Jensen et al., 2000; Meier et al., 2004). This may contribute to the prevention of the regeneration of entorhinal axons after axotomy, which do not extend beyond the transection site. To examine the contribution of MAG to the failure of entorhinal neurons to regenerate after EHP axotomy, we used entorhino-hippocampal organotypic co-cultures. First, we characterized the expression pattern of MAG in control and lesioned organotypic cultures (Figs. 5A–E). The perforant pathway was clearly distinguished in organotypic cultures using the anti-MAG antibody, demonstrating that myelination occurs after 15 days *in vitro* (Fig. 5A). In addition, *in situ* hybridization for MAG *in vitro* matched the mRNA distribution *in vivo* (Figs. 1 and 5B, D). In contrast to the *in vivo* situation, 2 days after axotomy of the EHP, there was no clear upregulation of MAG mRNA in the EC. However, an increased number of MAG-expressing cells was observed in the denervated stratum radiatum and SLM (Figs. 5C and E). This indicates that the overexpression of MAG in hippocampal fields that normally display low expression levels could contribute to preventing the entrance of entorhinal axons after lesion.

The gangliosides GD1a and GT1b have been proposed as neuronal receptors for MAG (Vinson et al., 2001; Vyas et al., 2002), and the removal of sialic acid residues with neuraminidase (NANase) reduces the inhibitory effect of MAG on neurite outgrowth *in vitro* (DeBellard et al., 1996; Tang et al., 1997b;



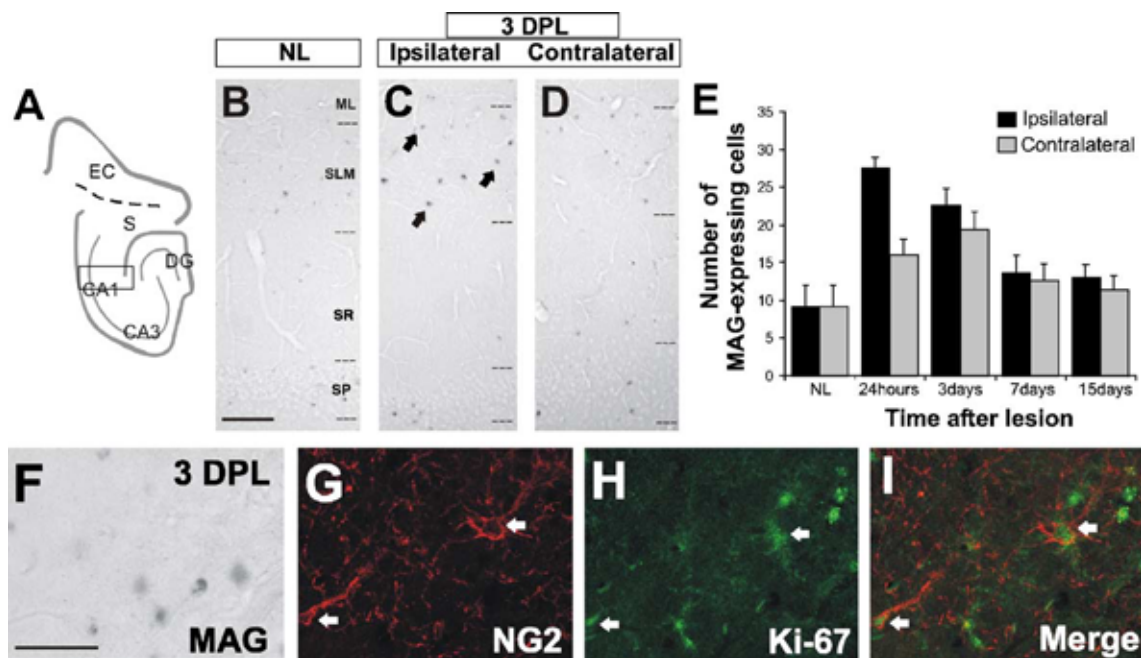


Fig. 4. Regulation of MAG in the hippocampus after EHP axotomy. (A) Schematic drawing of the entorhino-hippocampal system showing the localization of the transection site and the hippocampal area compared in B–D. (B–D) Photomicrographs illustrating MAG regulation in the CA1 region after EHP lesion (from the pyramidal layer to the SLM). The different hippocampal areas are indicated. An increase in the number of MAG-expressing cells is observed in the SLM 3 days after EHP axotomy (compare C–D with B) accompanied by an increase in the amount of MAG mRNA in the SLM of the ipsilateral hippocampus (arrows in C) that is not observed on the contralateral side (D). (E) Quantification of the number (mean \pm SEM) of MAG-positive cells in the ipsilateral and contralateral SLM at different times post-lesion. The number of MAG-expressing cells increases transiently after axotomy. (E–H) Double labeling of MAG mRNA (E) with NG2 (F) and Ki67 (G) at 3 dpl. Arrows point to double-labeled NG2/Ki67 cells. There is no colocalization with MAG mRNA labeling. Abbreviations as in Fig. 1. Scale bars: A–C = 100 μ m; E–H = 50 μ m.

Vinson et al., 2001). To determine the contribution of MAG to the regenerative failure of entorhinal axons after EHP axotomy, we treated entorhino-hippocampal organotypic cultures with neuraminidase (NANase) for 8 days following EHP transection performed at 15 days in vitro (Figs. 5G–J). Afterwards, a biocytin crystal was placed on the EC to label the perforant pathway and cultures were fixed the following day. The effective removal of sialic acids was confirmed by Western blotting to detect polysialylated NCAM (PSA-NCAM; Fig. 5F). When cultures were treated with NANase after lesioning, numerous axons were able to regrow into the hippocampus (Figs. 5G and I; 23.8 ± 6.7 , mean \pm SEM), with many of them reaching the SLM and terminating in growth cones (Figs. 5I–K). In contrast, few axons were able to enter the hippocampus in control cultures, and those that did stopped shortly afterwards (Figs. 5G–H; 5.7 ± 1.4 , mean \pm SEM). These data indicate that sialic acid-dependent inhibitors, such as MAG, are involved in preventing axonal regeneration of entorhinal afferents after in vitro axotomy.

Discussion

The regulation of myelin-associated glycoprotein (MAG) expression and the reactivity of mature oligodendrocytes after axotomy of cortical connections remain poorly understood. Here, we provide in vitro and in vivo evidence that MAG is overexpressed in response to axotomy of the entorhino-hippocampal connection, which may play important roles in the inhibition of axonal regeneration immediately after axotomy.

MAG expression is transiently upregulated in response to perforant pathway lesion

Analysis of MAG expression after in vivo axotomy revealed that MAG mRNA is transiently upregulated in both the hippocampus and the entorhinal cortex (EC). Transient overexpression of the myelin protein myelin basic protein (MBP) has also been described in the hippocampus after axotomy of the entorhino-

Fig. 3. MAG-overexpressing cells in the entorhinal cortex are non-proliferating mature oligodendrocytes and do not undergo apoptosis. (A–F) Double-labeling of MAG mRNA (B, D, F) with immunohistochemistry for NG2 (A) and GFAP (C, E) in the lesioned EC. (A–B) NG2+ cells in the EC do not express MAG. (C–D) There is no colocalization of astrocytes (GFAP+) with MAG mRNA labeling. (E–F) MAG mRNA (F) is not present in the glial scar, which is clearly labeled with GFAP (E). (G–I) Colocalization of MAG mRNA (G) with NG2 (H) and Ki67 (I). Ki67+ cells are present in the glial scar and in the EC. There is no colocalization with MAG mRNA labeling (G), but some cells are double labeled with NG2/Ki67 (white arrows in H–I). Insert shows detail of double-labeled NG2/Ki67 cell. The area represented in the insert appears squared in G–I. (J–K) OPCs do not differentiate into MAG-overexpressing cells. (J) The EC was divided in 50- μ m strips and the BrdU+ cells were counted. The same analysis was performed for MAG+ cells following in situ hybridization. (K) Result of the quantification of MAG- and BrdU+ cells. While BrdU+ cells localize preferentially around the glial scar, this area is devoid of MAG+ cells, which are distributed 150–300 μ m away from the lesion site. (L–Q) MAG-overexpressing cells are not apoptotic. (L–N) Sections were double stained for NeuN and Caspase-3 after MAG mRNA hybridization. At 3 dpl, apoptotic neurons (arrows in L), but not oligodendrocytes, are positively labeled for Caspase-3 (M–N). (O–Q) Example of hybridized sections counterstained with Hoechst. No pyknotic nuclei were observed in MAG-expressing cells (arrows) when stained with Hoechst. Scale bars: A–D = 20 μ m; E–F = 50 μ m; G–I = 100 μ m; J = 100 μ m; L–N = 50 μ m; O–Q = 50 μ m.

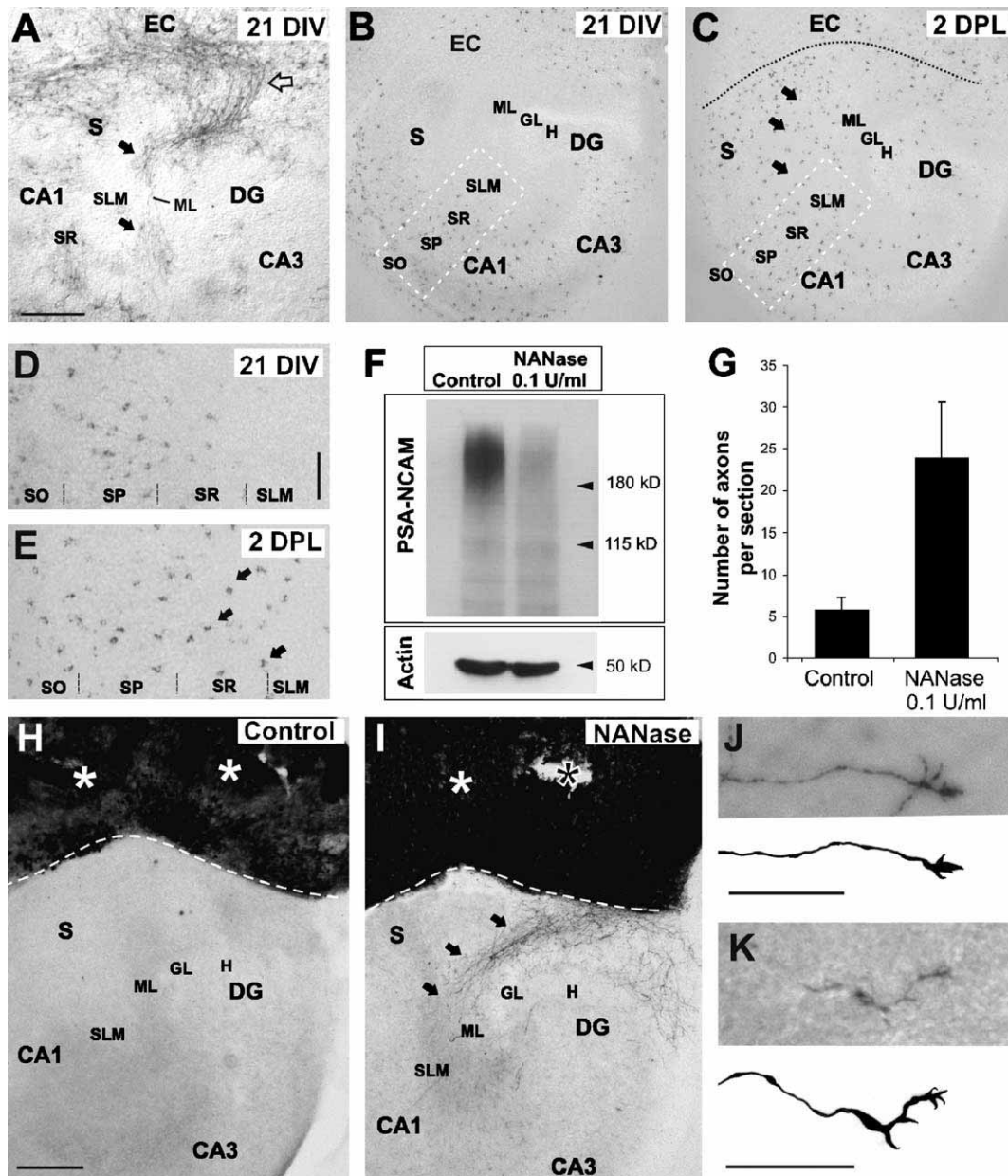


Fig. 5. MAG regulation in vitro and regeneration after NANase treatment. (A–E) MAG expression in organotypic cultures. (A) Immunohistochemistry for MAG demonstrates that myelination of the perforant pathway takes place in vitro as in vivo (open arrow), finishing in the prospective layers of the hippocampus (black arrows). (B–E) In situ hybridization for MAG in control (B and D) and lesioned (C and E) organotypic cultures. Two days after axotomy of the EHP, the number of MAG-expressing cells in the SLM and SR is increased compared to controls (arrowheads in C and E compared to control B and D). (F–J) NANase treatment promotes axonal regeneration after EHP axotomy. (F) The desialylation of cultures treated with NANase was monitored by Western blot analysis of the polysialylated form of NCAM. (G) Statistical analysis of the number of biocytin-labeled fibers in the deafferented hippocampus per section (Student's *t* test, $P = 0.051$ at 95% confidence level; error bars indicate standard error). (H–K) Entorhino-hippocampal cultures axotomized at 15 days in vitro (DIV). (H) EHP axotomized at 15 DIV did not show regeneration of lesioned fibers. (I) In contrast, in treated cultures, axotomized EHP axons regrew into the hippocampus and some reached the prospective SLM and molecular layer (arrows and J–K). (J–K) High magnification view and camera lucida drawings of two representative regrowing axons found in the SLM area showing terminal growth cones. Abbreviations as in Fig. 1. Scale bars: A–C = 250 μ m; D–E = 50 μ m; H–I = 250 μ m; J–K = 25 μ m.

hippocampal pathway (EHP) (Drojdahl et al., 2004; Jensen et al., 2000). MBP expression is upregulated in the stratum radiatum (SR) of CA3, the stratum lacunosum-moleculare (SLM), and the molecular layer of the dentate gyrus, peaking at 7 days post-lesion (dpl) (Jensen et al., 2000). Here we describe a transient upregulation of MAG by mature oligodendrocytes in the SLM of the hippocampus that precedes MBP upregulation. This may reflect

the different roles played by MAG and MBP during myelination, since MAG has been reported to be involved in the initial stages of myelination and MBP is important for myelin compaction and structural maintenance (Arquint et al., 1987; Martini and Schachner, 1997; Schachner and Bartsch, 2000).

In addition, we have described a previously unreported robust upregulation of MAG expression in the EC. This upregulation is

fast (reaching near maximum levels by 24 h post-lesion) and transient (peaking at 3 dpl and returning to control levels 2 weeks later). Furthermore, we have reported an increase in MAG and MBP protein levels in the EC at 4 and 7 days after EHP axotomy. These results indicate that MAG overexpression forms part of a reactive response of mature oligodendrocytes to axotomy that includes myelin reorganization.

Cell hypertrophy (increased size) and overexpression of specific proteins are both associated with glial activation (i.e., in reactive astrocytes and activated microglial cells) (Morgenstern et al., 2002). In addition, a normal response of activated or reactive glial cells to injury is cell proliferation (i.e., OPCs, astroglia and microglia), and the proliferation of mature oligodendrocytes has been reported previously (Ludwin, 1984; Ludwin and Bakker, 1988). However, we observed no expression of MAG mRNA by astrocytes or OPCs after lesion, ruling out the possibility that MAG is expressed by cells other than mature oligodendrocytes. Here, we report two types of oligodendrocyte-reactive response elicited in the EC and the hippocampus by EHP axotomy. In the EC, mature oligodendrocytes undergo a reactive response to axotomy that includes cell hypertrophy and overexpression of myelin-associated proteins, but not cell proliferation. In contrast, in the SLM, this process is parallel to the generation of new mature oligodendrocytes following cell proliferation (including NG2-positive cells) after EHP axotomy (see below).

Origin of MAG-expressing cells in the entorhinal cortex and the hippocampus after EHP axotomy

The reaction of myelinating mature oligodendrocytes after lesion has mainly been studied in animal models of remyelination such as cuprizone- or lyssolecithin-induced demyelination and remyelination in the spinal cord (Matsushima and Morell, 2001; Woodruff and Franklin, 1999). In these models, mature oligodendrocytes are specifically damaged, and OPCs proliferate to restore the population of mature myelinating oligodendrocytes in demyelinated areas (Matsushima and Morell, 2001). In contrast, we have shown that the total number of myelinating oligodendrocytes, as revealed by MAG expression, remains constant in the EC following knife-lesioning of the EHP. At least two hypotheses could explain this observation: the number of MAG-expressing cells could remain constant after EHP lesion without OPC differentiation, or alternatively, a putative decrease in the number of mature oligodendrocytes caused by cell death after axotomy may be compensated by the proliferation and differentiation of OPCs. To test these hypotheses, we performed a cumulative labeling with BrdU prior to EHP lesion in order to label the cycling population of OPCs in adult mice (Dawson et al., 2003) and followed their progress after axotomy. While the number of BrdU-labeled cells increases around the lesion site after axotomy and NG2+ cells frequently colocalize with Ki-67 in this area, MAG-positive cells are mainly localized between 150 and 300 μm from the lesion. Furthermore, displacement of BrdU-labeled cells from the glial scar to the upper layers of the entorhinal cortex was not observed at 7 dpl. Hence, it is unlikely that MAG-overexpressing cells in the EC derive from the proliferation and differentiation of OPCs, and this population probably corresponds to pre-existing mature oligodendrocytes.

Our finding that the number of MAG-expressing cells remains constant in the EC after EHP axotomy contrasts with the increase observed in the deafferented SLM. Immature oligodendrocytes in

the deafferented SLM may upregulate MAG and become detectable after injury without prior proliferation. Additionally, OPC proliferation may contribute to expansion of the MAG-expressing population. In support of this possibility, Drojdahl et al. reported the appearance of oligodendrocyte doublets in the molecular layer of the deafferented dentate gyrus 5 dpl, which eventually incorporated BrdU (Drojdahl et al., 2004). This is in agreement with our finding that the number of BrdU-positive cells labeled prior to lesion increases in the SLM, and NG2 and Ki67 colocalize in the same stratum. Thus we conclude that in the deafferented SLM, the overexpression of MAG by single oligodendrocytes is combined with an increase in the number of MAG-expressing cells, which, at least in part, can be attributed to cell proliferation (presumably of OPCs).

Finally, we addressed whether part of the population of MAG-expressing oligodendrocytes die in the EC or the deafferented SLM following EHP axotomy. Axonal degeneration after traumatic injury is associated with oligodendroglial apoptosis involving Caspase-3 activation (Casha et al., 2001). However, based on cleaved Caspase-3 labeling, we did not detect any apoptotic MAG-expressing cell at 3 dpl, when oligodendroglial reactivity (monitored by MAG overexpression) is maximal, although we did observe the degeneration of projecting neurons from the EC. Interestingly, oligodendrocytes undergo either apoptosis or cell lysis (necrosis) in response to diverse stimuli in different experimental models (Bonetti et al., 1997; D'Souza et al., 1996). After EHP axotomy, astrocytes overexpress Fas-ligand in the deafferented hippocampus (Bechmann et al., 2000), and Fas activation induces rapid oligodendrocyte lysis, without apoptosis features like Caspase-3 activation or DNA fragmentation, in multiple sclerosis (Bonetti et al., 1997; D'Souza et al., 1996). Therefore, we extended our analysis with other methods of detecting cell death, such as morphological criteria (the presence of aberrant cell morphologies) or the presence of pyknotic nuclei, all of which failed to provide evidence for cell death in the population of oligodendrocytes that express MAG mRNA. Although the present data do not rule out that oligodendrocytes may downregulate MAG mRNA before displaying characteristics of cell death, or that delayed cell death may occur, we conclude that cell death of MAG-expressing oligodendrocytes after EHP axotomy is a rare event for the time of MAG overexpression.

Modulation and functions of MAG overexpression after EHP axotomy

A combination of signals from the demyelinated axon and from reactive astrocytes and/or microglia stimulates adult OPCs to re-enter the cell cycle (Levine et al., 2001). In addition, several factors can regulate MAG overexpression after axotomy. First, axonal sprouting regulates myelin gene expression (Drojdahl et al., 2004; Gregersen et al., 2001; Jensen et al., 2000). The sprouting of associational and commissural afferents in the denervated hippocampus starts around day 4 post-axotomy and correlates with MAG and MBP overexpression (Jensen et al., 2000). Although the possibility that the upregulation of MAG expression and the increase in the number of oligodendrocytes in the SLM is an early response to axonal sprouting cannot be ruled out, this is unlikely to be the case in the EC. In addition, myelin gene expression by oligodendrocytes may be regulated by the CNS infiltration of non-CNS molecules and cells (which release inflammatory cytokines) as a result of damage to the blood–brain barrier (Silver and Miller,

2004), and by the cytokines and growth factors expressed by activated astrocytes and microglial cells after axotomy (Babcock et al., 2003; Diemel et al., 1998; Kiefer et al., 1995). In particular, after EHP axotomy, microglia synthesize IGF-1 and TGF β 1, which stimulate myelin gene expression, and microglial reaction is rapid, starting within a few days of lesion (Guthrie et al., 1995; Hailer et al., 1999). Taken together, these data indicate that the upregulation of MAG mRNA in the EC is likely to be induced by serum components, or cytokines and growth factors released by glial cells.

The strong upregulation of MAG in response to axotomy suggests that it plays important roles immediately after lesion. Different functions have been proposed for MAG (Filbin, 1995; Schachner and Bartsch, 2000). First, MAG participates in the process of myelin formation and maintenance (Schachner and Bartsch, 2000). Second, myelin exerts trophic effects on axons (Sanchez et al., 1996; Windebank et al., 1985) and the axonal atrophy observed in MAG knockout mice suggests that MAG plays a role in maintaining axonal integrity (Yin et al., 1998). Finally, MAG is a myelin-associated inhibitor, and its strong overexpression after axotomy may contribute to preventing the regeneration of entorhinal axons (see below). We have described two areas of MAG overexpression after EHP axotomy, one near the axotomized neurons, in the EC, and another in the target tissue, the hippocampal SLM. Thus, the function of MAG in the two areas may be different. The rapid overexpression of MAG in the EC could be related to the trophic support of axotomized neurons, while the increase in the number of MAG-expressing cells in the target area could contribute to the prevention of axonal regeneration (see below).

Removal of sialic-acid residues: neuraminidase treatment promotes axonal regeneration in vitro

We have investigated the role of MAG in limiting axonal regeneration using an in vitro model: axotomy of the EHP in entorhino-hippocampal slice cultures. This model has been used previously to test the role of factors that prevent axonal regeneration (del Rio et al., 2002; Li et al., 1996; Mingorance et al., 2004; Woodhams and Atkinson, 1996). Consistent with observations made in vivo, several changes occur after EHP axotomy in vitro, and inhibitory proteins are overexpressed by both reactive astrocytes and OPCs (Hailer et al., 1999). For example, Nogo-A and NgR are upregulated after axotomy of entorhinal axons in organotypic cultures (AM and JADR, unpublished observations). Although we did not observe a clear upregulation of MAG in the EC after lesion, an increase in the number of MAG-positive cells was clearly detectable in the hippocampus, which correlates with the presence of myelin debris around the lesion site (Supplementary Fig. 1; Jensen et al., 2000; Meier et al., 2004). These cells were numerous in layers that normally display low levels of MAG expression, such as the stratum pyramidale and the stratum radiatum of the CA1 region, and the SLM. Thus, MAG could contribute to preventing the regrowth of lesioned entorhinal afferents into the hippocampal fields.

Currently, there are few techniques available with which to block MAG without affecting the binding of Nogo-A and OMgp to NgR. Immunization with MAG and in vitro chromophore-assisted laser inactivation (CALI) of MAG promote axonal regeneration after spinal cord and optic nerve injury, respectively (Sicotte et al., 2003; Wong et al., 2003). However, the binding of MAG to sialic residues has been shown to potentiate neurite outgrowth inhibition

in vitro, and the neuraminidase (NANase) treatment successfully reduces MAG inhibition in vitro (DeBellard et al., 1996; Tang et al., 1997a,b, 2001; Vinson et al., 2001). Interestingly, Zheng et al. (2005) have recently shown that NgR is not essential for mediating inhibitory signals from CNS myelin, reinforcing the potential reduction of MAG-induced inhibition by interfering with its binding to gangliosides. Treatment of organotypic cultures with NANase after axotomy of the EHP increased the number of regenerating axons in the hippocampus (4-fold), supporting the hypothesis that sialic acid-dependent inhibitors such as MAG prevent axonal regeneration in the EHP in vitro. However, two observations suggest that this result should be interpreted with caution. First, treatment with NANase is not exclusive for MAG, and it may affect other molecules involved in neurite outgrowth (Muller et al., 1996). Second, treatment with NANase represents a reduction rather than a blockade of MAG-induced inhibition (Domeniconi et al., 2002; Liu et al., 2002; Tang et al., 1997a,b; Vinson et al., 2001). Nevertheless, taken together, our in vivo and in vitro results suggest that MAG actively participates in the failure of CNS cortical axons to regenerate.

We have described a strong regulation of MAG expression in both the origin and the target tissue as part of a reactive response of mature oligodendrocytes and OPCs to cortical axotomy. Although the function of MAG overexpression in the EC has yet to be fully elucidated, we have provided evidence that increase in MAG expression in the hippocampus could be related to the prevention of axonal regeneration. Our results extend previous observations relating to Nogo-A and NgR, and support the importance of myelin-associated inhibitors in the regenerative failure of cortical connections in the adult CNS.

Experimental methods

Surgical procedures and sample collection

All procedures were carried out in accordance with the guidelines approved by the Spanish Ministry of Science and Technology, following European standards. For developmental studies, a total of 7 OF1 pregnant mice (Iffa Credo, Lyon, France) were used. Females were mated overnight from 12 pm to 8 am. The mating day was considered as embryonic day 0 (E0) and the day of birth (in the night between E19 and E20) as postnatal day 0. Animals were killed at the following stages: P0, P5, P10, P15, and P21. Three to six animals from at least two different litters were processed for in situ hybridization (ISH) at each of the stages analyzed. Postnatal mice were anaesthetized and transcardially perfused with 4% paraformaldehyde in 0.1 phosphate buffer pH 7.3. After perfusion, the brains were removed from the skull and postfixed in the same fixative solution for additional 48 h, cryoprotected in 30% sucrose, and coronally sectioned on a freezing microtome (30 μ m thick).

In vivo axotomy of the perforant pathway was performed as described elsewhere (Mingorance et al., 2004). Adult mice (3 months old; $n = 43$) were subjected to knife lesioning of the perforant pathway using a wire knife (Kopf instruments, Consultants GmbH, Düsseldorf, Germany), essentially as described by Jensen et al. (1997). Briefly, animals were placed in a stereotaxic apparatus after pentobarbital anesthesia (50 mg/kg, b.w.) and a hole was drilled 1 mm posterior and 3 mm lateral to lambda. A closed wire knife was then inserted at an angle of 15° anterior and 15°

lateral. Four millimeters ventral to dura, the wire was unfolded (1.5 mm) and the perforant pathway was sectioned by retracting the knife 3 mm. After different survival times (24 h, 48 h, and 3, 4, 7, and 15 days), lesioned ($n = 35$) and sham-operated ($n = 10$) mice were processed as described for developmental studies and horizontally sectioned on a freezing microtome (30 μm thick).

Immunohistochemistry

Primary antibodies were used at the following concentrations: anti-gial fibrillary acidic protein (GFAP) (rabbit polyclonal; Chemicon) 1:500; anti-NG2 (rabbit polyclonal; Chemicon) 1:100; anti-Ki-67 (mouse monoclonal; Novocastra Laboratories Ltd) 1:100; anti-BrdU (mouse monoclonal; Dako) 1:75; anti-Caspase 3 (rabbit polyclonal; Cell Signalling Technology) 1:100; Anti-NeuN (mouse monoclonal; Chemicon) 1:50; anti-MAG (mouse monoclonal; Chemicon) 1:100; and anti-MBP (mouse monoclonal; Chemicon) 1:100. Fab fragments (Jackson ImmunoResearch) diluted at 1:50 were used to block endogenous immunoglobulins present in reactive microglia. Immunohistochemistry was performed as described elsewhere (Mingorance et al., 2004). After *in situ* hybridization, sections were incubated with primary antibodies for 2 days at 4°C, followed by immunofluorescence detection with Alexa-Fluor 488- and Alexa-Fluor 568-tagged secondary antibodies (Molecular Probes, Eugene, USA). Immunoreagents were diluted in PBS containing 0.5% Triton X-100, 0.2% gelatin, and 5% pre-immune serum. In some sections, the nuclei were counterstained with Hoechst 33258 (2-[2-(4-hydroxyphenyl)-6-benzimidazolyl]-6-(1-methyl, 4-piperazyl) benzimidazol]). After rinsing, sections were mounted and coverslipped with Mowiol. Immunohistochemical controls, including omission of the primary antibody or its substitution with normal serum, prevented immunostaining.

In situ hybridization

To detect MAG expression, we generated a probe recognizing both S-MAG and L-MAG. A 760-bp restriction fragment (base pairs 885–1645, shared by both S- and L-MAG) obtained by digestion of the full-length S-MAG cDNA with *EcoRI* and *XhoI* was cloned into pBlueScript SK+. MAG antisense probe was generated by linearization with *EcoRI*, followed by *in vitro* transcription with T7 RNA polymerase. Conversely, MAG sense probe was generated by linearization with *XhoI* followed by transcription with T3 RNA polymerase. Both sense and antisense riboprobes were labeled with digoxigenin according to the manufacturer's instructions (Roche Applied Science). *In situ* hybridization was carried out as described previously (Hunt et al., 2002; Mingorance et al., 2004).

BrdU experiments

To analyze cumulative BrdU uptake, 6 mice received a BrdU pulse injection every 24 h for 3 days and were lesioned on the fourth day. Operated mice were sacrificed 4 or 7 days after lesion and processed for immunohistochemistry. For BrdU detection, sections were pretreated with cold 0.1 N HCl (15 min) followed by 2 N HCl at 37°C (20 min) to denature DNA. After washing in borate buffer (pH 8.5), sections were blocked and incubated with primary antibody overnight (anti-BrdU 1:50; Dako). Primary antibody was detected with a biotinylated secondary antibody

and developed with DAB-Ni²⁺. In order to compare the distribution of MAG+ and BrdU+ cells after lesion, equivalent sections from different animals were used (processed for *in situ* hybridization and immunohistochemistry, respectively). MAG-positive and BrdU-positive cells were counted in the entorhinal cortex (EC) (400 \times 500 μm area, 2 areas per EC) and the SLM using a 40 \times oil immersion objective and a micrometric eyepiece. When required, the EC was divided into 50- μm strips and the BrdU+ cells counted. The same analysis was performed for MAG+ cells following *in situ* hybridization.

Entorhino-hippocampal organotypic slice co-cultures

Entorhino-hippocampal slice co-cultures were prepared from newborn OF1 mice as described elsewhere (Del Rio et al., 1997; Stoppini et al., 1991). P0 animals were anaesthetized by hypothermia, and the hippocampus and EC were dissected out. Horizontal sections (300–350 μm thick) were obtained using a McIlwain tissue chopper (Mickle Laboratory Engineering, Goshall, UK). Slices were laid on a porous Millicell CM-membrane (Millipore, Bedford, MA) and incubated using the interface culture technique (Stoppini et al., 1991). Incubation medium was 50% MEM, 25% horse serum, and 25% Hank's balanced salts, supplemented with 2 mM L-glutamine (GIBCO Life Technologies). The medium was changed after 24 h and subsequently every 48 h until the tissue was examined.

Axotomy of the entorhino-hippocampal projections *in vitro* and neuraminidase treatment

After 15 days *in vitro* (DIV), the entorhino-hippocampal connections were axotomized by cutting the co-cultures with a tungsten knife from the rhinal fissure to the ventricular surface along the entire entorhino-hippocampal interface (del Rio et al., 2002). α 2-3,6,8-Neuraminidase (NANase, from *Vibrio cholerae*; Calbiochem) was added every 2 days at a final concentration of 0.1 U/ml diluted in neuraminidase buffer (154 mM Sodium Chloride, 50 mM Sodium Acetate, and 9 mM Calcium Chloride, pH 5.5, and 1 \times protease inhibitor cocktail; Roche) to each lesioned culture (2 μl final volume/culture; control $n = 20$ and treated $n = 30$). Control cultures were treated with NANase buffer. After 7–10 days of treatment, a small crystal of biocytin (Sigma) was injected in the entorhinal slice to label the EHP. The following day, cocultures were fixed with paraformaldehyde and 50- μm -thick sections were obtained using a vibratome. Sections were incubated overnight with an avidin-biotin peroxidase complex (ABC-elite™, diluted 1:100; Vector Laboratories) and peroxidase activity was visualized using a nickel-enhanced diaminobenzidine (DAB) reaction. For quantification, the mean number of biocytin-labeled fibers that crossed a 400- μm segment in the hippocampus (located at a distance of 75–80 μm from the axotomy) was counted for each section using a 40 \times oil-immersion objective. Only cultures displaying equivalent biocytin labeling in the entorhinal cortex were considered for quantification. The statistical significance of the results was analyzed using Student's *t* test (95% confidence level).

To confirm the removal of sialic acids, organotypic cultures were incubated with 0.1 U/ml NANase diluted in NANase buffer or buffer alone for 3 h at 37°C. After incubation, the cultures were homogenized in lysis buffer containing protease inhibitors and samples of 20 μg were separated by electrophoresis. The presence

of polysialylated NCAM (Anti-PSA-NCAM 1:4000; AbCys SA) was confirmed by Western blot using the ECL-plus peroxidase Western kit (Amersham Biosciences).

Note added in proof

While the manuscript was under review, Venkatesh et al., 2005 reported that both NgR1 and NgR2 support MAG binding in a sialic acid-dependent neuraminidase-sensitive manner. We consider that these data support our results and reinforce our conclusions.

Acknowledgments

We thank Hisami Koito (Tokyo, Japan) for full-length S- and L-MAG plasmids and Robin Rycroft for linguistic advice. AM and XF are fellows from the Spanish Ministry of Education and Science (MEC). This work was supported by grants from the Spanish Ministry of Science and Technology (MCYT) (EET2002-05149 and BFI2003-03459), and Fundación Mutua Madrileña Automovilística to JADR; and from MCYT (SAF2001-3290 and SAF2004-07929) to ES.

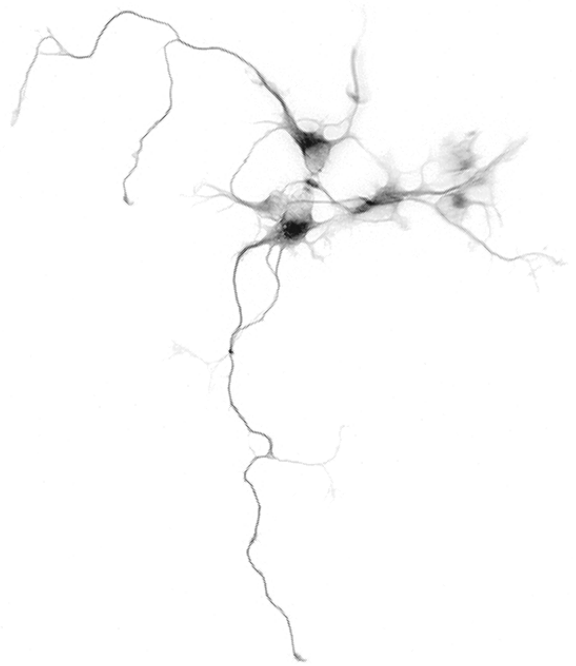
Appendix A. Supplementary data

Supplementary data associated with this article can be found, in the online version, at doi:10.1016/j.mcn.2005.03.016.

References

- Arquint, M., Roder, J., Chia, L.S., Down, J., Wilkinson, D., Bayley, H., Braun, P., Dunn, R., 1987. Molecular cloning and primary structure of myelin-associated glycoprotein. *Proc. Natl. Acad. Sci. U. S. A.* 84, 600–604.
- Babcock, A.A., Kuziel, W.A., Rivest, S., Owens, T., 2003. Chemokine expression by glial cells directs leukocytes to sites of axonal injury in the CNS. *J. Neurosci.* 23, 7922–7930.
- Bechmann, I., Nitsch, R., 2000. Involvement of non-neuronal cells in entorhinal–hippocampal reorganization following lesions. *Ann. N. Y. Acad. Sci.* 911, 192–206.
- Bechmann, I., Lossau, S., Steiner, B., Mor, G., Gimsa, U., Nitsch, R., 2000. Reactive astrocytes upregulate Fas (CD95) and Fas ligand (CD95L) expression but do not undergo programmed cell death during the course of anterograde degeneration. *Glia* 32, 25–41.
- Bonetti, B., Pohl, J., Gao, Y.L., Raine, C.S., 1997. Cell death during autoimmune demyelination: effector but not target cells are eliminated by apoptosis. *J. Immunol.* 159, 5733–5741.
- Cadelli, D.S., Schwab, M.E., 1991. Myelin-associated inhibitors of neurite outgrowth and their role in CNS regeneration. *Ann. N. Y. Acad. Sci.* 633, 234–240.
- Casha, S., Yu, W.R., Fehlings, M.G., 2001. Oligodendroglial apoptosis occurs along degenerating axons and is associated with FAS and p75 expression following spinal cord injury in the rat. *Neuroscience* 103, 203–218.
- Chen, M.S., Huber, A.B., van der Haar, M.E., Frank, M., Schnell, L., Spillmann, A.A., Christ, F., Schwab, M.E., 2000. Nogo-A is a myelin-associated neurite outgrowth inhibitor and an antigen for monoclonal antibody IN-1. *Nature* 403, 434–439.
- D'Souza, S.D., Bonetti, B., Balasingam, V., Cashman, N.R., Barker, P.A., Trout, A.B., Raine, C.S., Antel, J.P., 1996. Multiple sclerosis: fas signaling in oligodendrocyte cell death. *J. Exp. Med.* 184, 2361–2370.
- Dawson, M.R., Polito, A., Levine, J.M., Reynolds, R., 2003. NG2-expressing glial progenitor cells: an abundant and widespread population of cycling cells in the adult rat CNS. *Mol. Cell. Neurosci.* 24, 476–488.
- DeBellard, M.E., Tang, S., Mukhopadhyay, G., Shen, Y.J., Filbin, M.T., 1996. Myelin-associated glycoprotein inhibits axonal regeneration from a variety of neurons via interaction with a sialoglycoprotein. *Mol. Cell. Neurosci.* 7, 89–101.
- Del Rio, J.A., Heimrich, B., Borrell, V., Forster, E., Drakew, A., Alcantara, S., Nakajima, K., Miyata, T., Ogawa, M., Mikoshiba, K., Derer, P., M.Soriano, E., 1997. A role for Cajal–Retzius cells and reelin in the development of hippocampal connections. *Nature* 385, 70–74.
- del Rio, J.A., Sole, M., Borrell, V., Martinez, A., Soriano, E., 2002. Involvement of Cajal–Retzius cells in robust and layer-specific regeneration of the entorhino-hippocampal pathways. *Eur. J. Neurosci.* 15, 1881–1890.
- Diemel, L.T., Copelman, C.A., Cuzner, M.L., 1998. Macrophages in CNS remyelination: friend or foe? *Neurochem. Res.* 23, 341–347.
- Domeniconi, M., Cao, Z., Spencer, T., Sivasankaran, R., Wang, K., Nikulina, E., Kimura, N., Cai, H., Deng, K., Gao, Y., He, Z., Filbin, M., 2002. Myelin-associated glycoprotein interacts with the Nogo66 receptor to inhibit neurite outgrowth. *Neuron* 35, 283–290.
- Drojdahl, N., Fenger, C., Nielsen, H.H., Owens, T., Finsen, B., 2004. Dynamics of oligodendrocyte responses to anterograde axonal (Wallerian) and terminal degeneration in normal and TNF-transgenic mice. *J. Neurosci. Res.* 75, 203–217.
- Fawcett, J.W., Asher, R.A., 1999. The glial scar and central nervous system repair. *Brain Res. Bull.* 49, 377–391.
- Filbin, M.T., 1995. Myelin-associated glycoprotein: a role in myelination and in the inhibition of axonal regeneration? *Curr. Opin. Neurobiol.* 5, 588–595.
- Fournier, A.E., GrandPre, T., Strittmatter, S.M., 2001. Identification of a receptor mediating Nogo-66 inhibition of axonal regeneration. *Nature* 409, 341–346.
- GrandPre, T., Nakamura, F., Vartanian, T., Strittmatter, S.M., 2000. Identification of the Nogo inhibitor of axon regeneration as a Reticulon protein. *Nature* 403, 439–444.
- GrandPre, T., Li, S., Strittmatter, S.M., 2002. Nogo-66 receptor antagonist peptide promotes axonal regeneration. *Nature* 417, 547–551.
- Gregersen, R., Christensen, T., Lehrmann, E., Diemer, N.H., Finsen, B., 2001. Focal cerebral ischemia induces increased myelin basic protein and growth-associated protein-43 gene transcription in peri-infarct areas in the rat brain. *Exp. Brain Res.* 138, 384–392.
- Guthrie, K.M., Nguyen, T., Gall, C.M., 1995. Insulin-like growth factor-1 mRNA is increased in deafferented hippocampus: spatiotemporal correspondence of a trophic event with axon sprouting. *J. Comp. Neurol.* 352, 147–160.
- Hailer, N.P., Grampp, A., Nitsch, R., 1999. Proliferation of microglia and astrocytes in the dentate gyrus following entorhinal cortex lesion: a quantitative bromodeoxyuridine-labelling study. *Eur. J. Neurosci.* 11, 3359–3364.
- Hunt, D., Coffin, R.S., Anderson, P.N., 2002. The Nogo receptor, its ligands and axonal regeneration in the spinal cord; a review. *J. Neurocytol.* 31, 93–120.
- Hunt, D., Coffin, R.S., Prinjha, R.K., Campbell, G., Anderson, P.N., 2003. Nogo-A expression in the intact and injured nervous system. *Mol. Cell. Neurosci.* 24, 1083–1102.
- Jensen, M.B., Finsen, B., Zimmer, J., 1997. Morphological and immunophenotypic microglial changes in the denervated fascia dentata of adult rats: correlation with blood–brain barrier damage and astroglial reactions. *Exp. Neurol.* 143, 103–116.
- Jensen, M.B., Poulsen, F.R., Finsen, B., 2000. Axonal sprouting regulates myelin basic protein gene expression in denervated mouse hippocampus. *Int. J. Dev. Neurosci.* 18, 221–235.
- Josephson, A., Widenfalk, J., Widmer, H.W., Olson, L., Spenger, C., 2001. NOGO mRNA expression in adult and fetal human and rat nervous tissue and in weight drop injury. *Exp. Neurol.* 169, 319–328.
- Keirstead, H.S., Blakemore, W.F., 1999. The role of oligodendrocytes and

- oligodendrocyte progenitors in CNS remyelination. *Adv. Exp. Med. Biol.* 468, 183–197.
- Kelm, S., Pelz, A., Schauer, R., Filbin, M.T., Tang, S., de Bellard, M.E., Schnaar, R.L., Mahoney, J.A., Hartnell, A., Bradfield, P., et al., 1994. Sialoadhesin, myelin-associated glycoprotein and CD22 define a new family of sialic acid-dependent adhesion molecules of the immunoglobulin superfamily. *Curr. Biol.* 4, 965–972.
- Kiefer, R., Streit, W.J., Toyka, K.V., Kreutzberg, G.W., Hartung, H.P., 1995. Transforming growth factor-beta 1: a lesion-associated cytokine of the nervous system. *Int. J. Dev. Neurosci.* 13, 331–339.
- Kottis, V., Thibault, P., Mikol, D., Xiao, Z.C., Zhang, R., Dergham, P., Braun, P.E., 2002. Oligodendrocyte-myelin glycoprotein (OMgp) is an inhibitor of neurite outgrowth. *J. Neurochem.* 82, 1566–1569.
- Levine, J.M., Reynolds, R., Fawcett, J.W., 2001. The oligodendrocyte precursor cell in health and disease. *Trends Neurosci.* 24, 39–47.
- Li, D., Field, P.M., Raisman, G., 1996. Connectional specification of regenerating entorhinal projection neuron classes cannot be overridden by altered target availability in postnatal organotypic slice co-culture. *Exp. Neurol.* 142, 151–160.
- Liu, B.P., Fournier, A., GrandPre, T., Strittmatter, S.M., 2002. Myelin-associated glycoprotein as a functional ligand for the Nogo-66 receptor. *Science* 297, 1190–1193.
- Ludwin, S.K., 1984. Proliferation of mature oligodendrocytes after trauma to the central nervous system. *Nature* 308, 274–275.
- Ludwin, S.K., Bakker, D.A., 1988. Can oligodendrocytes attached to myelin proliferate? *J. Neurosci.* 8, 1239–1244.
- Martini, R., Schachner, M., 1997. Molecular bases of myelin formation as revealed by investigations on mice deficient in glial cell surface molecules. *Glia* 19, 298–310.
- Matsushima, G.K., Morell, P., 2001. The neurotoxicant, cuprizone, as a model to study demyelination and remyelination in the central nervous system. *Brain Pathol.* 11, 107–116.
- McKerracher, L., David, S., Jackson, D.L., Kottis, V., Dunn, R.J., Braun, P.E., 1994. Identification of myelin-associated glycoprotein as a major myelin-derived inhibitor of neurite growth. *Neuron* 13, 805–811.
- McTigue, D.M., Wei, P., Stokes, B.T., 2001. Proliferation of NG2-positive cells and altered oligodendrocyte numbers in the contused rat spinal cord. *J. Neurosci.* 21, 3392–3400.
- Meier, S., Brauer, A.U., Heimrich, B., Schwab, M.E., Nitsch, R., Savaskan, N.E., 2003. Molecular analysis of Nogo expression in the hippocampus during development and following lesion and seizure. *FASEB J.* 17, 1153–1155.
- Meier, S., Brauer, A.U., Heimrich, B., Nitsch, R., Savaskan, N.E., 2004. Myelination in the hippocampus during development and following lesion. *Cell. Mol. Life Sci.* 61, 1082–1094.
- Mingorance, A., Fontana, X., Sole, M., Burgaya, F., Urena, J.M., Teng, F.Y., Tang, B.L., Hunt, D., Anderson, P.N., Bethea, J.R., Schwab, M.E., Soriano, E., del Rio, J.A., 2004. Regulation of Nogo and Nogo receptor during the development of the entorhino-hippocampal pathway and after adult hippocampal lesions. *Mol. Cell. Neurosci.* 26, 34–49.
- Morgenstern, D.A., Asher, R.A., Fawcett, J.W., 2002. Chondroitin sulphate proteoglycans in the CNS injury response. *Prog. Brain Res.* 137, 313–332.
- Mukhopadhyay, G., Doherty, P., Walsh, F.S., Crocker, P.R., Filbin, M.T., 1994. A novel role for myelin-associated glycoprotein as an inhibitor of axonal regeneration. *Neuron* 13, 757–767.
- Muller, D., Wang, C., Skibo, G., Toni, N., Cremer, H., Calaora, V., Rougon, G., Kiss, J.Z., 1996. PSA-NCAM is required for activity-induced synaptic plasticity. *Neuron* 17, 413–422.
- Quarles, R.H., Everly, J.L., Brady, R.O., 1973. Myelin-associated glycoprotein: a developmental change. *Brain Res.* 58, 506–509.
- Sanchez, I., Hassinger, L., Paskevich, P.A., Shine, H.D., Nixon, R.A., 1996. Oligodendroglia regulate the regional expansion of axon caliber and local accumulation of neurofilaments during development independently of myelin formation. *J. Neurosci.* 16, 5095–5105.
- Sandvig, A., Berry, M., Barrett, L.B., Butt, A., Logan, A., 2004. Myelin-, reactive glia-, and scar-derived CNS axon growth inhibitors: expression, receptor signaling, and correlation with axon regeneration. *Glia* 46, 225–251.
- Savaskan, N.E., Plaschke, M., Ninnemann, O., Spillmann, A.A., Schwab, M.E., Nitsch, R., Skutella, T., 1999. Myelin does not influence the choice behaviour of entorhinal axons but strongly inhibits their outgrowth length in vitro. *Eur. J. Neurosci.* 11, 316–326.
- Schachner, M., Bartsch, U., 2000. Multiple functions of the myelin-associated glycoprotein MAG (siglec-4a) in formation and maintenance of myelin. *Glia* 29, 154–165.
- Schwab, M.E., 2004. Nogo and axon regeneration. *Curr. Opin. Neurobiol.* 14, 118–124.
- Sicotte, M., Tsatas, O., Jeong, S.Y., Cai, C.Q., He, Z., David, S., 2003. Immunization with myelin or recombinant Nogo-66/MAG in alum promotes axon regeneration and sprouting after corticospinal tract lesions in the spinal cord. *Mol. Cell. Neurosci.* 23, 251–263.
- Silver, J., Miller, J.H., 2004. Regeneration beyond the glial scar. *Nat. Rev. Neurosci.* 5, 146–156.
- Stoppini, L., Buchs, P.A., Muller, D., 1991. A simple method for organotypic cultures of nervous tissue. *J. Neurosci. Methods* 37, 173–182.
- Tang, S., Shen, Y.J., DeBellard, M.E., Mukhopadhyay, G., Salzer, J.L., Crocker, P.R., Filbin, M.T., 1997. Myelin-associated glycoprotein interacts with neurons via a sialic acid binding site at ARG118 and a distinct neurite inhibition site. *J. Cell Biol.* 138, 1355–1366.
- Tang, S., Woodhall, R.W., Shen, Y.J., deBellard, M.E., Saffell, J.L., Doherty, P., Walsh, F.S., Filbin, M.T., 1997. Soluble myelin-associated glycoprotein (MAG) found in vivo inhibits axonal regeneration. *Mol. Cell. Neurosci.* 9, 333–346.
- Tang, S., Qiu, J., Nikulina, E., Filbin, M.T., 2001. Soluble myelin-associated glycoprotein released from damaged white matter inhibits axonal regeneration. *Mol. Cell. Neurosci.* 18, 259–269.
- Tropak, M.B., Johnson, P.W., Dunn, R.J., Roder, J.C., 1988. Differential splicing of MAG transcripts during CNS and PNS development. *Brain Res.* 464, 143–155.
- Venkatesh, K., Chivatakarn, D., Lee, H., Joshi, P.S., Kantor, D.B., Newman, B.A., Mage, R., Rader, C., Giger, R.J., 2005. The Nogo-66 receptor homolog NgR2 is a sialic acid-dependent receptor selective for myelin-associated glycoprotein. *J. Neurosci.* 25, 808–822.
- Vinson, M., Strijbos, P.J., Rowles, A., Facci, L., Moore, S.E., Simmons, D.L., Walsh, F.S., 2001. Myelin-associated glycoprotein interacts with ganglioside GT1b. A mechanism for neurite outgrowth inhibition. *J. Biol. Chem.* 276, 20280–20285.
- Vyas, A.A., Patel, H.V., Fromholt, S.E., Heffer-Lauc, M., Vyas, K.A., Dang, J., Schachner, M., Schnaar, R.L., 2002. Gangliosides are functional nerve cell ligands for myelin-associated glycoprotein (MAG), an inhibitor of nerve regeneration. *Proc. Natl. Acad. Sci. U. S. A.* 99, 8412–8417.
- Windebank, A.J., Wood, P., Bunge, R.P., Dyck, P.J., 1985. Myelination determines the caliber of dorsal root ganglion neurons in culture. *J. Neurosci.* 5, 1563–1569.
- Wong, E.V., David, S., Jacob, M.H., Jay, D.G., 2003. Inactivation of myelin-associated glycoprotein enhances optic nerve regeneration. *J. Neurosci.* 23, 3112–3117.
- Woodhams, P.L., Atkinson, D.J., 1996. Regeneration of entorhino-dentate projections in organotypic slice cultures: mode of axonal regrowth and effects of growth factors. *Exp. Neurol.* 140, 68–78.
- Woodruff, R.H., Franklin, R.J., 1999. The expression of myelin protein mRNAs during remyelination of lysolecithin-induced demyelination. *Neuropathol. Appl. Neurobiol.* 25, 226–235.
- Woolf, C.J., 2003. No Nogo: now where to go? *Neuron* 38, 153–156.
- Yin, X., Crawford, T.O., Griffin, J.W., Tu, P., Lee, V.M., Li, C., Roder, J., Trapp, B.D., 1998. Myelin-associated glycoprotein is a myelin signal that modulates the caliber of myelinated axons. *J. Neurosci.* 18, 1953–1962.
- Zheng, B., Atwal, J., Ho, C., Case, L., He, X.L., Garcia, K.C., Steward, O., Tessier-Lavigne, M., 2005. Genetic deletion of the Nogo receptor does not reduce neurite inhibition in vitro or promote corticospinal tract regeneration in vivo. *Proc. Natl. Acad. Sci. U. S. A.* 102, 1205–1210.



Results

Chapter III

Regeneration of lesioned entorhino-hippocampal axons *in vitro* by combined degradation of inhibitory proteoglycans and blockade of Nogo-66/NgR signaling

Ana Mingorance, Marta Solé, Vanesa Muneton, Albert Martínez, Manolo Nieto-Sampedro, Eduardo Soriano and José A. del Río.

FASEB Journal, Submitted

FASEBJ/2005/051219

Regeneration of lesioned entorhino-hippocampal axons *in vitro* by combined degradation of inhibitory proteoglycans and blockade of Nogo-66/NgR signalling

Ana Mingorance¹, Marta Solé¹, Vilma Munetón², Albert Martínez¹, Manuel Nieto-Sampedro²; Eduardo Soriano¹ and José Antonio del Río¹.

1) Development and Regeneration of the CNS, Department of Cell Biology, IRB-PCB, Barcelona Science Park, University of Barcelona, Josep Samitier 1-5, 08028 Barcelona, Spain.

2) Regeneration of the CNS Unit, Cajal Institute, C.S.I.C., Dr. Arce 37, 28002 Madrid, Spain, and and National Hospital of Paraplegics, 45071 Toledo, Spain.

The authors thank M. López, S. Soriano and E. Márquez for technical assistance, R. Rycroft and T. Yates for editorial advice and B. Castellano, B. Gonzalez and L. Acarin (UAB, Spain) for their help with the NDPase histochemistry method. The authors also thank J.W. Fawcett (Cambridge, UK) for the gift of the 2B6 antibody. This study was supported by grants from the Spanish Ministry of Science and Technology (MCYT; BF12003-03594) and La Caixa Foundation to JADR, and MCYT (SAF2004-07929) to ES. AM and MS are fellows from the Spanish Ministry of Education and Science.

ABSTRACT

Damaged axons do not regenerate after axotomy in the adult mammalian central nervous system (CNS). This may be due to local inhibitory factors at the site of injury, such as over-expression of chondroitin sulfate (CS) proteoglycans (CSPG) and the presence of myelin-associated inhibitors (MAI). In order to overcome CSPG- or myelin-induced inhibition, strategies based on extrinsic and intrinsic treatments have been developed. For example, NEP1-40 is a synthetic peptide that promotes axonal regeneration by blocking Nogo-66/NgR interaction and Chondroitinase ABC (ChABC) degrades CS, thereby also promoting axon regrowth. Here we examined whether the combination of these complementary strategies facilitates regeneration of the lesioned entorhino-hippocampal pathway (EHP) in slice cultures. In this model, over-expressed CSPG and MAI impaired axon regrowth, which mimics regeneration failure *in vivo*. Both CS cleavage with ChABC and NEP1-40 strongly facilitated the regrowth of entorhinal axons after axotomy, permitting the re-establishment of synaptic contacts with target cells. However, the combined treatment did not improve the regeneration induced by ChABC alone, and the delayed treatment of ChABC, but not NEP1-40, had a less pronounced effect on axonal regrowth compared with acute treatment. These results provide insight into the development of new assays and strategies to enhance axon regeneration in injured cortical connections.

INTRODUCTION

Axons of the adult central nervous system (CNS) do not regenerate after injury mainly because of the presence of growth inhibitory molecules in the glial scar and in the CNS myelin. Three myelin-associated proteins, namely myelin-associated glycoprotein (MAG), Nogo-A, and oligodendrocyte myelin glycoprotein (OMgp), and various chondroitin sulfate (CS) proteoglycans (CSPG), like NG2 or Versican, have been proposed to be main molecular obstacles to nerve fibre regeneration (1-3). Myelin-derived molecules act mainly through a common neuronal receptor complex which comprises NgR, P75, TROY and LERN1/Lingo1 (4-6). In addition to this receptor complex, MAG inhibits axonal growth through binding to gangliosides and NgR2 (7, 8), whereas the receptors for the NiG domain of Nogo-A and the CSPG Versican remain to be identified (9).

PKC activation and the Rho GTPase pathway are common crosstalk points in myelin- and CSPG-induced intracellular inhibition (9-12). This intracellular redundancy may explain why axons do not regenerate in single genetic knock-out mice (13, 14) or when single inhibitory molecules are degraded or blocked (e.g., 15). Among others, current strategies to block myelin- and CSPG-induced inhibition include extrinsic approaches, such as treatment with anti-Nogo-A or NgR receptor antibodies, NgR antagonist peptide (NEP1-40), NgR-receptor extracellular fragments (16-18) and enzymatic proteoglycan hydrolysis with Chondroitinase ABC (ChABC) (19, 20). Intrinsic pharmacological treatments with Rho pathway inhibitors or PKC inhibitors (11, 21) have also been used. However, intracellular interference with these signalling pathways to alleviate axonal inhibition may have undesired side effects on other pathways (9). Recently, research has focused on the development of combined therapies. Most of these combine the blockade of several inhibitors with the promotion of neuronal survival (22-24). However, no study has addressed the combined blockade of myelin and CSPG inhibitors, after a cortical lesion. We have previously shown that the blocking of Nogo-A with specific antibodies (IN-1 and IN1-Fab) induces the regeneration of lesioned entorhinal axons (25). Here we combine two extrinsic approaches and analyze the potential use of ChABC and NEP1-40, which blocks Nogo-66 binding to NgR, to promote axonal regeneration of the lesioned entorhino-hippocampal pathway (EHP). We show that local administration of ChABC or NEP1-40 *in vitro* leads to the robust regeneration of lesioned entorhinal axons, which establish new synaptic contacts with their hippocampal target cells. Moreover, we demonstrate that the combination of these two drugs does not improve the results obtained with ChABC alone, and that their efficiency is affected when drug delivery is delayed. In conclusion, we believe that our results provide basic knowledge for the development of new strategies to enhance axon regeneration in injured cortical connections.

METHODS

Entorhino-hippocampal slice co-cultures and axotomy of the EHP

Entorhino-hippocampal slice co-cultures (n=290) were prepared from newborn mouse pups (n=40) as described (26). After 15-21 days *in vitro* (DIV) the EHP was axotomized by cutting the co-cultures from the rhinal fissure to the ventricular side along the entire entorhino-hippocampal interface (27). Control and treated cultures were allowed to grow for 3-15 days after axotomy and processed. In some cases, cultures were incubated with BrdU (1 μ M, 1 hour) on the first or the fourth day after axotomy, and then fixed and processed 3 or 7 days later.

Histological procedures

Microglial cells were labelled using their intrinsic NDPase activity with inosine 5'-diphosphate as substrate as described (28). For immunocytochemistry, vibratome sections (50 μ m thick) were permeabilized with DMSO and blocked with normal serum-containing Fab IgG fragments (Jackson Immunocytochemical, USA). Free-floating sections were incubated for two days with either anti-BrdU (clone Bu20a; diluted 1:75, Dako, Denmark), anti-GFAP (diluted 1:2000), anti-NG2 (diluted 1:1000, Chemicon, USA), anti-injured membrane heparan- and chondroitin-sulfate proteoglycan (IMP, clone 3PE8, diluted 1:200) or anti-chondroitin 4-6 sulfate (CS-56, diluted 1:200, Sigma, UK) primary antibodies and the ABC Kit (Vector Labs, USA). Controls, including omission of the primary antibody or its substitution by normal serum, showed immunostaining. Selected cultures were examined in the electron microscope using standard procedures (27).

Pharmacological treatment of axotomized cultures

For acute treatments, drugs were delivered to the cultures on days 0, 2, 4 and 6 post-axotomy. Alternatively, cultures were left untreated for four days and drugs were delivered on days 5, 7, 9 and 11 post-lesion (delayed treatment). In both cases, cultures were treated for seven days. After treatment, the EHP was labelled with biocytin crystals placed in the entorhinal cortex (26). For quantification, using a calibrated eyepiece, we counted the mean number of biocytin-labelled fibres that crossed a 400 μ m segment located at a distance of 75-80 μ m in the hippocampus parallel to the lesion interphase of consecutive sections from each culture (40x oil immersion oil objective). An ANOVA test was used to assess statistical significance. To degrade CS, ChABC (50, 100, 300 or 600 ng/ml; Seikagaku, Japan) was dissolved in TrisHCl 0.1M pH 8, sodium acetate 0.03M, supplemented with protease inhibitors (ChABC buffer) and pre-activated for one hour at 37° before use. To block Nogo-66/NgR interaction, NEP1-40 (Alpha Diagnostics, Texas) was dissolved in PBS (containing protease inhibitors) and applied at a final concentration of 100, 250 or 300 μ M. The doses used for each treatment were 50 ng/ml and 100 μ M respectively, since higher concentrations reduced culture viability. This was also the doses chosen for the combined treatments. Control cultures received ChABC buffer or PBS alone. To determine changes in microglial activation and phagocytic activity after drug treatment, several control and treated cultures were processed for GFAP immunostaining, NADPase histochemistry or, alternatively, living slices were incubated with fluorescence latex beads (1 μ m

Ø, Invitrogen-Molecular Probes, Spain) for 2 hours at 37° C, rinsed in culture media, and the level of intensity of fluorescence beads in the cultures were analyzed in an inverted microscope (Nikon, Japan) and using the Quantity One Image Analysis software (BioRad, USA).

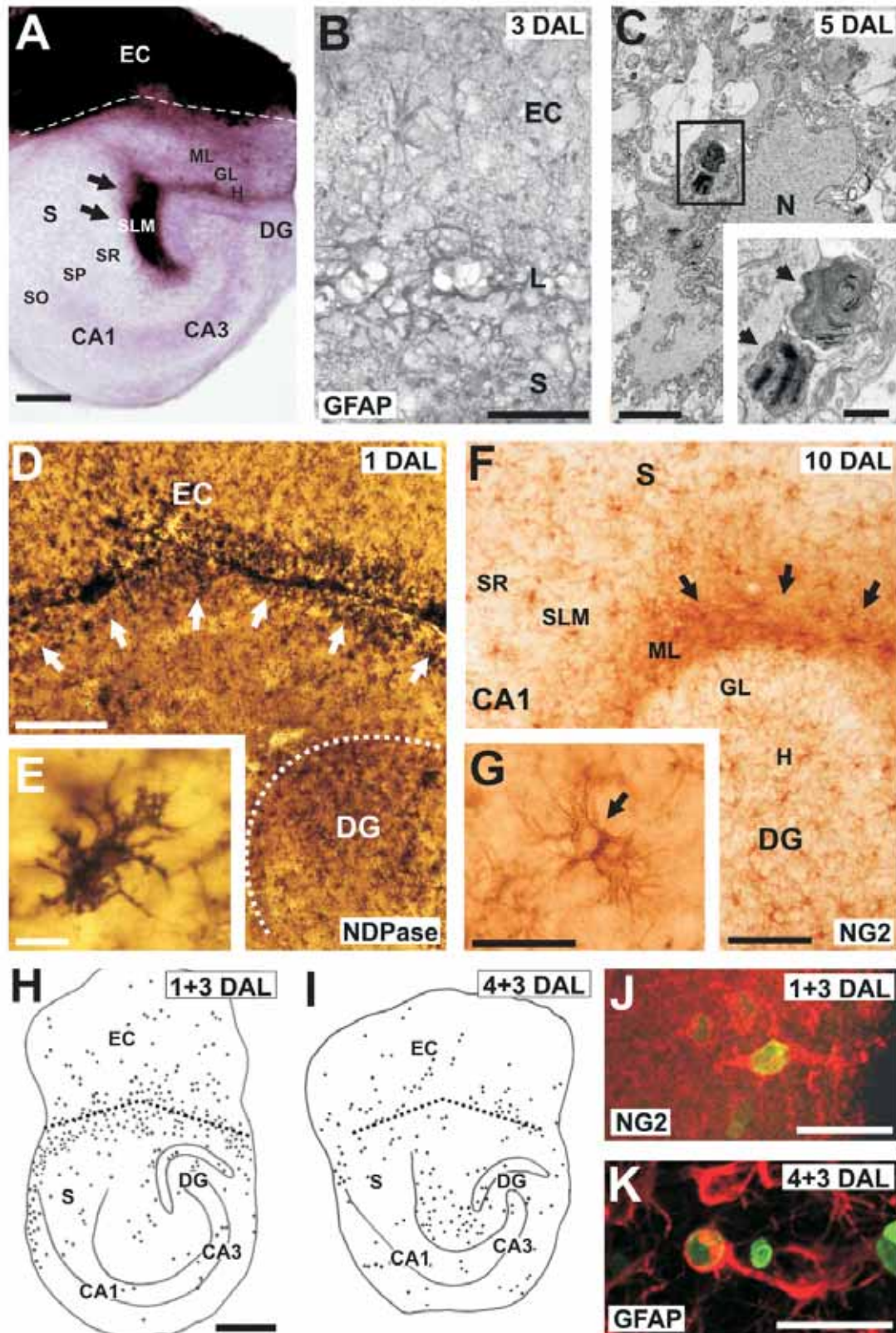


FIGURE 1. Glial reactivity after entorhino-hippocampal pathway (EHP) axotomy in slice co-cultures. A) Pattern of entorhino-hippocampal innervation in organotypic slice culture. The entorhinal cortex (EC) was labelled with the anterograde tracer biocytin after 7 days *in vitro* (DIV). Entorhinal fibres densely innervated the stratum lacunosum moleculare and the molecular layer (sml/ml, arrows). B) Immunoreactivity to GFAP 3 days after lesion (DAL) of the EHP at the subicular level (S). Note the small cavitation at the lesion site (L). C) Electron microscopy micrograph of sections through the lesioned area showing a reactive astrocyte. Arrows point to two large phagosomes in insert. D-G) Histochemistry to NDPase (D-E) and immunoreactivity of NG2 (F-G) in axotomized slice cultures at one (D-E) and ten (F-G) DAL. Note the intense NDPase labelling of microglial cells along the lesion site shortly after lesion (white arrows in D), and the characteristic amoeboid morphology of a "reactive" microglial cell (E). NG2-immunoreactivity increased after axotomy, especially in sml/ml (black arrows) (F). G) High power magnification of NG2-immunoreactive sections illustrating an example of juxtaposed mitotic NG2-positive cells at 10 DAL. H-I) Camera lucida drawings illustrating the distribution of BrdU-positive cells in lesioned slice cultures after BrdU exposure the first (H) or the fourth (I) DAL examined three days later. Immunoreactive nuclei were mostly located along the lesion site in H and in the sml/ml in I. J-K) Confocal photomicrograph showing double-labelled BrdU-NG2 (J) and BrdU-GFAP (K) in the sml/ml in equivalent cultures to H and I respectively. The transection of the EHP is labelled with a dotted line in H and I. Abbreviations: CA1-3, hippocampal fields; DG, dentate gyrus; EC, entorhinal cortex; GL, granule layer; H, hilus; L, lesion; ML, molecular layer; N, nucleous; S, subiculum; SLM, stratum lacunosum moleculare; SO, stratum oriens; SP, stratum pyramidale; SR, stratum radiatum. Scale bars: A=100 μ m; B = 50 μ m; C = 10 μ m; D, F = 50 μ m; E, G = 25 μ m; H-I= 100 μ m; J-K = 25 μ m.

RESULTS

Proliferation of glial cells after EHP axotomy *in vitro*

First, we checked the suitability of the organotypic slice culture assay to study axonal regeneration. The EHP lesion *in vitro* was followed by a robust glial reaction as observed by immunocytochemistry and NDPase-histochemistry (Fig 1). Slight cavitation (< 25-30 μ m) occurred during the first 5-7 days after lesion (DAL), with abundant astroglia, amoeboid microglia and NG2-positive oligodendrocyte progenitors on both sides of the transection (Fig 1B-G). After one week, the cavity was filled with a dense network of glial cells and processes. Using an electron microscope, we observed hypertrophic astroglial cells with dilated cytoplasm rich in intermediate filaments, and numerous phagocytic vacuoles (Fig. 1B-C). Subsequent BrdU-labelling experiments demonstrated that these reactive glial cells were generated by cell proliferation *in situ*, as double-labelled cells (GFAP- or NG2-BrdU) were observed near the lesion and the denervated stratum lacunosum moleculare/molecular layer (slm/ml; Fig. 1H-K).

Over-expression of CSPGs, Nogo-A and NgR after axotomy

The temporal evolution of CSPG-expression in control and lesioned slices was monitored using CS-56 and 3F8 antibodies (Fig. 2). In non-lesioned control co-cultures, CS-56 immunolabelling was present in all hippocampal layers, with a lower intensity in the slm/ml, target tissue for the EHP (Fig. 2A-B). From 2 to 15 DAL (the last DAL analyzed), a strong increase in CS-56 immunoreactivity occurred throughout the hippocampus, including the slm/ml, but not the entorhinal cortex (Fig. 2F), and glial cells resembling astroglia were immunostained with 3PE8 antibody in the slm/ml (Fig. 2C-D). In parallel to CSPG overexpression, a moderate increase in NgR and Nogo-A proteins, peaking at 2-5 DAL, was observed by Western blot (Fig. 3A). Thus, as *in vivo*, CSPG and Nogo-A could impair axonal regeneration of the EHP in slice cultures.

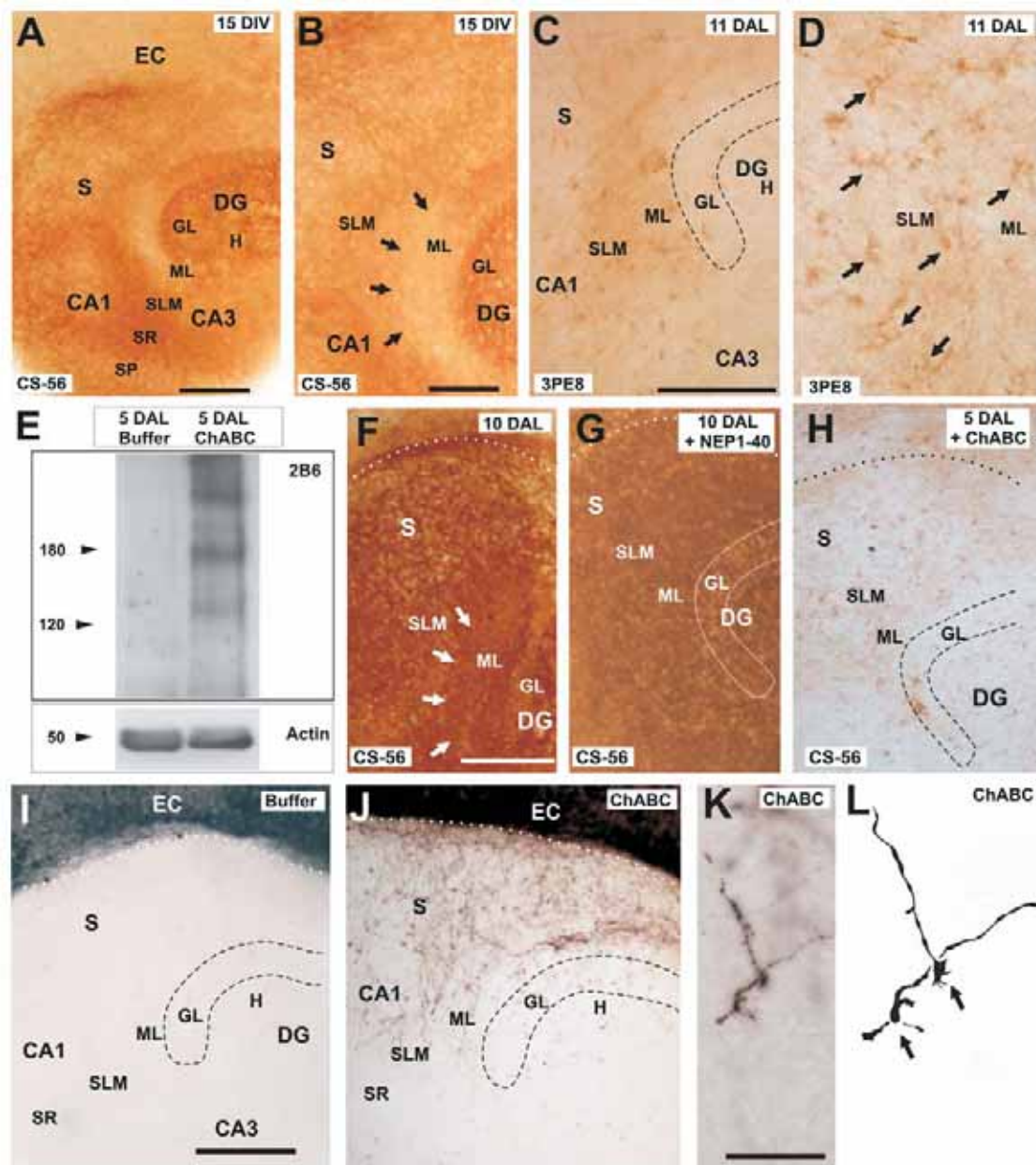


FIGURE 2. Overexpression of chondroitin-sulfate proteoglycans (CSPG) in axotomized co-cultures and axonal regeneration after chondroitinase ABC (ChABC) treatment. A-B) Pattern of CS-56 immunoreactivity in control (A-B) and lesioned (F) entorhino-hippocampal organotypic slices. Note the intense CS-56 immunoreactivity in the hippocampus after 15 DIV. Immunoreactivity was almost absent in the slm and the ml of the fascia dentata (arrows in B). 10 DAL of hippocampal afferents, CS-56 immunoreactivity strongly increased in the hippocampus, especially in the deafferented layers (F). This increase in immunoreactivity was not prevented by NEP1-40 treatment (G). C-D) Immunoreactivity of 3PE8 (to the CSPG IMP) in axotomized slice cultures 11 DAL. 3PE8-positive glial cells (arrows) were observed in the deafferented sml/ml (D). E) Western blot demonstration of the effectiveness of the ChABC treatment in EH organotypic co-cultures, determined by the retrieval of the stub antigen recognized by the 2B6 antibody. H) Example of CS-56 labelling in the hippocampus of a lesioned culture treated with ChABC for 5 days following EHP axotomy. Degradation of GAG residues is demonstrated by a marked decrease in CS-56 immunoreactivity in lesioned cultures after ChABC treatment. I-K) Pattern of entorhino-hippocampal innervation in control (I) and ChABC treated (J-K) cultures. The EC was labelled with biocytin as in Fig. A. The EHP lesioned at 15 DIV did not show regeneration of fibres after biocytin tracing at 7 DAL (I). ChABC-treated cultures displayed a high number of biocytin-labelled axons entering the hippocampus (J-K). K-L) High power magnification (K), and camera lucida drawing (L), of two examples of regenerating EH axons ending in growth cones (arrows) in the deafferented slm/ml after ChABC treatment. Abbreviations as in Fig. 1. The transection of the EHP is labelled with a dotted line in F-J. Scale bars: A = 200 μ m; B-D = 50 μ m; F-H = 100 μ m; I-J = 200 μ m; K = 25 μ m.

Blocking of CSPG- and Nogo-66/NgR-mediated axonal inhibition with ChABC and NEP1-40 after axotomy of the EHP

Acute treatment of axotomized organotypic cultures for seven days with ChABC (50 ng/ml), which degrades chondroitin-sulfate (CS) groups, resulted in the regrowth of numerous entorhinal axons into the hippocampus (Fig. 2J-K, 37.2 ± 8.4 ; mean \pm SEM). In contrast, in control cultures most of the axons stopped at the entorhino-hippocampal interface, and very few (3.7 ± 1.3) entered the hippocampus (Fig. 2I). Regenerating axons, ending in growth cones (Fig. 2K), did not always grow directly towards the slm/ml and often grew ectopically. However, in numerous cultures (33.3%) entorhinal axons preferentially innervated the slm/ml (e.g., Fig. 2J). The degradation of CS residues in ChABC-treated cultures was corroborated by a decrease in CS-56 immunostaining (Fig. 2H) accompanied by the appearance of the stub antigen recognized by the 2B6 antibody in Western blots (Fig. 2E). Control experiments demonstrated that drug treatments had no apparent effect on glial scar development and microglial activation, as assessed by GFAP immunostaining and NDPase histochemistry (Fig. 4A-F). In addition, the phagocytic properties of activated microglia after EHP axotomy were similar in control and treated cultures, as determined by the uptake of fluorescence latex microbeads in living slices (Fig. 4G-K).

Subsequently, we checked the contribution of Nogo-66 binding to NgR to the failure of entorhinal axons to regenerate. When compared with controls, acute NEP1-40 (100 μ M) treatment led to a significant increase in the number of regenerating biocytin-labelled axons that entered in the hippocampus (3.4 ± 1.2 vs. 19.7 ± 4.2 respectively; Fig. 3C and not shown). However, both the degree of regeneration and the layer specificity were lower in NEP1-40-treated cultures than those observed with ChABC treatment (Fig. 2J). Next, we examined the effect of combining the two treatments to enhance axonal regeneration of the lesioned EHP. While cultures treated with ChABC/NEP1-40 (Fig. 3D-F) displayed more regenerating axons than those receiving NEP1-40 alone (43.3 ± 6.9 vs. 19.7 ± 4.2), the difference with ChABC-treated cultures was not significant (37.2 ± 8.4). Notably, entorhinal axons receiving the combined treatment established asymmetric synaptic contacts with target hippocampal neurons, as assessed by electronic microscopy (Fig. 3G).

In parallel experiments, cultures were left untreated for four days after lesion, and were subsequently treated for seven days as for acute treatments. Although the efficiency of the ChABC treatment was reduced (37.2 ± 8.4 (acute) vs. 13.8 ± 7.5 (delayed)), delayed application of NEP1-40 gave similar regenerative results to acute treatment (Fig. 3H). We thus conclude that although the regenerative capacity of the EHP connection persists for several days after injury, the time window of effectiveness of some treatments, such as ChABC, may be limited to early application after lesion.

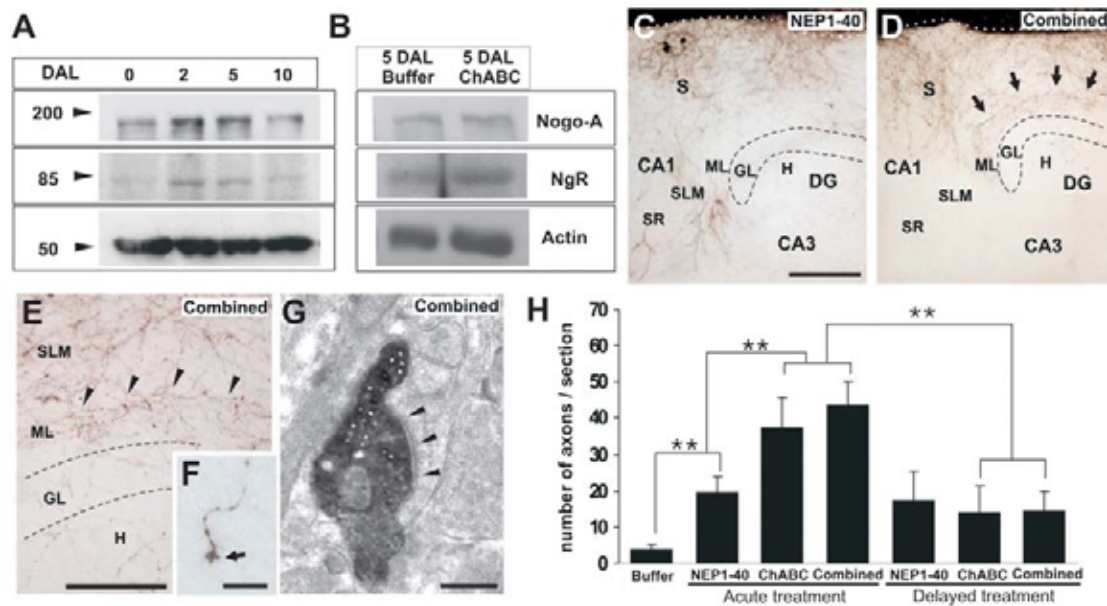


FIGURE 3. Regeneration of the EHP following combined treatment with NEP1-40 and ChABC. A) Western blotting analysis of the time course of Nogo-A, NgR and Actin protein levels in organotypic culture extracts after knife-cut axotomy. An increase in the amount of both Nogo-A and NgR was observed soon after lesion (at 2 DAL). B) Nogo-A and NgR protein levels are not affected by ChABC treatment after lesion. C-F) Pattern of entorhino-hippocampal innervation in lesioned cultures after NEP1-40 (C) and NEP1-40/ChABC (combined) treatments (D-F). Both treatments increased the number of regenerating entorhinal axons, although the combined treatment was more efficient and led to higher layer specificity (arrows in D). E) High power view of biocytin-labelled entorhinal axons displaying punctate labelling in the sml/ml (arrowheads). Insert F shows detail of a regenerating entorhinal axon ending in a growth cone (arrow) after combined treatment. G) Electron microscopy micrograph of a biocytin-labelled axon terminal in the deafferented sml/ml establishing asymmetric contact (arrowheads) with a dendrite. H) Histogram showing the mean number of biocytin-labelled fibers that crossed a 400 μm segment located at a distance of 75-80 μm in the hippocampus parallel to the transection of consecutive sections from each culture after NEP1-40, ChABC, or combined treatments in acute and delayed treatments. The transection of the EHP is labelled with a dotted line in C and D. Control n=40 cultures, NEP1-40 n= 43, ChABC n=26, Cocktail n=39, delayed NEP1-40 n=15, delayed ChABC n=11, delayed Cocktail n=11. Asterisks indicate significant difference (ANOVA test; ** $p < 0.05$). Abbreviations as in Fig. 1. Scale bars: C-D = 100 μm ; E = 50 μm ; F = 25 μm ; G = 2 μm .

DISCUSSION

This study examines the potential of several strategies to promote axonal regeneration of the lesioned EHP, taking advantage of the entorhino-hippocampal slice culture preparation. CSPG and myelin-derived molecules limit axonal regeneration (1, 3). After entorhinal lesions *in vivo*, glial cells proliferate and express increased levels of CSPG (e.g., neurocan, versican or NG2) and myelin-associated molecules (e.g., Nogo-A or MAG) (25, 29-31). Our findings demonstrate that glial reactivity after *in vitro* axotomy, including phagocytosis, proliferation and overexpression of CSPG and Nogo-A, mimics that occurring after *in vivo* lesion (32). Moreover, we show that the slice culture assay is well suited to test new approaches that aim to overcome CSPG- and myelin-mediated inhibition after EHP axotomy.

Potential of the blockade of CSPG- and Nogo-A/NgR-induced axonal inhibition to enhance EHP regeneration

ChABC releases GAG residues of the CS, thereby reducing CSPG-induced inhibition, but preserves heparan (HS) and keratan (KS) sulfate proteoglycans (19, 20). Therefore, given that HSPGs bind to numerous growth-promoting molecules (e.g., NCAM or Laminin), ChABC-treatment may also favor axonal regeneration by providing a more permissive substrate for entorhinal axons (e.g., HSPG-enriched). Nogo-A inhibits axonal regeneration through distinct domains, including NiG and Nogo-66. In our hands, NEP1-40 (which blocks Nogo-66 binding to NgR) is more efficient in promoting axonal regeneration than IN-1 antibody (against NiG; 25) and is useful in delayed treatment, as also observed after spinal cord lesions (33). This difference in efficiency may be attributable to the better penetration of the peptide compared with the IgM immunoglobulin. Alternatively, the contribution of Nogo-66 to Nogo-A-dependent inhibition may be greater than that of NiG, since NEP1-40 blocked the former but not other inhibitory regions of Nogo-A. Our results also reflect the relative contribution of CSPG and Nogo-66 to axonal growth inhibition in the EHP when ChABC and NEP1-40 are used separately and, surprisingly, demonstrate that the combined use of these two drugs has no synergistic effect, as it did not improve the results obtained with ChABC alone. In control experiments, NEP1-40 treatment did not modify CSPG up-regulation and conversely, ChABC treatment did not affect Nogo-A or NgR expression levels. Recently, an intracellular convergence in the signaling pathways activated by CSPG and myelin has been reported (10-12). Thus, ChABC alone may reduce inhibitory intracellular pathways (e.g., Rho or PKC activity) to an inactivated level at which the incubation with NEP1-40 has no additive effect. The lack of synergism between the two drugs supports the notion of signaling convergence and highlights the importance of selecting appropriate treatments with complementary intracellular effects for use in combination.

Nevertheless, the levels of axonal regeneration obtained with these extrinsic treatments were modest compared to the regeneration obtained by cell transplantation (27). Although the regulation of the inhibitory molecules after juvenile hippocampal transplantation in organotypic slices remains unknown, our present results indicate that other molecules may be involved in preventing EHP axon regeneration. These molecules may also act via PKC or Rho, since the pharmacological blockade of PKC also elicits robust regeneration of the EHP (34). However, this last study raises the question of whether intrinsic pharmacological treatments that block Rho or PKC lead to the specific regeneration of the EHP without affecting other neuronal functions. In our experiments, ChABC/NEP1-40 treatment resulted in the formation of mature synaptic contacts between regenerating entorhinal axons and their hippocampal target cells.

Finally, we determined the time window of effectiveness of ChABC and NEP1-40 after lesion. Although post-lesion delivery of ChABC and NEP1-40 led to axonal regeneration of the EHP, the degree of regrowth was reduced in cultures treated with the former. This may reflect the incapacity of ChABC to digest the increased amount of CSPG that accumulate in the lesioned hippocampus after five days. Unfortunately, culture viability was compromised at doses of ChABC higher than 50-100 ng/ml. On the contrary, NEP1-40 delivery can be delayed at least

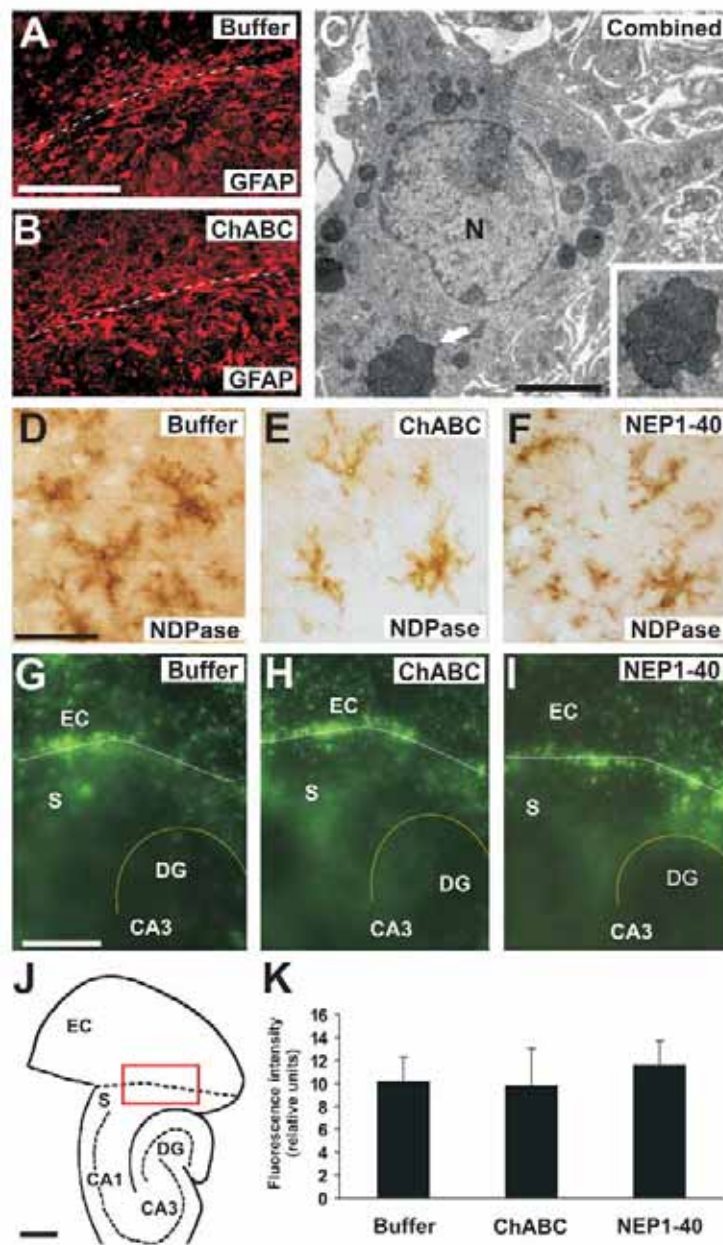


Figure 4. Effects of ChABC and NEP1-40 on glial scar development, microglial activation and phagocytic capability of activated microglia after lesion. A-B) Distribution pattern of GFAP-immunoreactive cells at the entorhino-hippocampal interphase at 5 DAL after ChABC treatment (50 ng/ml; B) compared to control (A). ChABC-treated cultures displayed no relevant changes in the distribution pattern of reactive astrocytes around the lesion compared to control cultures. C) Electron microscopy micrograph of a reactive astrocyte in the lesion in a ChABC/NEP1-40-treated culture at 7 DAL. As in control untreated cultures, several phagosomes containing cellular debris (insert in C) can be observed in the dilated cytoplasm (arrow). D-F) High power views of NDPase-positive microglial cells in layer II-III of the EC in control (D), NEP1-40- (E) and ChABC- (F) treated organotypic co-cultures at 5 DAL. No relevant differences in the gross morphology of microglial cells between control and treated cultures can be seen. G-I) Low power fluorescence micrograph of the distribution of FITC-tagged microbeads in control (G), NEP1-40- (H) and ChABC-treated (I) cultures for 4 days. Distribution of uptaken microbeads and intensity of fluorescence along the lesion site showed no differences between the different treatments indicating similar phagocytic activity by reactive microglia in all cases. J) Schematic diagram illustrating the *in vitro* axotomy model and the counting areas in the microbead experiment. The EHP was axotomized at 15 DIV (dashed line). After incubation with FITC-tagged microbeads, the intensity of fluorescence was measured in a box of (200 x 100 μ m, red box) centered in the transection trajectory and further corrected to background fluorescence levels. K) Histogram showing level of fluorescence intensity (mean \pm SEM) in control (n = 4) and treated (n = 5, NEP1-40; n = 5 ChABC) cultures. Scale bars: A-B = 25 μ m; C = 2 μ m; D-F = 50 μ m; G-I = 100 μ m; J = 100 μ m.

for 5 days without loss of efficiency. Our results are consistent with other studies and indicate that, in order to promote axonal regeneration, ChABC treatment must be started before or immediately after lesion (23). In conclusion, these results highlight the participation of Nogo-66 and CSPG in EHP regeneration failure and provide insight into the development of new assays and strategies to enhance axon regeneration in injured cortical connections.

References

1. Sandvig, A., Berry, M., Barrett, L. B., Butt, A., and Logan, A. (2004) Myelin-, reactive glia-, and scar-derived CNS axon growth inhibitors: expression, receptor signaling, and correlation with axon regeneration. *Glia* **46**, 225-251
2. Carulli, D., Laabs, T., Geller, H. M., and Fawcett, J. W. (2005) Chondroitin sulfate proteoglycans in neural development and regeneration. *Curr Opin Neurobiol* **15**, 116-120
3. Silver, J., and Miller, J. H. (2004) Regeneration beyond the glial scar. *Nat Rev Neurosci* **5**, 146-156
4. Park, J. B., Yiu, G., Kaneko, S., Wang, J., Chang, J., and He, Z. (2005) A TNF Receptor Family Member, TROY, Is a Coreceptor with Nogo Receptor in Mediating the Inhibitory Activity of Myelin Inhibitors. *Neuron* **45**, 345-351
5. Shao, Z., Browning, J. L., Lee, X., Scott, M. L., Shulga-Morskaya, S., Allaire, N., Thill, G., Levesque, M., Sah, D., McCoy, J. M., Murray, B., Jung, V., Pepinsky, R. B., and Mi, S. (2005) TAJ/TROY, an Orphan TNF Receptor Family Member, Binds Nogo-66 Receptor 1 and Regulates Axonal Regeneration. *Neuron* **45**, 353-359
6. Mi, S., Lee, X., Shao, Z., Thill, G., Ji, B., Relton, J., Levesque, M., Allaire, N., Perrin, S., Sands, B., Crowell, T., Cate, R. L., McCoy, J. M., and Pepinsky, R. B. (2004) LINGO-1 is a component of the Nogo-66 receptor/p75 signaling complex. *Nat Neurosci* **7**, 221-228
7. Vyas, A. A., Patel, H. V., Fromholt, S. E., Heffer-Lauc, M., Vyas, K. A., Dang, J., Schachner, M., and Schnaar, R. L. (2002) Gangliosides are functional nerve cell ligands for myelin-associated glycoprotein (MAG), an inhibitor of nerve regeneration. *Proc Natl Acad Sci U S A* **99**, 8412-8417
8. Venkatesh, K., Chivatakarn, O., Lee, H., Joshi, P. S., Kantor, D. B., Newman, B. A., Mage, R., Rader, C., and Giger, R. J. (2005) The Nogo-66 receptor homolog NgR2 is a sialic acid-dependent receptor selective for myelin-associated glycoprotein. *J Neurosci* **25**, 808-822
9. Schweigreiter, R., Walmsley, A. R., Niederost, B., Zimmermann, D. R., Oertle, T., Casademunt, E., Frentzel, S., Dechant, G., Mir, A., and Bandtlow, C. E. (2004) Versican V2 and the central inhibitory domain of Nogo-A inhibit neurite growth via p75NTR/NgR-independent pathways that converge at RhoA. *Mol Cell Neurosci* **27**, 163-174
10. He, Z., and Koprivica, V. (2004) The Nogo signaling pathway for regeneration block. *Annu Rev Neurosci* **27**, 341-368
11. Sivasankaran, R., Pei, J., Wang, K. C., Zhang, Y. P., Shields, C. B., Xu, X. M., and He, Z. (2004) PKC mediates inhibitory effects of myelin and chondroitin sulfate proteoglycans on axonal regeneration. *Nat Neurosci* **7**, 261-268
12. Hasegawa, Y., Fujitani, M., Hata, K., Tohyama, M., Yamagishi, S., and Yamashita, T. (2004) Promotion of axon regeneration by myelin-associated glycoprotein and Nogo through divergent signals downstream of Gi/G. *J Neurosci* **24**, 6826-6832
13. Bartsch, U., Bandtlow, C. E., Schnell, L., Bartsch, S., Spillmann, A. A., Rubin, B. P., Hillenbrand, R., Montag, D., Schwab, M. E., and Schachner, M. (1995) Lack of evidence that myelin-associated glycoprotein is a major inhibitor of axonal regeneration in the CNS. *Neuron* **15**, 1375-1381

14. Zheng, B., Ho, C., Li, S., Keirstead, H., Steward, O., and Tessier-Lavigne, M. (2003) Lack of enhanced spinal regeneration in Nogo-deficient mice. *Neuron* **38**, 213-224
15. Oudega, M., Rosano, C., Sadi, D., Wood, P. M., Schwab, M. E., and Hagg, T. (2000) Neutralizing antibodies against neurite growth inhibitor NI-35/250 do not promote regeneration of sensory axons in the adult rat spinal cord. *Neuroscience* **100**, 873-883
16. Schwab, M. E. (2004) Nogo and axon regeneration. *Curr Opin Neurobiol* **14**, 118-124
17. Lee, D. H., Strittmatter, S. M., and Sah, D. W. (2003) Targeting the Nogo receptor to treat central nervous system injuries. *Nat Rev Drug Discov* **2**, 872-878
18. Li, W., Walus, L., Rabacchi, S. A., Jirik, A., Chang, E., Schauer, J., Zheng, B. H., Benedetti, N. J., Liu, B. P., Choi, E., Worley, D., Silvan, L., Mo, W., Mullen, C., Yang, W., Strittmatter, S. M., Sah, D. W., Pepinsky, B., and Lee, D. H. (2004) A neutralizing anti-Nogo66 receptor monoclonal antibody reverses inhibition of neurite outgrowth by central nervous system myelin. *J Biol Chem* **279**, 43780-43788
19. Bradbury, E. J., Moon, L. D., Popat, R. J., King, V. R., Bennett, G. S., Patel, P. N., Fawcett, J. W., and McMahon, S. B. (2002) Chondroitinase ABC promotes functional recovery after spinal cord injury. *Nature* **416**, 636-640
20. Moon, L. D., Asher, R. A., Rhodes, K. E., and Fawcett, J. W. (2001) Regeneration of CNS axons back to their target following treatment of adult rat brain with chondroitinase ABC. *Nat Neurosci* **4**, 465-466
21. Fournier, A. E., Takizawa, B. T., and Strittmatter, S. M. (2003) Rho kinase inhibition enhances axonal regeneration in the injured CNS. *J Neurosci* **23**, 1416-1423
22. Ji, B., Li, M., Budel, S., Pepinsky, R.B., Walus, L., Engber, T.M., Strittmatter, S.M., Relton, J.K. (2005) Effect of combined treatment with methylprednisolone and soluble Nogo-66 receptor after rat spinal cord injury. *Eur J Neurosci* **22**, 587-594.
23. Steinmetz, M.P., Horn, K.P., Tom, V.J., Miller, J.H., Busch, S.A., Nair, D., Silver, D.J., Silver, J. (2005) Chronic enhancement of the intrinsic growth capacity of sensory neurons combined with the degradation of inhibitory proteoglycans allows functional regeneration of sensory axons through the dorsal root entry zone in the mammalian spinal cord. *J Neurosci* **25**, 8066-8076.
24. Schnell, L., Schneider, R., Kolbeck, R., Barde, Y.A., Schwab, M.E. (1994) Neurotrophin-3 enhances sprouting of corticospinal tract during development and after adult spinal cord lesion. *Nature* **367**, 170-173.
25. Mingorance, A., Fontana, X., Sole, M., Burgaya, F., Urena, J. M., Teng, F. Y., Tang, B. L., Hunt, D., Anderson, P. N., Bethea, J. R., Schwab, M. E., Soriano, E., and del Rio, J. A. (2004) Regulation of Nogo and Nogo receptor during the development of the entorhino-hippocampal pathway and after adult hippocampal lesions. *Mol Cell Neurosci* **26**, 34-49
26. Del Rio, J. A., Heimrich, B., Borrell, V., Forster, E., Drakew, A., Alcantara, S., Nakajima, K., Miyata, T., Ogawa, M., Mikoshiba, K., Derer, P., Frotscher, M., and Soriano, E. (1997) A role for Cajal-Retzius cells and reelin in the development of hippocampal connections. *Nature* **385**, 70-74

27. del Rio, J. A., Sole, M., Borrell, V., Martinez, A., and Soriano, E. (2002) Involvement of Cajal-Retzius cells in robust and layer-specific regeneration of the entorhino-hippocampal pathways. *Eur J Neurosci* **15**, 1881-1890
28. Castellano, B., Gonzalez, B., Jensen, M. B., Pedersen, E. B., Finsen, B. R., and Zimmer, J. (1991) A double staining technique for simultaneous demonstration of astrocytes and microglia in brain sections and astroglial cell cultures. *J Histochem Cytochem* **39**, 561-568
29. Meier, S., Brauer, A. U., Heimrich, B., Schwab, M. E., Nitsch, R., and Savaskan, N. E. (2003) Molecular analysis of Nogo expression in the hippocampus during development and following lesion and seizure. *FASEB J* **17**, 1153-1155
30. Deller, T., Haas, C. A., and Frotscher, M. (2000) Reorganization of the rat fascia dentata after a unilateral entorhinal cortex lesion. Role of the extracellular matrix. *Ann N Y Acad Sci* **911**, 207-220
31. Mingorance, A., Fontana, X., Soriano, E., and Del Rio, J. A. (2005) Overexpression of myelin-associated glycoprotein after axotomy of the perforant pathway. *Mol Cell Neurosci* **29**, 471-483
32. Bechmann, I., and Nitsch, R. (2000) Involvement of non-neuronal cells in entorhinal-hippocampal reorganization following lesions. *Ann N Y Acad Sci* **911**, 192-206
33. Li, S., Strittmatter, S.M. (2003) Delayed systemic Nogo-66 receptor antagonist promotes recovery from spinal cord injury. *J Neurosci* **23**, 4219-4227.
34. Prang, P., Del Turco, D., and Kapfhammer, J. P. (2001) Regeneration of entorhinal fibers in mouse slice cultures is age dependent and can be stimulated by NT-4, GDNF, and modulators of G-proteins and protein kinase C. *Exp Neurol* **169**, 135-147

Copyright permission

Chapter I and II have been reprinted from

Mingorance A., Fontana X., Solé M., Burgaya F., Ureña JM., Teng FY., Tang BL., Hunt D., Anderson PN., Bethea JR., Schwab ME., Soriano E. and JA. del Río. (2004) Regulation of Nogo and Nogo receptor during the development of the entorhino-hippocampal pathway and after adult hippocampal lesions. *Molecular and Cellular Neuroscience*. 26: 34-49

and

Mingorance A., Fontana X., Soriano E. and del Río JA. (2005) Overexpression of Myelin-Associated Glycoprotein after axotomy of the perforant pathway. *Molecular and Cellular Neuroscience*. 29: 471-483

with permission from Elsevier.

Chapter III content is reprinted from

Mingorance A., Solé M., Muneton V., Martínez A., Nieto-Sampedro M., Soriano E. and del Río JA. (2006) Regeneration of lesioned entorhino-hippocampal axons in vitro by combined degradation of inhibitory proteoglycans and blockade of Nogo-66/NgR signaling. *FASEB Journal*, DOI10.1096/fj.05-5121fje

with permission form FASEB publications.